BIOCHEMICAL AND FUNCTIONAL CHARACTERIZATION OF FATTY ACID TRASNPORT PROTEINS

A DISSERTATION
SUBMITTED TO THE FACULTY OF THE GRADUATE SCHOOL
OF THE UNIVERSITY OF MINNESOTA
BY

Brian Michael Wiczer

IN PARTIAL FULFILLMENT OF THE REQUIREMENTS
FOR THE DEGREE OF
DOCTOR OF PHILOSOPHY

David A. Bernlohr

July 2009

Acknowledgements

I would like to thank my advisor and mentor, Dr. Dave Bernlohr, for all of his support and guidance throughout my graduate studies. He gave me practically unimpeded freedom to develop and test my own hypotheses, even despite the times when he himself was unsure what direction they would go. The experience I had during these six years of graduate school would not have been as entertaining and stimulating as it was if it weren't for all the lab members, both past and present. I am thankful for all their help and camaraderie, not too mention the willingness they displayed to help me complete an experiment the day my wife went into labor. I must also specifically acknowledge Brian Thompson and Ann Hertzel. I consider them two additional mentors without whom I would certainly not have developed into the scientist I am. Finally, the afternoon "coffee club" will also always hold a special place in my heart, and I will miss the sometimes serious, sometimes whimsical discussions.

Dedication

This dissertation is dedicated to my wife, Liz, and my son, Christopher. Liz has been my rock during the last three years of my graduate career. She has stood together with me through this rollercoaster ride, celebrating with me at the highs and suffering with me as well as supporting me at the lows. The recent addition of Christopher has also helped me to enjoy life every day, even when work has felt dark. Thank you both for all that you have given and I love you so much.

Abstract

The adipocyte fatty acid transport proteins (FATPs), FATP1 and FATP4, have been implicated in both lipid influx and storage and understanding their role in adipose tissue would gain insight into the persistence of metabolic disorders, such as type 2 diabetes. FATP1 was previously determined to be an acyl-CoA synthetase and work described in this thesis additionally explored the acyl-CoA synthetase activity of purified FATP4. FATP4 was found to be a more robust acyl-CoA synthetase than FATP1. Through the use of RNAi in cultured adipocytes, silencing the expression of either FATP1 or FATP4 results in cellular phenotype demonstrating improved insulin responsiveness. Interestingly, silencing FATP1 abolished insulin-stimulated long-chain fatty acid (LCFA) influx, whereas silencing FATP4 had no effect on LCFA influx despite its higher activity. Furthermore, the expression of FATP1 was demonstrated to be important for the activation of the AMP-activated protein kinase during insulin-stimulated LCFA influx. In addition to the cytoplasmic localization of FATP1, it was also found to exhibit mitochondrial localization. Further analysis demonstrated a novel role in the regulation of TCA cycle function and mitochondrial energy metabolism, in part, through the interaction of FATP1 with the 2-oxoglutarate dehydrogenase complex, a rate-limiting step in the TCA cycle. This work shines light on how FATPs may play broader roles in metabolism that previously appreciated and the potential implications associated with such roles.

Table of Contents

List of Tables

List of Figures

List of Abbreviations

ACC	acetyl-CoA carboxylase
ACS	acyl-CoA synthetase
ACSL1	acyl-CoA synthetase 1
AFABP/aP2	adipocyte fatty acid binding protein
AMPK	AMP-activated protein kinase
BCKDH	branched-chain keto acid dehydrogenase
BSA	bovine serum albumin
C/EBPα	CCAAT/enhancer binding protein alpha
$C_{12}E_8$	octaethylene glycol monododecyl ether
CD36	fatty acid translocase
DDM	n-dodecyl-β-D-matlopyranoside
DOPC	dioleoylphosphatidylcholine
DOPE	dioleoylphosphatidylethanolamine
DOPS	dioleoylphosphatidyl-L-serine
$FABP_{PM}$	plasma membrane fatty acid binding protein
FAT/CD36	fatty acid translocase / CD36 antigen
FATP	fatty acid transport protein
FATP1	fatty acid transport protein 1
FATP4	fatty acid transport protein 4
HPLC	high pressure liquid chromatography
KRH	Krebs-Ringer's HEPES
LCFA	long-chain fatty acid
OGDH	2-oxoglutarate dehydrogenase complex
PDH	pyruvate dehydrogenase complex
PPARγ	peroxisome proliferator activated receptor γ
SAX	strong anion exchange
shRNA	short hairpin RNA
SUVs	small unilamellar vesicles
TCA	tricarboxylic acid

CHAPTER 1:

ADIPOCYTE LIPID METABOLISM AND FATTY ACID TRANSPORT PROTEINS

Portions of this chapter are taken directly from: **Biochemistry of Lipids, Lipoproteins and Membranes**, edition 5 (2008) Vance and Vance; Chapter 10: Lipid Metabolism in Adipose Tissue, Hertzel, A. H., Thompson, B. R., **Wiczer, B. M.**, Bernlohr, D. A.; Elsevier Press; and **Transport of Fatty Acids into Adipocytes**; **Wiczer, B. M.**, Lobo, S., Bernlohr, D. A. (2006) *Future Lipidol.* **1**(3), 291-298

1 Metabolic Syndrome and Lipids

Obesity and other metabolic disorders, such as type 2 diabetes and dyslipidemia, have become a serious health issue and the prevalence is increasing worldwide in both adults and children. It is therefore vital to understand the biological mechanisms that are contributing to the onset and persistence of these metabolic disorders. Because these pathologies are often related, they have been grouped together and termed the metabolic syndrome (1). One aspect of metabolic syndrome is dysregulation of cellular fatty acid influx and metabolism, especially in highly metabolic tissues (i.e., liver, skeletal muscle, and adipose tissue).

Long-chain fatty acids (LCFA) and their acyl-CoA derivatives play a variety of processes in regulatory and metabolic biology. Activation of phospholipase A_2 leads to the production of polyunsaturated LCFA, the most common substrate for lipid second messenger signaling systems (2-4). The oxidation of LCFA to prostaglandins, leukotrienes, and thromboxanes leads to signaling molecules whose functions are often linked to rapid metabolic responses facilitated through G-protein coupled receptor signaling and result in various inflammatory responses dependent on the effector lipid-derived molecule (5-7). In contrast, the metabolism of LCFA to the corresponding acyl-CoAs provides substrates for a variety of metabolic processes including glycerophospholipid and sphingolipid synthesis, cholesterol ester formation, β-oxidation, protein acylation, nuclear receptor regulation, and triacylglycerol biosynthesis. Such metabolic and/or regulatory uses of acyl-CoAs are often linked to long-term or chronic regulation of metabolism.

Of the cells that avidly utilize LCFA for both regulatory and metabolic processes, the adipocyte exhibits perhaps the most robust metabolism, producing lipid second messengers for activation of nuclear peroxisome proliferator activated receptor γ as well as acyl-CoAs for metabolic storage and utilization (Figure 1). Therefore, aberrant adipocyte metabolism would result in LCFA metabolic dysfunction, greatly increased pro-inflammatory signaling, and contribute to the onset of metabolic syndrome (8). Fatty acid transport proteins (FATPs) are a family of proteins comprised of six members (FATP1-6) and have been implicated in both LCFA influx and storage. Adipose tissue only express FATP1 and FATP4, however, their specific cellular functions have remained unclear. Consistent with the important role adipocytes play in LCFA metabolism and overall energy homeostasis, aberrant adipocyte LCFA influx and acyl-CoA production greatly contributes to metabolic syndrome (8,9). In light of this, understanding the biochemical and functional roles of FATP1 and FATP4 in adipocytes is of great interest.

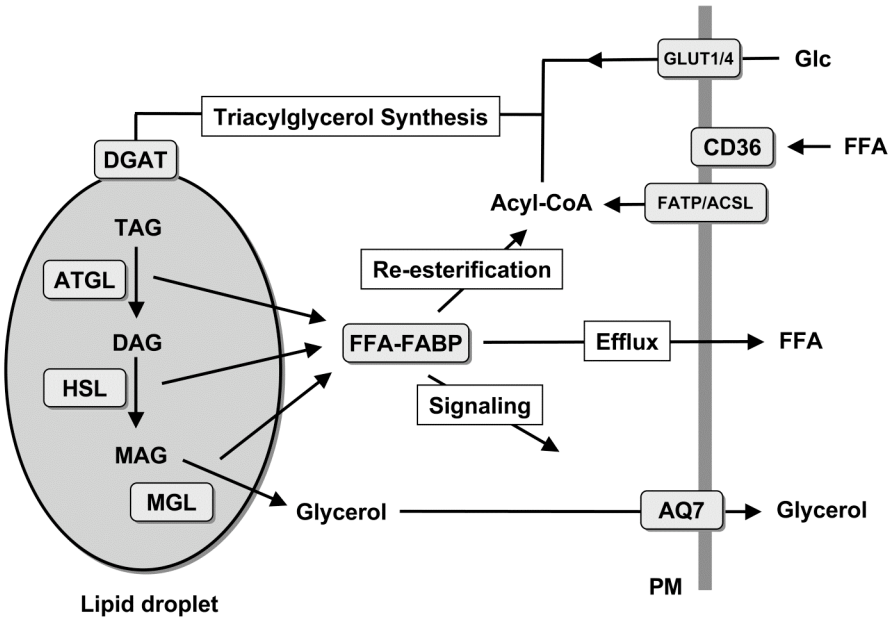

Fig. 1

Figure 1. Lipid cycling in adipocytes. Adipocytes transport glucose (Glc via GLUT 1 or 4) and fatty acids (FFA via CD36 /ACSL) into the cell in response to insulin stimulation leading to the synthesis of triacylglycerol, the terminal step of which is catalyzed by diacylglycerol acyltransferase (DGAT). Triacylglycerol synthesis is balanced by hydrolysis catalyzed by a series of triacylglycerol (adipose triacylglycerol lipase; ATGL), diacylglycerol (hormone sensitive lipase; HSL) and monoacylglycerol (MGL) lipases. Glycerol produced by complete TAG hydrolysis is exported from the adipocyte via an aquaporin protein (AQ7) while FFA are bound by intracellular fatty acid binding proteins (FABP) and subjected to re-esterification, efflux, or metabolized to signaling molecules. TAG, triacylglycerol; DAG, diacylglycerol; MAG, monoacylglycerol; ACSL, long-chain acyl-CoA synthetase.

2 Adipocyte Lipid Metabolism

2.1 Lipids and Insulin Signaling

A primary function of adipose tissue is to serve as a storage site for the excess energy derived from food consumption. Energy stored in the form of triacylglycerol can be

utilized by the organism to fulfill subsequent metabolic requirements during times of little or no consumption (Figure 1). In the case of WAT, these requirements entail efficient storage of large amounts of energy in a form that can be readily mobilized to supply the needs of peripheral organs and tissues. Lipids, particularly fatty acids, are exceptionally efficient fuel storage species. The highly reduced hydrocarbon tail of triacylglycerol can be readily oxidized to produce large quantities of NADH and $FADH_2$ and subsequently ATP. At the same time, the very hydrophobic nature of the hydrocarbon tail precludes concomitant storage of excess water that would increase the mass and spatial requirements of the organism. Also, the relatively straight, chain-like structure of the fatty acid permits dense packing of many molecules into each cell, maximizing the use of storage space available. BAT also stores energy in lipid form, but more frequently produces heat by oxidizing fatty acids within the adipocyte, rather than by supplying free fatty acids for use by other cell types.

During feeding, pancreatic β cells secrete insulin in response to both elevated blood glucose levels and elevated blood lipid levels. Insulin is the most important physiological stimulus for energy storage. The effect of insulin directly counteracts the effects of glucagon and the catecholamines. The insulin receptor is found in many diverse cell and tissue types, not the least significant of which is adipose.

The insulin receptor is an integral membrane protein and a receptor tyrosine kinase that functions as a tetramer composed of two α and two β subunits. The β subunits each span the plasma membrane once, and the α subunits are covalently attached to the β

subunit extracellularly by disulfide bonds. The insulin-binding site is extracellular and the intracellular domains contain many tyrosine phosphorylation sites. Ligand binding induces autophosphorylation of several intracellular domains, activating the kinase activity of each β subunit. A complex series of interactions follows in which the insulin receptor phosphorylates some of its substrates directly, such as insulin receptor substrate-1 (IRS-1) and IRS-2, or recruits various adaptor proteins, such as Shc and Grb2 that transmit the insulin signal (10).

Insulin binding to the adipocyte insulin receptor simultaneously stimulates lipogenesis and inhibits lipolysis. Insulin action effectively clears fatty acids and glucose from the blood both by increasing uptake and storage, and by decreasing mobilization of stored energy. The mechanisms by which these effects are accomplished are highly complex and involve an integrated series of regulated events (11). In regards to insulin-stimulated glucose uptake, the insulin receptor acts mainly through the phosphatidylinositol-3-kinase (PI3 kinase) pathway. Activated insulin receptor binds and phosphorylates IRS-1, thereby allowing PI3 kinase to bind IRS-1. PI3 kinase subsequently phosphorylates its substrate, phosphatidylinositol-4,5-bisphosphate, forming phosphatidylinositol-3,4,5-trisphosphate at the plasma membrane. The kinases AKT/protein kinase B (PKB) and PDK1 are recruited to the plasma membrane by binding phosphatidylinositol-3,4,5-trisphosphate. PDK1 phosphorylates and activates AKT/PKB. AKT/PKB then transmits the signal to increase glucose uptake through the phosphorylation of the AKT substrate of 160 kDa, which is a Rab-GTPase activating protein. This activation of AKT substrate of 160 kDa, through an unknown mechanism,

facilitates the translocation of GLUT4, to the plasma membrane and stimulates glucose transport (Figure 2).

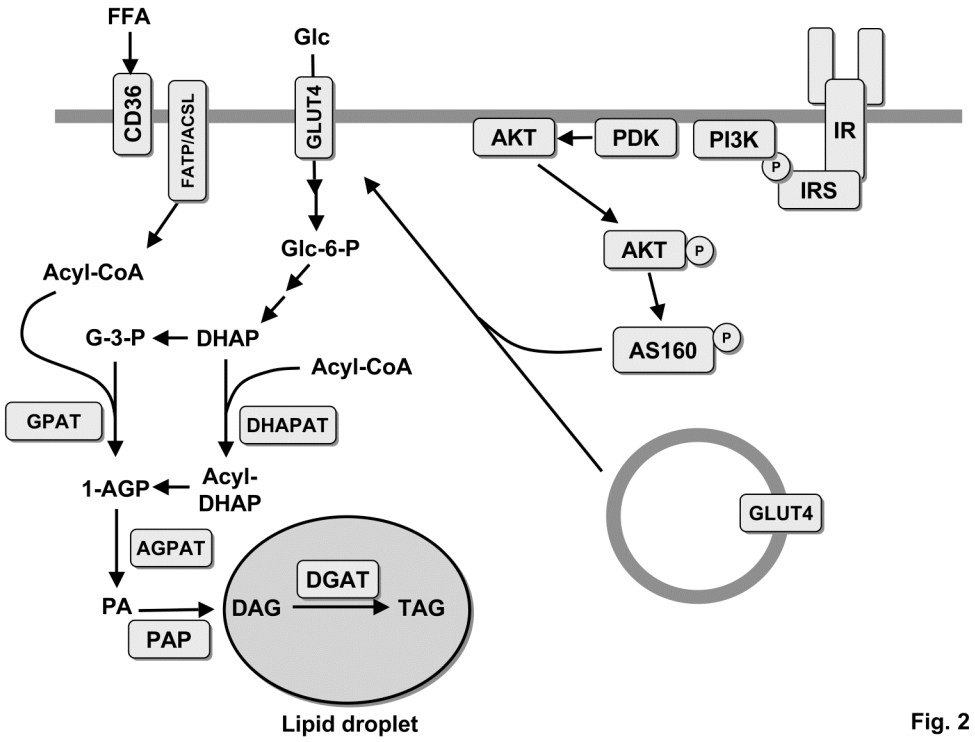

Fig. 2

Figure 2. Insulin-stimulated glucose uptake and triacylglycerol biosynthesis. Activation of the insulin receptor (IR) upon insulin binding results in the recruitment of IRS to the insulin receptor and subsequent tyrosine phosphorylation of IRS. This allows the subsequent recruitment and activation of phosphatidylinositol 3-phosphate kinase (PI3K), phosphatidylinositol-dependent protein kinase (PDK), and AKT/PKB. PDK phosphorylates and activates AKT at the plasma membrane. AKT dissociates from the plasma membrane and phosphorylates AS160. Phosphorylated AS160 facilitates the translocation of GLUT4 containing vesicles to the plasma membrane, resulting in an increase in glucose transport. Glucose (Glc) transported into the adipocyte is phosphorylated (Glc-6-P) and converted to dihydroxyacetone phosphate (DHAP) via glycolysis and, subsequently, glycerol-3-phosphate (G-3-P). DHAP is converted to acyl-dihydroxyacetone phosphate (Acyl-DHAP) via DHAPAT and, subsequently, to 1-acyl-glycerolphosphate (1-AGP). 1-AGP is also directly produced from G-3-P via GPAT. AGPAT, then, adds a second acyl-CoA to 1-AGP to form phosphatidic acid (PA). PA is dephosphorylated by PAP to form diacylglycerol (DAG) and DGAT esterifies a third acyl-CoA with DAG to create triacylglycerol (TAG). IRS, insulin receptor substrate; AS160, AKT substrate of 160 kDa; DHAPAT, dihydroxyacetone phosphate:acyltransferase; GPAT, glycerolphosphate:acyltransferase; AGPAT, acyl-glycerolphosphate:acyltransferase; PAP, phosphatidic acid phosphatase; DGAT, diacylglycerol:acyltransferase.

2.2 Fatty Acid and Triacylglycerol Biosynthesis

Adipocytes readily convert the products of glycolysis into fatty acids via the de novo biosynthetic pathway. Briefly, surplus citrate is transported from the mitochondrion and cleaved to produce cytosolic acetyl-CoA. This acetyl-CoA is acted upon by acetyl-CoA carboxylase producing malonyl-CoA. The next steps of the fatty acid biosynthetic pathway are carried out by the multifunctional fatty acid synthase that utilizes NADPH to catalyze multiple condensations of malonyl-CoA with acetyl-CoA or the elongating lipid, eventually generating palmitate.

De novo fatty acid synthesis is, in part, negatively regulated by the AMP-activated protein kinase (AMPK). When the adipocyte is in an energy deficit state due to the lack of available glucose or other cellular stresses, ATP levels decrease and AMP levels increase. This causes the AMP:ATP ratio in the adipocyte to increase and thus AMP binds and activates AMPK kinase, LKB. AMP also binds to AMPK, which allows LKB to recognize AMPK as a substrate and results in the phosphorylation and activation of AMPK. Active AMPK phosphorylates acetyl-CoA carboxylase, deactivating it and, hence, decreasing fatty acid synthesis (12).

Triacylglycerol synthesis combines the products of glycolysis, glycerolphosphate and dihydroxyacetone phosphate with acyl-CoAs (Figure 2). In adipocytes, two pathways exist for the production of phosphatidic acid. In one, glycerol-3-phosphate is sequentially esterified with two acyl-CoAs to produce 1-acylglycerolphosphate and 1,2-

diacylglycerolphosphate. In the second pathway, dihydroxyacetone phosphate is esterified with acyl-CoA to produce acyl-dihydroxyacetone phosphate. An acyl-dihydroxyacetone phosphate reductase subsequently produces 1-acylglycerolphosphate that leads to the production of 1,2-diacylglycerolphosphate. The resultant phosphatidic acid is dephosphorylated generating 1,2-diacylglycerol and triacylglycerol is formed through the activity of diacylglycerol acyltransferase (DGAT).

The DGAT catalyzed reaction is crucial for it represents a branch point for hydrocarbon flow towards either the triacylglycerol or phospholipid pathways. However, this view has been modified through the production of DGAT null mice. DGAT deficient mice are viable, are resistant to diet induced obesity, and have reduced triacylglycerol synthesis, though they still have significant amounts of triacylglycerol. This implies that either an alternate triacylglycerol biosynthetic pathway is utilized or additional DGAT isoforms are present in adipose cells. To address this question, Farese and colleagues identified a second DGAT (DGAT2) with kinetic properties distinct from the original DGAT (now termed DGAT1) (13). DGAT2 null mice have lipopenia and skin barrier abnormalities. The DGAT2 null mice also have severely reduced triacylglycerol synthesis and triacylglycerol content in their tissues, suggesting that DGAT2 is responsible for the majority of triacylglycerol biosynthesis (14). Moreover, additional DGAT-like sequences are present in the murine and human genome suggesting an unappreciated complexity in diacylglycerol metabolism.

2.3 Triacylglycerol Mobilization

Lipolysis refers to the process by which triacylglycerol molecules are hydrolyzed to fatty acids and glycerol. During times of metabolic stress (i.e. during fasting or prolonged strenuous exercise when the body's energy needs exceed the circulating nutrient levels), the triacylglycerol droplet within an adipocyte is degraded producing fatty acids to be used as an energy source by other tissues. Numerous stimuli are capable of eliciting the lipolytic response in adipocytes (15). A family of lipases, adipose triglyceride lipase (ATGL), hormone sensitive lipase (HSL) and monoacylglycerol lipase catalyzes the hydrolysis of the triacylglycerol ester bonds producing glycerol and three moles of fatty acids.

The process of triacylglycerol hydrolysis is a complex phenomenon that involves at least three lipases, lipid droplet associated proteins and FABPs, although other adipocyte lipases (i.e. triacylglycerol hydrolase) may play a role in basal lipolysis. The data at this time support the model that three lipases are the major contributors to adipocyte lipolysis. Complete hydrolysis of triacylglycerol involves the hydrolysis of three ester bonds to liberate three fatty acids and a glycerol moiety. ATGL catalyzes hydrolysis of the first ester bond to release one fatty acid and results in diacylglycerol formation (16). HSL can catalyze the hydrolysis of triacylglycerol, but has 10-fold greater activity towards diacylglycerol, hydrolyzing the second ester bond at either the *sn*-1 or *sn*-3 position. A third enzyme, monoacylglycerol lipase, catalyzes hydrolysis of the remaining ester to yield a third fatty acid and glycerol (Figure 1). Since adipocytes do not express glycerol kinase to any great extent (although they might when PPARγ is

activated), they are generally unable to reuse glycerol. Therefore, glycerol is transported out of adipocytes via aquaporin 7 and must be shuttled back to the liver for oxidation or gluconeogenesis. Mono- and diacylglycerols can be re-esterified by the endoplasmic reticulum acyltransferases. During a lipolytic stimulus, re-esterification is minimized so that the net direction of these reactions is toward fatty acid efflux from the cell.

Free fatty acids are minimally soluble in the aqueous cytoplasm. The charged carboxylate group provides enough electrostatic hindrance to prevent association with the neutral triacylglycerols whereas the hydrocarbon tail reduces solubility in water. At sufficiently high concentrations, fatty acids exert a detergent-like effect that would disrupt membranes and/or they could cluster together in micelles in the crowded cytoplasm. To alleviate this problem, the adipocyte and other lipid-metabolizing cell types have evolved intracellular fatty acid binding proteins (FABPs), a family of small, soluble, highly abundant proteins that bind and sequester fatty acids. Adipocytes express two FABPs, the adipocyte and epithelial FABPs. Once outside the adipocyte, fatty acids are immediately bound to serum albumin and carried in the bloodstream to the liver, muscle and other tissues for oxidation.

2.4 Long-chain Fatty Acid Influx

Long-chain fatty acids (LCFAs) presented to adipocytes for internalization are derived from the hydrolysis of triglycerides found in either chylomicrons (whose origin is dietary fat) or very low-density lipoprotein (VLDL, whose origin is excess dietary

carbohydrate and protein). Adipose lipoprotein lipase is tethered on the surface of the capillary endothelial cell and hydrolyzes circulating triglycerides producing LCFA that are bound by albumin. The albumin-LCFA complex traverses the fenestrated capillary epithelial layer delivering dietary lipid to the surface of the adipocyte where the LCFA is taken up by the cell in a complex, ATP-dependent process. While appreciated for decades, the molecular mechanism(s) that control and mediate LCFA uptake into fat cells remain poorly defined from a structural, mechanistic, and regulatory viewpoint.

The mechanism by which LCFAs are taken up by adipocytes has been enveloped in controversy for years and is largely framed within two processes: either diffusion-mediated uptake or protein-mediated uptake (17). The velocity of fatty acid influx across the plasma membrane can be defined by the sum of the two respective terms shown in equation 1.

$$V([LCFA_u]) = k_d[LCFA_u] + (V_{max} \bullet [LCFA_u]) / (K_m + [LCFA_u])$$

$V([LCFA_u])$ is the initial velocity of uptake as a function of unbound $[LCFA_u]$, V_{max} is the maximal velocity, $K_m = [LCFA_u]$ at half-maximal uptake, and k_d is the rate constant for diffusional uptake. In diffusion-mediated fatty acid uptake represented by the first term in the equation, the rate of fatty acid influx across the membrane is proportional to the free fatty acid concentration. The rate constant differs for each LCFA and is dependent in part on the permeability of a ligand through the lipid bilayer. The macroscopic k_d shown in Equation 1 groups together three individual microscopic rate constants which represent the three steps of fatty acid diffusion: association with the outer leaflet of the plasma membrane, flip-flop from outer to inner membrane, and

dissociation from the inner membrane to the aqueous space. Biophysical studies of fatty acid flip-flop, or transversal, across model lipid membranes have revealed that fatty acids are able to transverse from the membrane outer leaflet to the inner leaflet with rate constants inversely proportional to the curvature of the lipid membrane (18,19). Indeed, some studies have demonstrated that fatty acid flip-flop (ff) in small unilamellar vesicles is very fast ($k_{ff} > 100\ s^{-1}$) as compared to fatty acid dissociation rates from the inner membrane leaflet to the aqueous space ($k_d = 12\ s^{-1}$), suggesting that diffusion is sufficient for adequate movement of fatty acids into cells (18). However, contrasting data suggests that the rate of fatty acid flip-flop is slower than dissociation ($k_{ff} = 2\ s^{-1}$), making fatty acid flip-flop rate limiting (18). The latter view implies that the membrane bilayer presents a barrier to fatty acids and additional mechanisms might be involved in facilitating fatty acid influx. While these two views of fatty acid transbilayer movement are debated, the use of classical or molecular genetic approaches have led to identification of protein(s) that facilitate LCFA influx into cells and fueled interest into the biochemistry of fatty acid transport (18,20).

Evidence for a protein component in fatty acid transport has been suggested by studies revealing substantially reduced LCFA import upon treatment of adipocyte membranes with proteases, amino acid modification reagents, and reactive fatty acid analogues. Four major classes of proteins are thought to play a role in protein-mediated fatty acid uptake: 1) plasma membrane fatty acid binding protein (FABPpm), 2) caveolin, 3) fatty acid translocase (FAT/CD36), and 4) fatty acid transport proteins (FATPs).

Mitochondrial aspartate aminotransferase (mAspAT), a critical component of the malate-aspartate shuttle, has been implicated in adipocyte LCFA influx. Using a direct protein chemistry approach involving long-chain acyl group affinity chromatography, a plasma membrane fatty acid binding protein (FABPpm) on the surface of adipocytes, hepatocytes, enterocytes, and cardiomyocytes was identified. Subsequent molecular analysis and protein sequencing identified FABPpm as mAspAT (21). Incubation of 3T3-L1 adipocyte monolayers with anti-FABPpm antibodies selectively inhibited the uptake of oleate but had no effect on uptake of either 2-deoxyglucose or the medium chain fatty acid octanoate. The mRNA levels of FABPpm are up-regulated in adipose tissue isolated from Zucker fatty rats and ob/ob mice (22,23) and recently, Bonen and colleagues demonstrated in myocytes that FABPpm is found within an intracellular endosomal pool that is translocated to the plasma membrane in response to 5-amino-4-imidazolecarboxamide ribonucleoside (AICAR), a cell-permeable activator of AMP-activated protein kinase (AMPK) (24).

Caveolae are specialized flask-shaped plasma membrane invaginations formed by clusters of lipid microdomains in association with the structural proteins caveolin-1, -2, and -3. Adipocyte plasma membranes are rife with numerous caveolae whose functions have been linked to signaling systems, receptor mediated endocytosis, and more recently LCFA influx (25). Inhibition of caveolar function by either depletion of membrane cholesterol using cyclodextrin, overexpression of a dominant negative caveolin-3 mutant (26), or disruption of the caveolae-actin structure by actin-depolymerizing agents all reduced LCFA uptake without decreasing LCFA

esterification. In contrast, loading 3T3-L1 adipocytes with cholesterol increased caveolin-1 expression and LCFA influx. A caveolin-1 null mouse lacking caveolae exhibited reduced adipocyte lipid droplet size, was resistant to diet-induced obesity and had higher post-prandial levels of triglycerides and free fatty acids (27). It is not clear if caveolae *per se* play a role in LCFA influx or simply present a physical structure that facilitates uptake by other proteins such as FAT/CD36.

FAT/CD36 is a 53 kDa integral membrane protein with an apparent molecular mass of 88 kDa due to a high degree of glycosylation. FAT/CD36 belongs to the family of class B scavenger receptors and exhibits broad tissue distribution but is largely expressed in adipocytes, macrophages, heart, and skeletal muscle. FAT/CD36 binds a variety of hydrophobic ligands including oxidized low-density lipoproteins, long-chain fatty acids, thrombospondin, collagens, and sickle erythrocytes. Studies involving both FAT/CD36 null and transgenic mice have suggested that the protein is intimately connected to LCFA uptake in adipocytes and muscle leading to influences on whole body insulin sensitivity (28,29). In 3T3-L1 cells FAT/CD36 is localized to caveolae containing detergent resistant lipid microdomains in the plasma membrane (DRM) as well as detergent soluble intracellular membranes (DSM). The LCFA transport function of FAT/CD36 is regulated by translocation from intracellular DSMs to the plasma membrane DRMs. Disruption of lipid microdomains by cyclodextrin and specific inhibition of FAT/CD36 by sulfo-N-succinimidyl oleate resulted in a 60% decrease in oleate uptake. Based on these observations the authors proposed a model in which caveolin-1 in lipid rafts might target FAT/CD36 to the plasma membrane thus

controlling LCFA uptake by regulating surface availability of FAT/CD36 (30). FAT/CD36 may in turn facilitate LCFA influx via endocytotic mechanisms or alternatively providing a high local LCFA environment producing a concentration gradient across the plasma membrane facilitating uptake by other proteins. Importantly, fatty acid uptake in heart and muscle is inhibited by the FAT/CD36 inhibitor SSO as well as by FABPpm selective antibodies, though not in an additive manner (31,32). Based on this, it has been proposed that FAT/CD36 and FABPpm may cooperate with each other to transport fatty acids across the plasma membrane (33). While FAT/CD36 homologues are found in a variety of higher eukaryotes, no such homologue exists in yeast. As such, FAT/CD36 in higher eukaryotes may be part of a more complex LCFA influx system that may allow the organism to finely control cellular LCFA uptake and maintain energy homeostasis throughout periods of nutrient abundance or depletion.

3 Fatty Acid Transport Proteins

3.1 Expression and Localization

Fatty acid transport proteins (FATPs) are a family of integral membrane proteins with an approximate molecular mass of 71 kDa and are important for the uptake of long-chain and very long-chain fatty acids in adipocytes. Most mammals have six paralogs, identified as FATP1-6, each with unique tissue expression patterns. FATP1 and FATP4 are the predominant forms present in adipocytes. Additionally, FATP4 is expressed in brain, muscle, liver, kidney, skin and heart, however it is the only FATP isoform expressed in the small intestine. FATP1 is also expressed in brain, muscle, and heart (34). Topology mapping of FATP1 (35) as well as hydropathy analysis suggest that

FATPs contain a single transmembrane domain at the N-terminus that may serve as a membrane anchor. Subcellular fractionation and immunochemical analysis of 3T3-L1 and mouse primary adipocytes have revealed FATP1 to be localized primarily to detergent-soluble membranes (30) within the plasma membrane, high density membranes (endoplasmic reticulum, golgi) and to a lesser amount in low density membranes (vesicles, endosomes) (36). FATP4 has also been shown to share a similar broad subcellular distribution (36).

3.2 Transcriptional Regulation

Transcription of the FATP1 is controlled by both peroxisome proliferators-activated receptors (PPARs) and insulin, where as FATP4 is only known to be controlled by PPARs. Ligands and activators of two distinct classes of PPARs, PPARα and PPARγ have been shown to induce transcription of FATP1 in tissue-specific manner. PPARα activation induces FATP1 transcription only in the liver and, as determined more recently, trophoblasts (37). PPARγ activation, on the other hand, induces FATP1 expression in adipose and skeletal muscle and induces FATP4 in trophoblasts (38). In support of these observations, a PPAR response element has been mapped to the FATP1 gene (39). The resultant increase in mRNA levels was found to coincide with the concomitant increase in LCFA uptake observed in adipose and skeletal muscle. The transcriptional regulation of FATP1 by PPAR activators could be reproduced *in vitro* in cell culture systems (40). Activators of retinoid X receptor (RXR), the heterodimeric PPAR nuclear receptor partner were also found to increase FATP1 gene transcription in 3T3-L1 adipocytes (39) and FATP4 transcription in trophoblasts (38). Additional

studies in primary human trophoblasts have demonstrated that p38 MAPK modulates the activity and influence of the PPARγ/RXR heterodimer on fatty acid uptake and expression of FATPs (38). Taken together, these observations indicate that while FATP1 and FATP4 can be regulated by both PPARγ/RXR and PPARα/RXR, only PPARγ/RXR regulates FATP1 and 4 in adipocytes.

In contrast to the activating effects of PPARγ on FATP1 expression, insulin negatively regulates the expression of FATP1 in 3T3-L1 adipocytes. Consistent with insulin being a negative regulator of FATP1 expression, FATP1 mRNA levels are up-regulated in several murine models of insulin resistance. Lipopolysaccharides and cytokines such as TNFα and IL-1 were also shown to down regulate FATP1 mRNA levels in adipocytes (41).

3.3 FATPs and Acyl-CoA Synthetases

In general, FATPs share 20-40% sequence identity with the long-chain acyl-CoA synthetases (ACSLs), enzymes that catalyze the esterification of a long-chain fatty acid (LCFA) with coenzyme A via an ATP-dependent mechanism yielding fatty acyl-CoA, AMP, and pyrophosphate. The sequence identity between ACSLs and FATPs is greatest in two motifs referred to as the ATP-binding motif and the fatty acyl-CoA signature (FACS) motif. This FACS motif has previously been proposed to be the site of fatty acid binding. Gertow et al. (42) carried out homology modeling of FATP4 using the known crystal structure of *Salmonella enterica* acetyl-CoA synthetase as a

template while Wiczer et al (unpublished) modeled FATP1 based on the *Thermus thermophilus* long-chain acyl-CoA synthetase crystal structure (Figure 3). The two FATP models agree with each other, revealing similar structural characteristics, including the location of the ATP-binding motif, the FACS motif, and a β-sheet-like region that Gertow et al. propose to be peripherally associated with the lipid membrane. Purification of mouse FATP1 (43) revealed that the proteins do in fact possess both long-chain and very long-chain acyl-CoA synthetase activity. Based on sucrose gradient sedimentation velocity studies, FATP1 forms homodimers in vivo (44) and in vitro [B. Wiczer, D. Bernlohr, unpublished]. When compared with the enzymatic activity of ACSL1, the major acyl-CoA synthetase in adipose tissue, FATP1 possesses similar very long-chain acyl-CoA synthetase activity but 35-fold lower long-chain acyl-CoA synthetase activity. The biochemical characterization of FATP4 is discussed in Chapter 2.

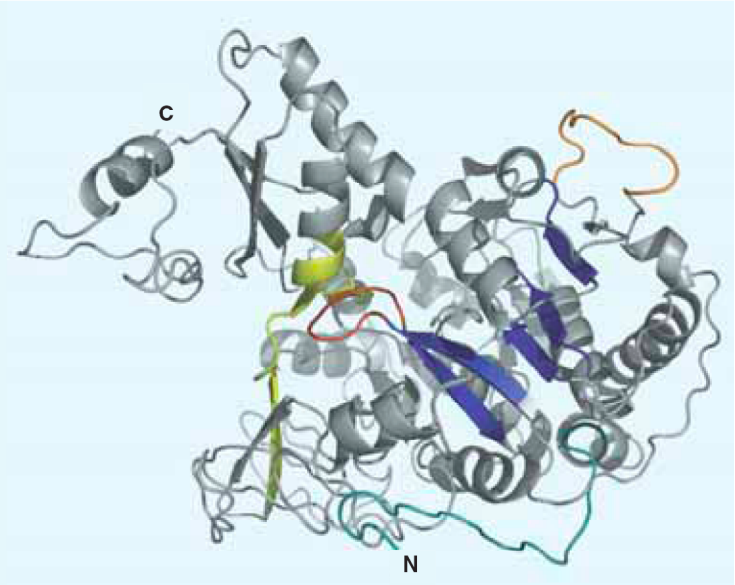

Figure 3. Homology model of FATP1 lacking the 43 N-terminal amino acids, which are predicted to comprise the transmembrane domain. FATP1 model based on the known crystal structure of the long-chain acyl-CoA synthetase from *Thermus thermophilus* as a template, and modeled using SWISS-MODEL. *Red*, ATP-binding motif; *yellow*, fatty acyl-CoA signature (FACS) motif; *blue*, β-sheet-like region; *orange*, flexible loop region.

The acyl-CoA synthetase activity of FATPs is essential for its fatty acid transport activity. Richards et al. found that NIH 3T3 cells expressing a catalytically inactive FATP1-S250A mutant showed a 5-fold decrease in LCFA uptake as compared to cells expressing wild-type FATP1 (44). This suggests that LCFA uptake is mechanistically coupled to the acyl-CoA synthetase activity of the transporter in a process termed vectoral acylation. Indeed, in *E. coli* LCFA influx is driven by the bacterial peripheral membrane associated acyl-CoA synthetase, FadD (45). This paradigm, LCFA influx coupled to CoA dependent esterification, does not address the mechanisms involved in the lipid traversal across the membrane. Diffusion could be implied as the mechanism controlling LCFA bilayer movement, with the acyl-CoA synthetase activity of FATP

facilitating bilayer movement by driving a flux of LCFAs across the membrane, trapping the lipid intracellularly via CoA dependent esterification. Zou et al (46) have suggested based on mutagenesis analysis of the yeast FATP homologue, Fat1p, that activation of transport and LCFA esterification are separable functions. However, while the mutations are broadly dispersed within the amino acid sequence, molecular modeling (Figure 3) predicts that they all cluster to the physical region surrounding either the ATP binding or LCFA binding region implying some indirect effects on catalysis. The ability of certain mammalian FATP forms to complement the yeast *Fat1* disruption provides a facile system for future structure-function relationships.

In 3T3-L1 adipocytes FATP1 is found to co-localize with fatty acyl-CoA synthetase (ACSL1) (47) (also found in the same molecular genetic screen that identified FATP1) as a protein involved in fatty acid uptake. ACSL1 is a 75 kDa protein that is peripherally associated with the plasma membrane. Evidence for a functional interaction between the yeast fatty acyl-CoA synthetase (Faa1p, Faa4p) and fatty acid transport protein (Fat1p) was provided by yeast two-hybrid assay and co-immunoprecipitation studies. This discovery suggests that FATP1 and ACSL1 may form a broad substrate range complex within adipocytes, coupling fatty acid uptake and esterification to augment LCFA uptake at the plasma membrane. Currently however there is no biochemical data from mammalian systems to physically link FATP1 and ACSL1 although Schaffer and colleagues have shown that co-expression of FATP1 and ACSL1 in NIH-3T3 cells results in increased LCFA influx above the activity of either protein alone (47). Increase in LCFA uptake observed in overexpression studies of

ACSL5 in rat hepatoma McArdle-RH7777 cells (48) as well as *in vitro* reconstitution studies of purified ACSL1 into large unilamellar vesicles implies that acyl-CoA synthetase activity drives LCFA import by activating and increasing the flux of LCFA across the membrane.

3.4 Loss- and Gain-of-function Models

The role of FATP1 and FATP4 in fatty acid uptake has been documented by a variety of loss of function/gain of function model systems using cultured cells and transgenic animals. Hatch et al. demonstrated that LCFAs taken up into HEK 293 cells in a FATP1-dependent manner are channeled into triglyceride biosynthesis (49) and is consistent with the model that triglyceride synthesis occurs at the plasma membrane in adipocytes (50). A transgenic mouse (Tg) model with cardiac-specific expression of FATP1 demonstrated a 2-fold increase in myocardial LCFA uptake (51). Interestingly, the Tg mouse exhibited a 50% decrease in glucose uptake and metabolism. Hence, overexpression of FATP1 in the heart tends to shift the metabolic fuel preference to LCFAs. As opposed to the results observed with overexpression of FATP1 in 293 cells, cardiac expression of FATP1 did not lead to any difference in complex lipid synthesis such as TAG, cholesterol esters, sphingomyelin, and phospholipids with the exception of a 50% decrease in phosphatidylglycerol. The Tg mice had impaired diastolic function consistent with impaired cardiac myocyte function, which could be attributed to FFA accumulation as well as the changes in substrate utilization. In contrast to the FATP1 transgenic model, mice harboring at total ablation of FATP1 maintain insulin sensitivity on a high-fat diet and decreased intramuscular fatty acid and fatty acid

metabolites (LCFA, fatty acyl-CoA, DAG, TAG, ceramides) (52). The observed effects of FATP1 KO and cardiac-specific FATP1 Tg mouse on glucose uptake provides compelling models for evaluation of the cellular mechanisms regulating substrate utilization and their connectivity to fat-induced insulin resistance in the pathophysiology of type 2 diabetes. The FATP1 KO mouse model, however, does not address what tissues are contributing to the observed phenotype.

When over expressed in HEK 293 cells, FATP4 was shown to enhance fatty acid uptake (53,54), whereas incubation of isolated enterocytes with *FATP4*-targeted anti-sense nucleotides led to a 50% decrease in oleate and palmitate uptake (53). The role of FATP4 in adipocytes has been difficult to evaluate for deletion of FATP4 results in early embryonic lethality (54) or death shortly after birth (55). In those animals that die shortly after birth, *Fatp4*-/- mice displayed features of neonatal lethal restrictive dermopathy, suggesting a critical function of FATP4 is in the formation of a functional epidermal barrier. The role of FATP4 in fatty acid metabolism and the etiology of insulin resistance have been linked via the identification of a Gly209Ser polymorphism in the FATP4 gene in healthy middle-aged Swedish men. Heterozygotes with the rare Ser209 polymorphism had significantly low body mass index, lower triacylglycerol and insulin concentration, systolic blood pressure and homeostasis model assessment index, factors implying higher insulin sensitivity compared to the common homozygous Gly209 counterparts (42). The Gly209Ser polymorphism is modeled to be located on a surface-accessible loop based on the FATP model (Figure 3). Gertow et al. have suggested that the nature and location of this loop resembles a region that would be

involved in protein-protein interactions and exchange of the glycine with the hydrogen bonding serine could prevent such interactions.

4 Concluding Remarks

Because adipose is one of the most robust tissues in terms of LCFA metabolism and generation of lipid-derived signaling molecules, understanding the mechanisms underlying adipocyte LCFA influx and storage is vital for the development of therapies for metabolic syndrome. FATP1 and FATP4 have been implicated in cellular LCFA influx and storage using a number of overexpression models; however, their physiological functions in adipocytes have remained elusive. Subsequent chapters characterize the biochemical properties of FATP4 (Chapter 2) and investigate the functional roles of FATP1 (Chapter 3, 4, and 5) and FATP4 in adipocytes (Chapter 3). These studies reveal novel insights into the roles of FATPs and challenge the paradigm that FATP family members function solely in cellular LCFA flux.

5 References

1. Schmidt, M. I., Watson, R. L., Duncan, B. B., Metcalf, P., Brancati, F. L., Sharrett, A. R., Davis, C. E., and Heiss, G. (1996) *Metabolism* **45**, 699-706
2. Morrow, J. D., and Roberts, L. J. (1997) *Prog Lipid Res* **36**, 1-21
3. Kunkel, S. L., Spengler, M., May, M. A., Spengler, R., Larrick, J., and Remick, D. (1988) *J Biol Chem* **263**, 5380-5384
4. Tobias, L. D., and Hamilton, J. G. (1979) *Lipids* **14**, 181-193
5. Maroon, J. C., and Bost, J. W. (2006) *Surg Neurol* **65**, 326-331
6. Liang, X., Wang, Q., Shi, J., Lokteva, L., Breyer, R. M., Montine, T. J., and Andreasson, K. (2008) *Ann Neurol* **64**, 304-314
7. Linton, M. F., and Fazio, S. (2003) *Int J Obes Relat Metab Disord* **27 Suppl 3**, S35-40
8. Rajala, M. W., and Scherer, P. E. (2003) *Endocrinology* **144**, 3765-3773

9. Sauer, S. W., Okun, J. G., Hoffmann, G. F., Koelker, S., and Morath, M. A. (2008) *Biochim Biophys Acta* **1777**, 1276-1282
10. Marshall, S. (2006) *Sci STKE* **2006**, re7
11. Cohen, P. (2006) *Nat Rev Mol Cell Biol* **7**, 867-873
12. Hardie, D. G., Hawley, S. A., and Scott, J. W. (2006) *J Physiol* **574**, 7-15
13. Cases, S., Stone, S. J., Zhou, P., Yen, E., Tow, B., Lardizabal, K. D., Voelker, T., and Farese, R. V., Jr. (2001) *J Biol Chem* **276**, 38870-38876
14. Stone, S. J., Myers, H. M., Watkins, S. M., Brown, B. E., Feingold, K. R., Elias, P. M., and Farese, R. V., Jr. (2004) *J Biol Chem* **279**, 11767-11776
15. Carmen, G. Y., and Victor, S. M. (2006) *Cell Signal* **18**, 401-408
16. Zimmermann, R., Strauss, J. G., Haemmerle, G., Schoiswohl, G., Birner-Gruenberger, R., Riederer, M., Lass, A., Neuberger, G., Eisenhaber, F., Hermetter, A., and Zechner, R. (2004) *Science* **306**, 1383-1386
17. Berk, P. D., and Stump, D. D. (1999) *Mol Cell Biochem* **192**, 17-31
18. Cupp, D., Kampf, J. P., and Kleinfeld, A. M. (2004) *Biochemistry* **43**, 4473-4481
19. Brunaldi, K., Miranda, M. A., Abdulkader, F., Curi, R., and Procopio, J. (2005) *J Lipid Res* **46**, 245-251
20. Hamilton, J. A. (2003) *Curr Opin Lipidol* **14**, 263-271
21. Cechetto, J. D., Sadacharan, S. K., Berk, P. D., and Gupta, R. S. (2002) *Histol Histopathol* **17**, 353-364
22. Berk, P. D., Zhou, S. L., Kiang, C. L., Stump, D., Bradbury, M., and Isola, L. M. (1997) *J Biol Chem* **272**, 8830-8835
23. Memon, R. A., Fuller, J., Moser, A. H., Smith, P. J., Grunfeld, C., and Feingold, K. R. (1999) *Diabetes* **48**, 121-127
24. Chabowski, A., Coort, S. L., Calles-Escandon, J., Tandon, N. N., Glatz, J. F., Luiken, J. J., and Bonen, A. (2005) *FEBS Lett* **579**, 2428-2432
25. Pohl, J., Ring, A., Ehehalt, R., Herrmann, T., and Stremmel, W. (2004) *Proc Nutr Soc* **63**, 259-262
26. Pol, A., Martin, S., Fernandez, M. A., Ferguson, C., Carozzi, A., Luetterforst, R., Enrich, C., and Parton, R. G. (2004) *Mol Biol Cell* **15**, 99-110
27. Razani, B., Combs, T. P., Wang, X. B., Frank, P. G., Park, D. S., Russell, R. G., Li, M., Tang, B., Jelicks, L. A., Scherer, P. E., and Lisanti, M. P. (2002) *J Biol Chem* **277**, 8635-8647
28. Febbraio, M., Guy, E., Coburn, C., Knapp, F. F., Jr., Beets, A. L., Abumrad, N. A., and Silverstein, R. L. (2002) *Mol Cell Biochem* **239**, 193-197
29. Heron-Milhavet, L., Haluzik, M., Yakar, S., Gavrilova, O., Pack, S., Jou, W. C., Ibrahimi, A., Kim, H., Hunt, D., Yau, D., Asghar, Z., Joseph, J., Wheeler, M. B., Abumrad, N. A., and LeRoith, D. (2004) *Endocrinology* **145**, 4667-4676
30. Pohl, J., Ring, A., Korkmaz, U., Ehehalt, R., and Stremmel, W. (2005) *Mol Biol Cell* **16**, 24-31
31. Luiken, J. J., Turcotte, L. P., and Bonen, A. (1999) *J Lipid Res* **40**, 1007-1016
32. Turcotte, L. P., Swenberger, J. R., Tucker, M. Z., Yee, A. J., Trump, G., Luiken, J. J., and Bonen, A. (2000) *Mol Cell Biochem* **210**, 53-63

33. Glatz, J. F., Luiken, J. J., and Bonen, A. (2001) *J Mol Neurosci* **16**, 123-132; discussion 151-127
34. Watkins, P. A. (2008) *J Biol Chem* **283**, 1773-1777
35. Lewis, S. E., Listenberger, L. L., Ory, D. S., and Schaffer, J. E. (2001) *J Biol Chem* **276**, 37042-37050
36. Stahl, A., Evans, J. G., Pattel, S., Hirsch, D., and Lodish, H. F. (2002) *Dev Cell* **2**, 477-488
37. Xu, Y., Cook, T. J., and Knipp, G. T. (2005) *Toxicol Sci* **84**, 287-300
38. Schaiff, W. T., Bildirici, I., Cheong, M., Chern, P. L., Nelson, D. M., and Sadovsky, Y. (2005) *J Clin Endocrinol Metab* **90**, 4267-4275
39. Frohnert, B. I., Hui, T. Y., and Bernlohr, D. A. (1999) *J Biol Chem* **274**, 3970-3977
40. Martin, G., Poirier, H., Hennuyer, N., Crombie, D., Fruchart, J. C., Heyman, R. A., Besnard, P., and Auwerx, J. (2000) *J Biol Chem* **275**, 12612-12618
41. Memon, R. A., Feingold, K. R., Moser, A. H., Fuller, J., and Grunfeld, C. (1998) *Am J Physiol* **274**, E210-217
42. Gertow, K., Bellanda, M., Eriksson, P., Boquist, S., Hamsten, A., Sunnerhagen, M., and Fisher, R. M. (2004) *J Clin Endocrinol Metab* **89**, 392-399
43. Hall, A. M., Smith, A. J., and Bernlohr, D. A. (2003) *J Biol Chem* **278**, 43008-43013
44. Richards, M. R., Listenberger, L. L., Kelly, A. A., Lewis, S. E., Ory, D. S., and Schaffer, J. E. (2003) *J Biol Chem* **278**, 10477-10483
45. Weimar, J. D., DiRusso, C. C., Delio, R., and Black, P. N. (2002) *J Biol Chem* **277**, 29369-29376
46. Zou, Z., DiRusso, C. C., Ctrnacta, V., and Black, P. N. (2002) *J Biol Chem* **277**, 31062-31071
47. Gargiulo, C. E., Stuhlsatz-Krouper, S. M., and Schaffer, J. E. (1999) *J Lipid Res* **40**, 881-892
48. Mashek, D. G., McKenzie, M. A., Van Horn, C. G., and Coleman, R. A. (2005) *J Biol Chem*
49. Hatch, G. M., Smith, A. J., Xu, F. Y., Hall, A. M., and Bernlohr, D. A. (2002) *J Lipid Res* **43**, 1380-1389
50. Ost, A., Ortegren, U., Gustavsson, J., Nystrom, F. H., and Stralfors, P. (2005) *J Biol Chem* **280**, 5-8
51. Chiu, H. C., Kovacs, A., Blanton, R. M., Han, X., Courtois, M., Weinheimer, C. J., Yamada, K. A., Brunet, S., Xu, H., Nerbonne, J. M., Welch, M. J., Fettig, N. M., Sharp, T. L., Sambandam, N., Olson, K. M., Ory, D. S., and Schaffer, J. E. (2005) *Circ Res* **96**, 225-233
52. Kim, J. K., Gimeno, R. E., Higashimori, T., Kim, H. J., Choi, H., Punreddy, S., Mozell, R. L., Tan, G., Stricker-Krongrad, A., Hirsch, D. J., Fillmore, J. J., Liu, Z. X., Dong, J., Cline, G., Stahl, A., Lodish, H. F., and Shulman, G. I. (2004) *J Clin Invest* **113**, 756-763
53. Stahl, A., Hirsch, D. J., Gimeno, R. E., Punreddy, S., Ge, P., Watson, N., Patel, S., Kotler, M., Raimondi, A., Tartaglia, L. A., and Lodish, H. F. (1999) *Mol Cell* **4**, 299-308

54. Gimeno, R. E., Hirsch, D. J., Punreddy, S., Sun, Y., Ortegon, A. M., Wu, H., Daniels, T., Stricker-Krongrad, A., Lodish, H. F., and Stahl, A. (2003) *J Biol Chem* **278**, 49512-49516
55. Moulson, C. L., Martin, D. R., Lugus, J. J., Schaffer, J. E., Lind, A. C., and Miner, J. H. (2003) *Proc Natl Acad Sci U S A* **100**, 5274-5279

CHAPTER 2:

ENZYMATIC PROPERTIES OF PURIFIED MURINE FATTY ACID TRANSPORT PROTEIN 4 AND ANALYSIS OF ACYL-COA SYNTHETASE ACTIVITIES IN TISSUES FROM FATP4 NULL MICE

This chapter is a reprint of a published manuscript of the same title with minor alterations. Hall, A. M., **Wiczer, B. M.**, Herrmann, T., Stremmel, W., and Bernlohr, D. A. (2005) *J. Biol. Chem.* **280**, 11948-11954.

Brian Wiczer's contribution to this chapter was Figure 1, 2, 5, and 6A, and preparation of the text and discussion.

SUMMARY

Fatty acid transport protein 4 (FATP4) is an integral membrane protein expressed in the plasma and internal membranes of the small intestine and adipocyte as well as the brain, kidney, liver, skin, and heart. FATP4 has been hypothesized to be bifunctional, exhibiting both fatty acid transport and acyl-CoA synthetase activities that work in concert to mediate fatty acid influx across biological membranes. To determine if FATP4 is an acyl-CoA synthetase, the murine protein was engineered to contain a C-terminus flag epitope tag, expressed in COS1 cells via adenoviral-mediated infection and purified to near homogeneity using α-FLAG affinity chromatography. Kinetic analysis of the enzyme was carried out for long-chain (palmitic acid, C16:0) and very long-chain (lignoceric acid, C24:0) fatty acids as well as for ATP, and CoA. FATP4 exhibited substrate specificity for C16:0 and C24:0 fatty acids with a V_{max}/K_m (C16:0) / V_{max}/K_m (C24:0) of 1.5. Like purified FATP1, FATP4 was insensitive to inhibition by triacsin C but was sensitive to feedback inhibition by acyl-CoA. Although purified FATP4 exhibited high levels of palmitoyl-CoA and lignoceroyl-CoA synthetase activity, extracts from the skin and intestine from FATP4 null mice exhibit reduced esterification for C24:0, but not C16:0 or C18:1 suggesting that in vivo, defects in very long-chain fatty acid uptake may underlie the skin disorder phenotype of null mice.

INTRODUCTION

Studies in multiple tissue types, including cardiomyocytes and adipocytes (1), support the hypothesis that fatty acid transport occurs by a saturable, protein-mediated mechanism and several candidate proteins responsible for FA uptake have been identified. These include the fatty acid binding protein from the plasma membrane ($FABP_{PM}$), the fatty acid translocase (FAT / CD36), as well as the fatty acid transport protein family of molecules (FATP) reviewed in (2). In mammalian cells, FATP isoforms 1-6 have been identified based on sequence similarity and have distinct tissue-specific distributions of expression (3). When expressed into cultured cells, FATP1 increases fatty acid import and stimulates triacylglycerol synthesis (4). Genetic and biochemical analyses have shown that the FATP homologue in yeast (Fat1p) is required for fatty acid uptake (5) in cells with compromised *de novo* fatty acid biosynthesis.

Previous work from this laboratory has demonstrated that purified FATP1 possesses intrinsic acyl-CoA synthetase activity directed to both long and very long-chain fatty acids (6). Watkins and colleagues have also shown that FATP3 is also an acyl-CoA synthetase but that the protein does not facilitate fatty acid internalization into cultured cells (7). These results suggested that the acyl-CoA synthetase and transport functions of FATPs might be separable functions. Indeed, Black and DiRusso have identified yeast *FAT1* mutants that are deficient in either transport, or acyl-CoA synthetase activity, or both (8). However, the S250A mutant of murine FATP1 as well as multiple yeast *FAT1* mutants lacking acyl-CoA synthetase activity exhibit greatly diminished FA influx supporting the hypothesis that that fatty acid uptake into cells is linked, at least in

part, to their esterification with coenzyme A in a process termed vectoral acylation (9,10).

The importance of FATP4 in fatty acid utilization has been illustrated through the use of ablated mice that display extreme phenotypes linked to skin biology. FATP4 loss of function due to either a spontaneous transposon insertion in exon 3, or targeted disruption of exon 3, results in mice with a phenotype reminiscent of restrictive dermopathy (11,12). These animals die shortly after birth and have tight, wrinkle-free skin and disrupted skin barrier function. There may be additional phenotypes linked to fat absorption in the intestine (13), but these have not been examined in detail. Moreover, polymorphisms in the human FATP4 locus have been linked to the development of insulin resistance suggesting that this protein may be a major contributor to lipid uptake in the adipocyte as well (14,15).

The objective of the study was to determine if FATP4 is an acyl-CoA synthetase, to assess the substrate specificity and intrinsic catalytic efficacy of the purified protein, and to compare those properties to FATP1 in order to determine if fatty acid transport proteins have similar or discretely definable catalytic properties. To that end, murine FATP4 was engineered to contain a C-terminus flag epitope tag, expressed in COS1 cells, and purified to near homogeneity by affinity chromatography. Herein we present data characterizing FATP4 as a high velocity enzyme with specificity for long and very long-chain fatty acids as well as the acyl-CoA synthetase activity of tissues from wild

type and FATP4 ablated mice suggesting that *in vivo*, the transport or acyl-CoA synthetase activity for very long-chain fatty acids is critical for FATP4 function.

EXPERIMENTAL PROCEDURES

Reagents—[^{3}H] palmitic acid and [^{3}H]-lignoceric acid were obtained from American Radiochemicals Company. All non-labeled fatty acid was obtained from NuChek Prep, Inc., Elysian, MN. Triacsin C was obtained from BIOMOL. Cell culture reagents were obtained from GIBCO. All other reagents were of analytical grade and obtained from Sigma Chemical Co., St. Louis, MO. Dr. Paul Watkins, Kennedy Krieger Institute, kindly provided Baltimore, MD the anti-FATP4 antibody.

Generation of FATP4 Recombinant Adenovirus and Expression in COS1 cells—A recombinant adenovirus expressing both the green fluorescent protein and murine FATP4 was constructed by recombination in Escherichia coli using the methods described by He and colleagues (16). The resulting construct was recombined into pADEasy in E. coli BJ5183 cells recreating the replication-deficient adenovirus genome. Linear constructs of the recombinant adenovirus were transfected (LipofectAMINE; GIBCO-BRL, Gaithersburg, MD) into 293 cells (American Type Culture Collection, Manassas, VA) to allow packaging and amplification of the adenovirus. Large-scale adenovirus preparations from twenty 10-cm plates of infected cells were propagated until approximately 50% of the cells lysed. The cells and media were collected and the remaining cells lysed by three freeze/thaw cycles. The medium

was centrifuged at 20,000 x g for 10 min to pellet the cellular debris and the supernatant containing virus particles was recovered and frozen in aliquots at –70° C.

For protein expression, COS1 cells were plated in 10-cm plates and grown to approximately 80% confluence at 37° C in a 5 % CO_2 incubator. For infection, the effective concentration of infectious adenoviral particles was experimentally determined by monitoring green fluorescent protein expression and COS1 cell viability seventy-two hours post infection. Adenovirus particles that yielded ~90-100 % infection were delivered in 8 mL of DMEM supplemented with 10 % FBS per plate. Seventy-two hours post-transfection, cells were harvested by centrifugation, immediately frozen and stored at -70° C.

Affinity Purification of Recombinant FATP4 Protein—COS1 cells expressing FATP4-flag were thawed in buffer A (150 mM Tris-HCL, pH 7.5, 250 mM sucrose, and 150 mM NaCl), subjected to five freeze/thaw cycles, and solubilized with 1% n-dodecyl-β-D-matlopyranoside (DDM) for four hours at 4° C. The soluble fraction was separated from debris by centrifugation at 100,000 x g for 1 hour at 4° C, recovered, and glycerol was added to a final concentration of 20%. For purification of recombinant FATP4-flag, α-FLAG matrix beads (Sigma) equilibrated with buffer A was incubated with the protein extract for 6 hours, washed, and eluted with flag peptide in Buffer A containing 0.1% DDM. Eluates were pooled, aliquoted, and stored at -70° C until use. To determine the amount of purified protein, samples were precipitated (17) and protein

concentration determined by the bicinchoninic acid method (Pierce) with bovine serum albumin as the standard.

Fatty acyl-CoA synthetase assays—Samples were assayed for acyl-CoA synthetase activity by the conversion of [^{3}H]-palmitate or [^{3}H]-lignocerate to their CoA derivatives by a modified method from Nagamatsu et al. (18) as described by Hall et al (6). All kinetic studies reported used 0.5-2 μg of purified FATP4 for 2 min at pH 7.5 and 30 mM NaCl in 250 μL of a buffer containing 20 μM fatty acid delivered bound to α-cyclodextrin, 100 mM Tris-HCl (pH 7.5), 10 mM ATP, 5 mM $MgCl_2$, 200 μM CoA, and 200 μM dithiothreitol. Addition of enzyme purified in the presence of 0.1% DDM resulted in a final concentration of 0.02% DDM in all standard assays. Reactions were terminated with the addition of 1.25 mL of isopropenol:heptane:H_2SO_4 (40:10:1, v/v/v), 0.5 mL of H_20 and 0.75 mL of heptane to facilitate organic phase separation. The aqueous phase was extracted three times with 0.75 mL of heptane to remove unreacted fatty acids and the radioactivity determined by liquid phase scintillation counting. The enzyme activity was stable in the elution buffer and activity was retained for 2 months without significant loss of activity when stored at -70° C.

Stability of purified FATP4 in DDM-detergent micelles— Purified FATP4 was thawed on ice and then maintained at either 4 °C or 37 °C for various lengths of time and then assayed for acyl-CoA synthetase activity at 37 °C with [^{3}H]-lignoceric acid. The zero time point represents assayed activity immediately after thawing.

Competition studies— Due to the unavailability of commercially radiolabeled fatty acids, the fatty acid substrate specificity of the purified FATP4 was indirectly determined by a competitive enzymatic inhibition by the addition of unlabelled fatty acids at a constant concentration of 15 μM in the reaction in addition to either [^{3}H] palmitic acid or [^{3}H]-lignoceric acid. A selectivity series for fatty preference was generated by determining the fraction of acyl-CoA synthetase activity at 1/2 $[S]_{max}$.

Acyl-CoA synthetase activity in murine tissues—Tissues from FATP4 null mice (11) (intestine, liver, lung, brain, and skin) were excised from killed newborn mice, weighed, washed in cold phosphate-buffered saline, and snap-frozen in liquid nitrogen. The tissues were ground to a fine homogenate in a glass homogenizer in a total volume of 800 μL phosphate-buffered saline containing 1 % protease inhibitor cocktail P 8340 (Sigma). Protein concentrations were determined by Bradford assay. All mouse procedures were in compliance with the guidelines of the institutional animal care and use committees and in accordance with governmental guidelines.

RESULTS

Previous studies in crude extracts from cells over expressing FATP4 have suggested that the protein is an acyl-CoA synthetase (19). To determine if FATP4 exhibits intrinsic fatty acid CoA synthetase activity and to kinetically assess the properties of such a reaction, murine FATP4 was purified and studied. To facilitate purification, FATP4 was C-terminal tagged with a flag epitope and over expressed in COS1 cells by a recombinant adenoviral infection method. To obtain FATP4 protein in a highly

purified form that retains biological activity, membranes were extracted with a variety of different detergents and solubilized protein and acyl-CoA synthetase activity compared. Figure 1A shows the immunoblotting analysis of the membranes extracted with different detergents. Extraction of membranes with 1% DDM solubilized FATP4 from COS1 to the greatest extent in comparison to the other detergents tested. The degree of FATP4 solubilization obtained for each detergent was generally proportional to the acyl-CoA synthetase activity (Figure 1B) with the exception of $C_{12}E_8$. While the extractable activity obtained with $C_{12}E_8$ was high, the amount of enzyme obtained was relatively low; as such, DDM was chosen for further analyses.

The purification involved detergent extraction of FATP4 from the membrane with 1% DDM and chromatography through α-FLAG-agarose resin. Figure 1C presents the SDS-PAGE analysis of pooled elution fractions collected during a typical FATP4 purification, along with the corresponding immunoblotting analysis with α-FATP4 antibody. The purified FATP4 migrated as a single band on a 7% SDS-polyacrylamide gel and was judged to be at least ~80% pure by silver staining. The level of murine FATP4 enrichment obtained from the α-FLAG column purification was ~2000-fold as assessed by comparison of the specific activity of the crude cell fraction to the eluted fraction (Table 1).

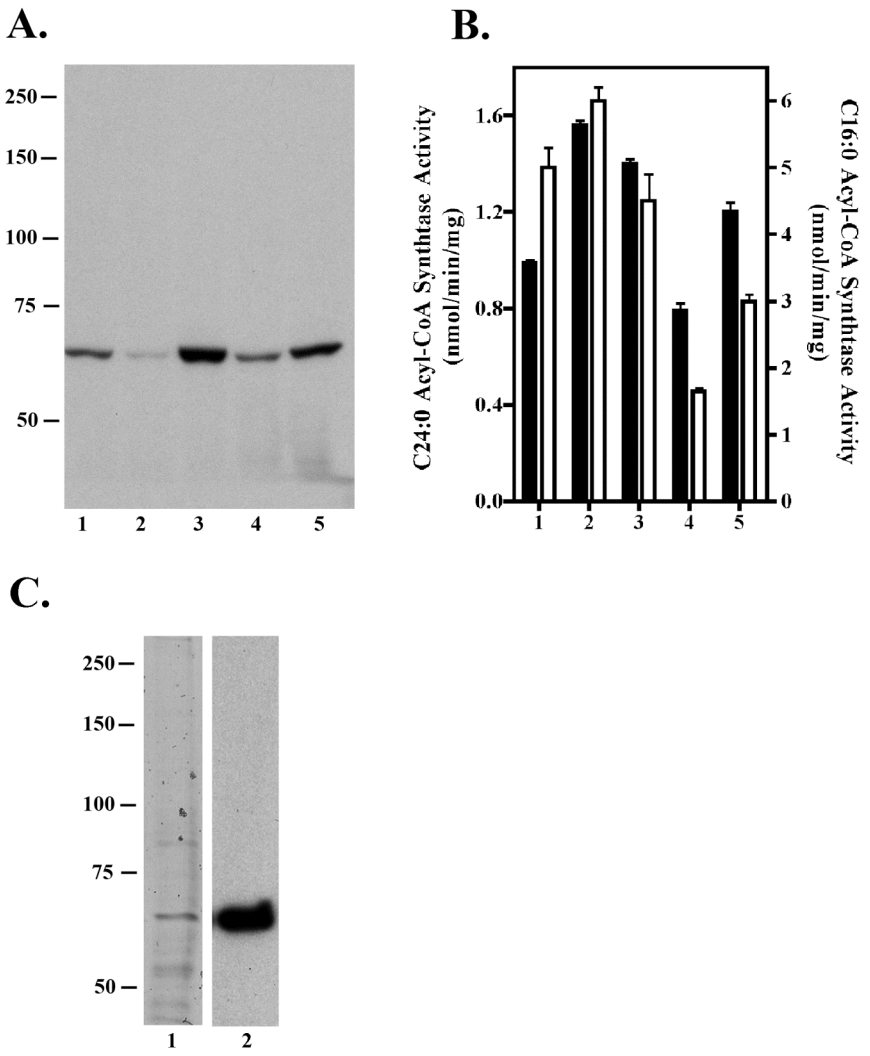

Figure 1. Immunoblot analysis of detergent soluble extracts of FATP4 from COS1 cells and SDS-PAGE analysis of purified FATP4. FATP4-Flag plasmid was transfected into COS1 cells and 72 h post-transfection, cells were harvested by centrifugation and extracts prepared in buffer A (150 mM Tris-HCL, pH 7.5, 250 mM sucrose, and 150 mM NaCl) containing either 1% Triton X-100, 2% octaethylene glycol monododecyl ether ($C_{12}E_8$), 1% n-dodecyl-β-D-matlopyranoside (DDM), 2% n-octyl-β-D-glucopyranoside (OG), or 1% 1,2-diheptanoylphosphatidylcholine (DHPC). Panel A, equal volumes of extracts were separated on a 7% SDS-polyacrylamide gel and analyzed for the presence of FATP4 immunochemically using α-FATP4 antibodies. Detection was accomplished using HRP-conjugated goat anti-rabbit IgG secondary antibody and enhanced chemiluminescence. Lane 1, 1% Triton X-100; lane 2, 2% $C_{12}E_8$; lane 3, 1% DDM; lane 4, 2% OG; lane 5, 1% DHPC. Numbers on y-axis represent molecular mass markers in kDa. Panel B, the FATP4 soluble crude extracts were assayed for C24:0 (■) and C16:0 ( ) acyl-CoA synthetase activity. Numbers on x-axes correspond to western blot lanes. The values are expressed as the mean ± standard deviation. Data presented is from a representative experiment of three independent determinations. Panel C, silver stain (lane 1) and immunodetection with α-FATP4 antibody (lane 2) of pooled elution fractions from an FATP4 purification. Numbers on y-axes represent molecular mass markers in kDa.

Table 1.
FATP4 purification profile

Recombinant FATP4 was expressed and purified as described under "Experimental Procedures". Fractions were taken at various steps throughout the purification and assayed for lignoceroyl-CoA synthetase activity as described under "Experimental Procedures". Values are reported as the mean ± standard deviation.

Step	Volume (mL)	Protein (mg/mL)	Sp. Act. nmol/min/mg	Fold purification
Crude extract	3.75	15.8	0.34 ± 0.01	1
Detergent soluble	3.75	10.3	0.6 ± 0.1	1.8
α-Flag elution	5.0	0.005	723 ± 68	2125

Previous studies on FATP1 have demonstrated that Triton X-100 has an inhibitory effect on its acyl-CoA synthetase activity (6), presumably due to sequestration of the substrates into detergent micelles. To determine whether FATP4 acyl-CoA synthetase activity was sensitive to DDM, purified enzyme was assayed with increasing concentrations detergent. FATP4 acyl-CoA synthetase activity was sensitive to DDM in the reaction buffer, with both C16:0 and C24:0 acyl-CoA synthetase activity decreasing with increasing DDM concentration (Figure 2A). The activity of FATP4 was found to be relatively insensitive to DDM below 0.03% DDM; as such, a final concentration of 0.02% DDM was adopted for all assays. To test the stability of purified FATP4 in DDM-detergent micelles, purified FATP4 was thawed on ice and maintained at either 4° C or 37° C for various times and then assayed for acyl-CoA synthetase activity (Figure 2B). Purified FATP4 in DDM micelles retained activity at 4° C for up to one hour but lost activity quickly when maintained at 37° C.

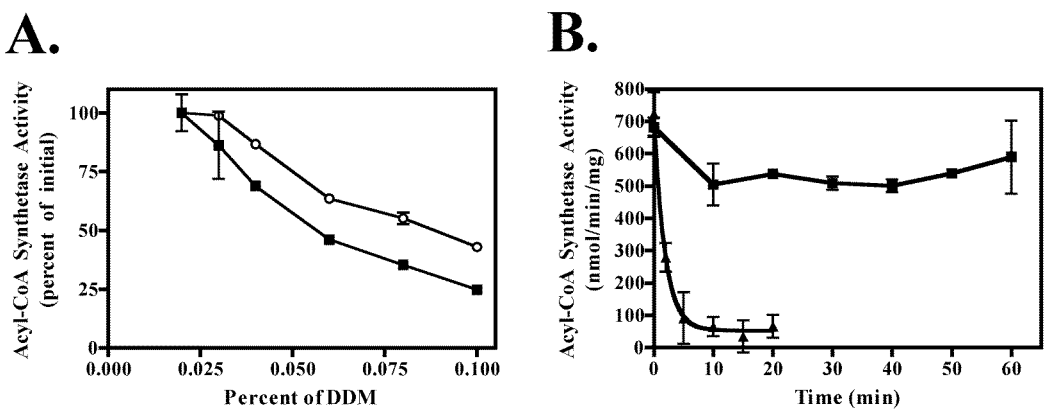

Figure 2. FATP4 sensitivity and stability in DDM. Panel A, purified FATP4 was assayed for acyl-CoA synthetase activity with C16:0 (○) or C24:0 (■) in the presence of increasing concentrations of DDM. Initial acyl-CoA synthetase activity is defined as the activity in the presence of 0.02% DDM. Initial C24:0 activity was 194 nmol/min/mg and initial C16:0 activity was 410 nmol/min/mg. Panel B, stability of FATP4 at 4° C (■) and 37° C (▲) was determined by assaying acyl-CoA synthetase activity with C24:0 at various time points. The values are expressed as the mean ± standard deviation. Data presented is from a representative experiment of three independent determinations.

The FATP4 acyl-CoA synthetase activity was optimized with respect to several standard reaction parameters for both long-chain (C16:0) and very long-chain (C24:0) fatty acids. As shown in Figure 3, the activity was proportional to the amount of enzyme added to the reaction (3A) as well as time of reaction (3B). In addition, the pH sensitivity of the reaction was evaluated (3C), as was the influence of ionic strength (3D). The purified FATP4 has broad pH dependence with 7.0–8.5 being generally optimal and enzymatic activity was sensitive to the NaCl concentration when varied from 30 mM to 500 mM. Synthetase activity was modestly activated at lower ionic strength and then was inhibited at salt concentration in excess of 300 mM.

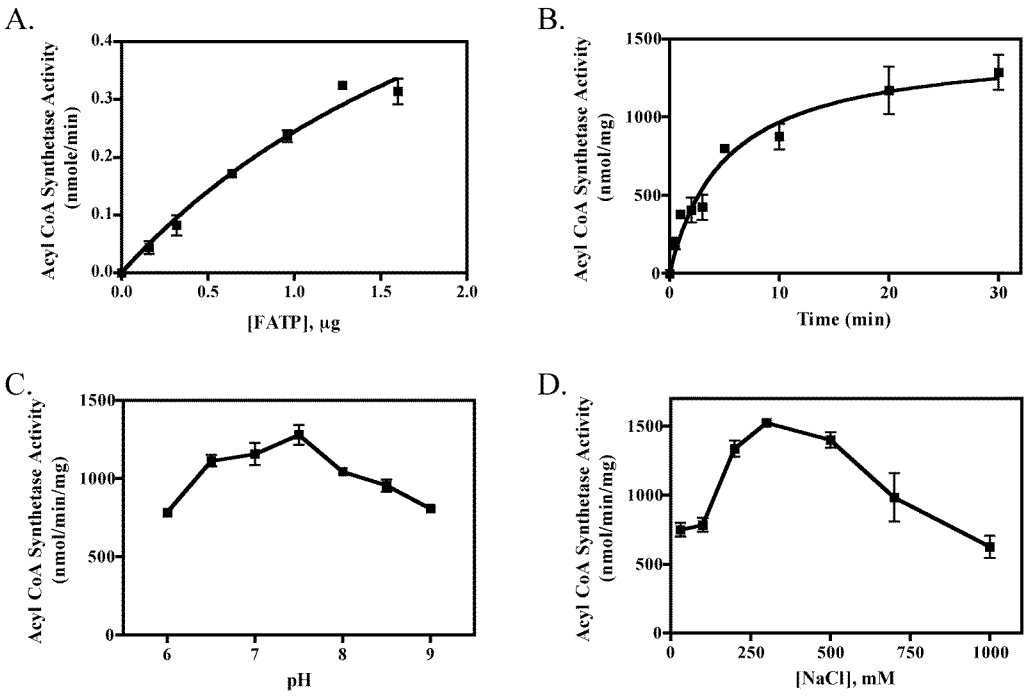

Figure 3. **FATP4 acyl-CoA synthetase reaction conditions.** Panel A, acyl-CoA synthetase activity as a function of FATP4. Panel B, time course of C16:0 esterification by FATP4. Panel C, effect of pH on FATP4 acyl-CoA synthetase activity. Panel D, effect of ionic strength on FATP4 acyl-CoA synthetase activity. Data points are expressed as the mean ± standard deviation. Data presented is from a representative experiment of three independent determinations.

The fatty acid esterification properties of purified FATP4 were measured for two model lipid substrates as well as for CoA and ATP. The apparent K_m values of the purified enzyme were determined for palmitic acid (C16:0), lignoceric acid (C24:0), ATP, and CoA at 37° C (Figure 4). FATP4 demonstrated high affinity toward its substrates and co-substrates exhibiting a K_m of 13 μM for C16:0, 4.8 μM for C24:0, 1.4 mM for ATP, and 47 μM for CoA (Table 2). It should be stressed that because these studies are done in the presence of detergent, and using lipid delivered using α-cyclodextrin mediated solubilization, the free unbound concentration of fatty acids cannot be determined and

the K_m values reported for each fatty acid represent apparent values assuming all lipid was available to the enzyme. Since the solubility of lignoceric acid and palmitic acid vary greatly, this assumption is likely to be incorrect, but represents an experimentally tractable method for analyzing the data and comparing one enzyme to another. The maximal specific activity of ~4300 nmol/ min/ mg was measured for C16:0 and ~1050 nmol/ min/ mg for C24:0 which were 40 and 5-fold greater than those measured for purified FATP1, respectively (6).

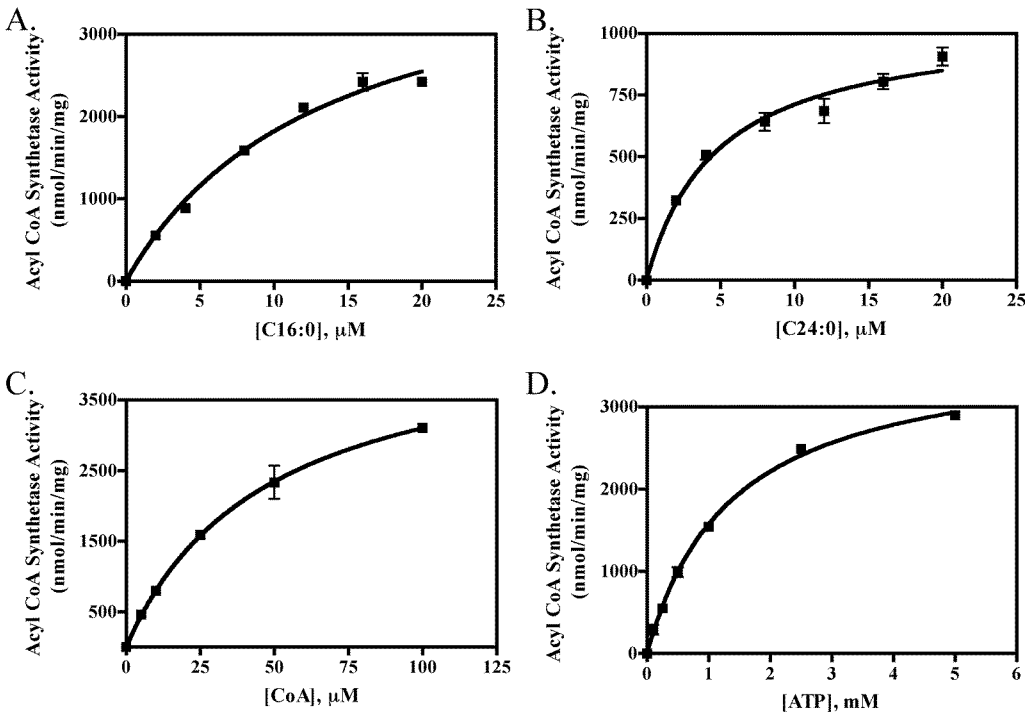

Figure 4. Substrate analysis for purified FATP4 (■). Panel A, activity as a function of C16:0. Panel B, activity as a function of C24:0. Panel C, activity as a function of ATP. Panel D, activity as a function of CoA. Data points are expressed as the mean ± standard deviation. Data presented is from a representative experiment of three independent determinations.

Table 2.

Comparison of kinetic constants for FATP4, FATP1 and ACSL1

Recombinant FATP4 was expressed, purified, and assayed for lignoceroyl-CoA and palmitoyl-CoA synthetase activities as described under "Experimental Procedures". Data are representative of at least two individual trials ± standard deviation and should be considered apparent rather than true values due to the presence of detergent in the analysis. (*) denotes values determined using palmitic acid (C16:0) as substrate.

		FATP4	FATP1[#]	ACSL1[#]
ATP[*]				
	K_m (mM)	1.4 ± 0.1	0.85 ± 0.1	0.32 ± 0.3
	V_{max} (nmol/min/mg)	3740 ± 90	160 ± 0.1	5003 ± 100
	V_{max}/K_m	2700	190	15,600
CoA[*]				
	K_m (μM)	47 ± 4	8.3 ± 1.6	6.4 ± 0.7
	V_{max} (nmol/min/mg)	4570 ± 170	169 ± 10	4602 ± 144
	V_{max}/K_m	100	20	720
C16:0				
	K_m (μM)	13 ± 3	21 ± 5	33 ± 4
	V_{max} (nmol/min/mg)	4248 ± 420	122 ± 40	3232 ± 400
	V_{max}/K_m	330	6	100
C24:0				
	K_m (μM)	4.8 ± 1.0	13 ± 3	18 ± 8
	V_{max} (nmol/min/mg)	1051 ± 69	243 ± 30	240 ± 50
	V_{max}/K_m	220	20	13

Data from reference 6.

Because a large number of different fatty acids are not commercially available in radiolabeled form, the fatty acid substrate specificity of the purified FATP4 was indirectly determined by a competitive enzymatic inhibition by the addition of unlabelled fatty acids in the reaction in addition to either [^{3}H] palmitic acid or [^{3}H]-lignoceric acid (Figure 5). Esterification of labeled lignoceric acid was inhibited only slightly by the addition of 15 μM of two long-chain fatty acids, C16:0 and C20:4. In contrast, the conversion of [^{3}H]-palmitate to palmitoyl-CoA was decreased by the addition of very long-chain fatty acids with the rank order of C24:0 = C20:0 > C16:0.

As with the other kinetic analysis, due to the differing solubilities of the various competing fatty acids, true K_i values cannot be determined and a simple selectivity series is presented. As such, these results suggest that the true K_m value for lignoceric acid is quite low and that the enzyme is much more specific for very long-chain FA rather than long-chain FA.

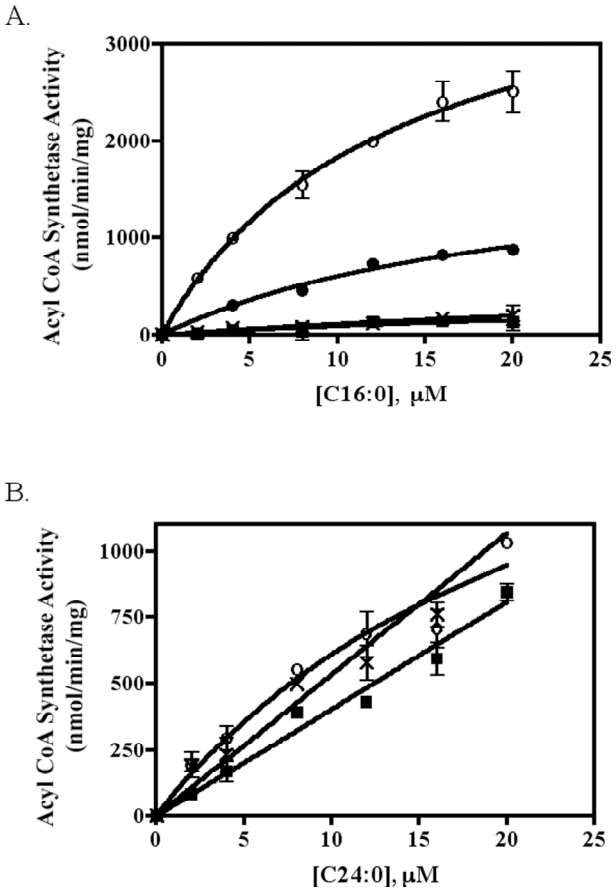

Figure 5. Competition studies with various long-chain and very long-chain fatty acids. Purified FATP4 was assayed for long-chain or very long-chain acyl-CoA synthetase activity in the presence of indicated fatty acids at 15 μM. Panel A, C16:0 (○) esterification was evaluated with the following competitor fatty acids: C24:0 (■), C20:0 (✖), and C16:0 (●). Panel B, C24:0 (■) esterification was evaluated with the following competitor fatty acids: C20:4 (✖) and C16:0 (○). The values are expressed as the mean ± standard deviation. Data presented is from a representative experiment of two independent determinations.

Reports of the cellular concentration of long-chain acyl-CoA esters vary between 5 and 160 μM (5). To determine whether FATP4 is regulated by feedback inhibition, increasing concentrations of palmitoyl-CoA were titrated into the standard reaction conditions (Figure 6A) and the activity of FATP4 evaluated. At a concentration of 10 μM palmitoyl-CoA, the FATP4 acyl-CoA synthetase reaction was inhibited by ~35%, where as 100 μM inhibited the reaction by greater than 90% for both C16:0 and C24:0. Triacsin C has been reported to be a potent competitive inhibitor of ACSL1 and ACSL4 (20), but does not inhibit FATP1 (6). To test whether triacsin C inhibits purified FATP4, various concentrations were added to the standard reaction mixture (Figure 6B) and the conversion of C16:0 and C24:0 to their CoA derivatives evaluated. Surprisingly, Triacsin C had no effect on FATP4 acyl-CoA synthetase activity toward C24:0 esterification, but inhibited C16:0 esterification in a dose-dependent manner with an IC_{50} of ~30 μM. Troglitazone inhibition of CoA synthetase activity paralleled the result with Triacsin C; C24:0 esterification was unaffected by concentrations up to 50 μM and inhibited C16:0 conversion with an IC_{50} of ~20 μM (Figure 6C). These results are consistent with the proposal that FATP4 is more specific for very long-chain FA esterification than for long-chain esterification.

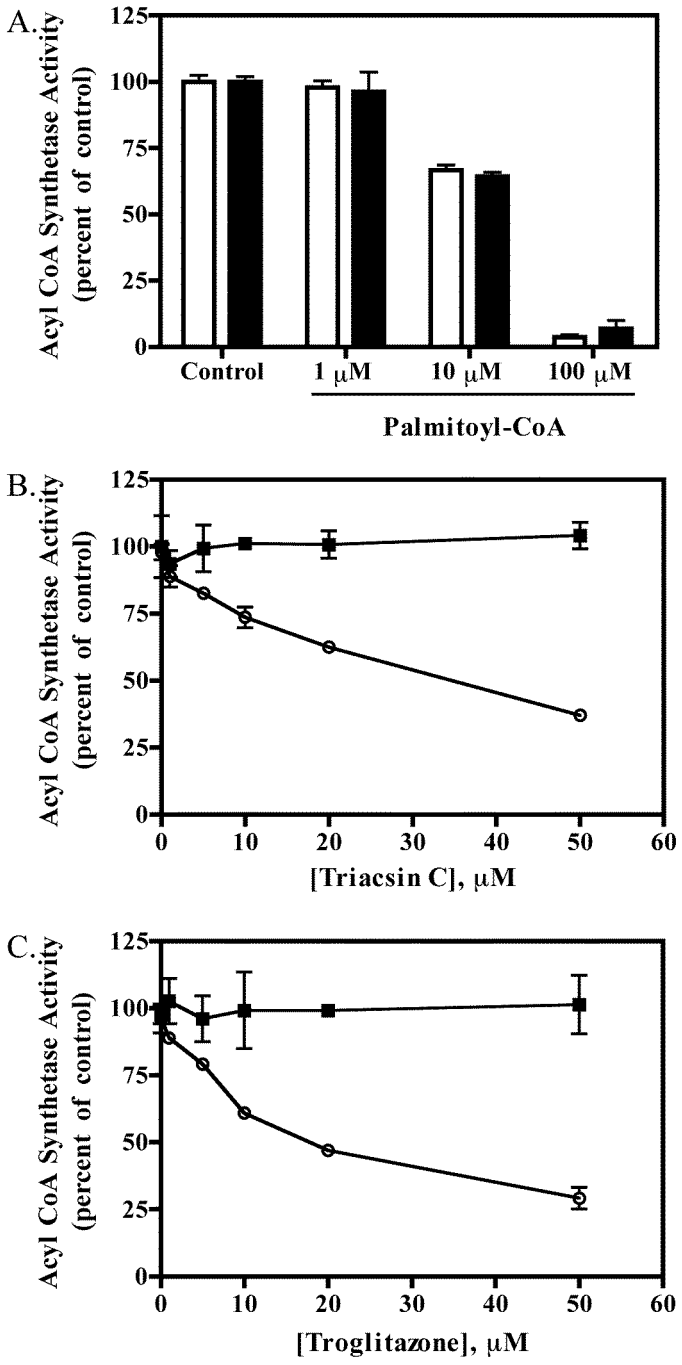

Figure 6. Inhibition of FATP4 synthetase activity. Purified FATP4 was assayed for C16:0 (open symbols) and C24:0 (closed symbols) acyl-CoA synthetase activity in the presence of increasing concentrations of (A) palmitoyl-CoA, (B) Triacsin C, and (C) troglitazone. The values are expressed as the mean ± standard deviation. Data presented is from a representative experiment of three independent determinations.

The phenotype of FATP4 null mice suggests defects in lipid uptake and/or metabolism. To evaluate the relevance of the FATP4 acyl-CoA synthetase activity to the phenotype of the null mice, the esterification of a variety of long and very long-chain FA was evaluated in extracts from FATP4 null mice (Figure 7). Although the C16:0 esterification activity of purified FATP4 exceeded that for C24:0, there were no statistically significant changes in palmitic or oleic acid esterification measured in any tissue. This is likely due to the presence of other acyl-CoA synthetases capable of C16:0 esterification. In contrast, esterification of C24:0 was significantly decreased in the intestine, brain, and skin samples from the FATP4 null mice when compared to wild type littermates, but was identical in the liver and lung samples where additional FATP family members are expressed (3). These results are consistent with the *in vitro* characterization of FATP4 activity and strongly suggest that in vivo, the loss of FATP4-mediated very long-chain fatty acid esterification may underlie the null phenotype.

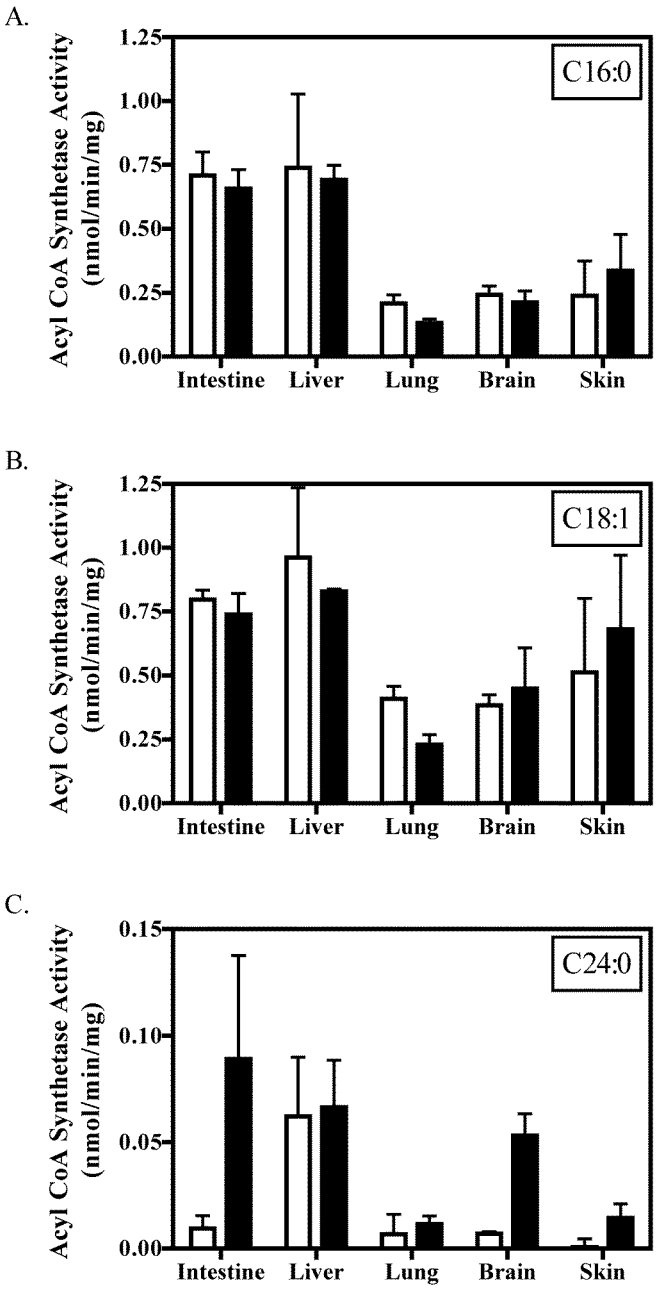

Figure 7. Acyl-CoA Synthetase activity in FATP4 null mice. Tissues from FATP4 null mice and wild type littermates were assayed for (A) C16:0, (B) C18:1, and (C) C24:0 acyl-CoA synthetase activity. * denotes p-values <0.05. The values are expressed as the mean ± standard deviation. Data presented is from a representative experiment of three independent determinations.

DISCUSSION

The FATP family of proteins was originally identified by the ability to facilitate fatty acid uptake using a fluorescent fatty acid internalization assay (21). Subsequently, mammalian FATP family members have been shown to catalyze fatty acid uptake using a variety of assays in multiple systems including evaluation in stable cell lines, transient transfection into 293, COS or CHO cells, and complementation of deletions in the yeast orthologue (3,4,22). Moreover, the purified FATP1 is an acyl-CoA synthetase and based on work from the yeast system has been postulated to function in a process termed vectoral acylation. Vectoral acylation links CoA dependent esterification of fatty acids to their influx thereby trapping the internalized lipid, preventing its diffusion or transport from the cell. It is unclear if FATPs facilitate both transbilayer movement of fatty acids and esterification or simply esterification of a fatty acid that has diffused across the membrane. However, yeast *FAT1* mutants have been identified with separable transport and esterification activity suggesting that the mammalian FATP family, if functioning similarly, may too be bifunctional (8). This hypothesis does not exclude the participation of other proteins such as CD36 that may function as a fatty acid receptor presenting a high local concentration of fatty acid at the plasma membrane, or ACSL1 another acyl-CoA synthetase, that collectively may work in concert with FATP. Vectoral acylation therefore is a functional parallel to the glucose transport-hexokinase system functioning in sugar import.

The current study was undertaken to evaluate the catalytic properties of the FATP4 acyl-CoA synthetase reaction. Here we demonstrate that *in vitro*, purified FATP4 has a

robust acyl-CoA synthetase activity with moderate specificity for long-chain fatty acids over very long-chain fatty acids. FATP4 is a high velocity enzyme comparable to ACSL1, the traditional enzyme believed to esterify fatty acids broadly in cells. FATP4 prefers long-chain fatty acid to very long-chain fatty acids, although care must be taken to consider that this conclusion is based on kinetic evaluations that consider all the substrate available to the enzyme. Given the differences in chemical solubility between C16:0 and C24:0, the ability to make absolute statements is tenuous at best.

The kinetic properties of purified FATP4 protein are interesting when compared to those exhibited by ACSL1 purified similarly. Purified his-tagged ACSL1 demonstrated the expected high affinities toward C16:0, ATP, and CoA, with K_m values of 33 μM, 320 μM, and 6.4 μM respectively (Table 2). Interestingly, ACSL1 also utilized very long-chain fatty acids (C24:0) with a K_m of 18 μM. The maximal velocity of ACSL1 for C16:0 was about 3200 nmol/ min/ mg, but was greatly reduced for C24:0 to 240 nmol/ min/mg. Consistent with the reduced velocity for very long-chain fatty acids, ACSL1 was 10-fold more active toward C16:0 than C24:0 as demonstrated by V_{max}/K_m values of 100 and 13 respectively. In contrast FATP4 exhibited higher activity toward C16:0 and increased specificity for C16:0 (V_{max}/K_m of 330) over C24:0 (V_{max}/K_m of 220). For very long-chain fatty acids, FATP4 was ~5-fold more active than was ACSL1 while the enzymes had comparable long-chain fatty acid esterification activity. In general FATP4 is a more robust acyl-CoA synthetase than is ACSL1.

FATP4 demonstrates a preference for C16:0 over C24:0 in these *in vitro* studies.

However, a number of experimental observations suggest that C24:0 may be the preferred substrate for FATP4 *in vitro* and *in vivo*. First, two fatty acid analogs Triacsin C and troglitazone were effective inhibitors of C16:0 esterification but not for C24:0. Second, in competition studies, lignoceric acid could compete for C16:0 conversion; however, C16:0 did not inhibit C24:0 esterification. Finally, tissues from FATP4 null animals were only defective for C24:0 esterification, while C16:0 or C18:1 conversion were unaltered. While the apparent K_m values for C16:0 and C24:0 were essentially identical, these observations suggest the actual K_m value for C24:0 is much lower that that of C16:0.

A comparative analysis of the two purified FATP proteins reveal significant differences between the enzymes. FATP4 is a high velocity acyl-CoA synthetase with preference for C24:0 over C16:0. Additionally, the FATP4 reaction is sensitive to a number of potential inhibitors including the product palmitoyl-CoA, and two fatty acid analogs, Triacsin C and troglitazone. On the other hand, FATP1 is comparatively a low velocity enzyme with broad specificity for fatty acids of 16 to 24 carbons. The FATP1 reaction is insensitive to Triacsin C and troglitazone, but subject to product inhibition. The relative abundance and cellular locations of FATP1 and FATP4 in adipocytes are not known. However if both enzymes are located on the plasma membrane, based upon the relative velocities of the two enzymes, FATP4 may be the major contributor to vectoral acylation. This may explain the lack of effects on adipose tissue lipid metabolism observed in FATP1 null mice where the major metabolic effect is centered in muscle (23).

Tissue extracts of the intestine, brain, and skin from FATP4 null mice exhibit reduced esterification for C24:0, but not C16:0 or C18:1 suggesting that in vivo, the very long-chain acyl-CoA synthetase activity of FATP4 contributes to the skin disorder phenotype of null mice. This conclusion is supported by lipid composition analysis of the FATP4 null mice. The epidermis of the FATP4 -/- mice had a reduced molar content of phosphatidylcholine, phosphatidylethanolamine, and cholesteryl ester, but increased ceramide compared to wild type littermates. Furthermore, detailed analysis of the ceramide species demonstrated the null mice had a significantly lower portion of very long-chain fatty acids (C26:0 and C26:0-OH) and an increased proportion of fatty acids with less than 26 carbons. This shift to shorter chain fatty acids was also observed for phosphatidylcholine and phosphatidylserine. The lack of effects in other tissues is likely due to the expression of other acyl-CoA synthetases, including FATP isoforms, in those cell types.

In sum, these results demonstrate that FATP4 exhibits intrinsic acyl-CoA synthetase activity and is a high velocity enzyme relative to FATP1 and ACSL1. For long-chain fatty acids, the FATP4 enzyme exhibits a V_{max} / K_m similar to ACSL1. This may suggest that ACS family members could functionally compensate for disruptions of FATP for some but not all lipid substrates. However, striking evidence from FATP4 null mice (12) that exhibit a wrinkle-free phenotype reminiscent of essential fatty acid deficiency suggests unique specialized roles for the fatty acid transport proteins in very long-chain fatty acids metabolism and that their physiological significance is central to normal lipid homeostasis.

ACKNOWLEDGEMENTS

We thank members of the Bernlohr laboratory for their advice during this study.

Supported in part by grants from the NIH DK53189 (to DAB), the AHA (to AMH) and the Minnesota Obesity Center

REFERENCES

1. Luiken, J. J., Schaap, F. G., van Nieuwenhoven, F. A., van der Vusse, G. J., Bonen, A., and Glatz, J. F. (1999) *Lipids* **34 Suppl**, S169-175
2. Frohnert, B. I., and Bernlohr, D. A. (2000) *Prog Lipid Res* **39**, 83-107
3. Hirsch, D., Stahl, A., and Lodish, H. F. (1998) *Proc Natl Acad Sci U S A* **95**, 8625-8629
4. Hatch, G. M., Smith, A. J., Xu, F. Y., Hall, A. M., and Bernlohr, D. A. (2002) *J Lipid Res* **43**, 1380-1389
5. Faergeman, N. J., DiRusso, C. C., Elberger, A., Knudsen, J., and Black, P. N. (1997) *J Biol Chem* **272**, 8531-8538
6. Hall, A. M., Smith, A. J., and Bernlohr, D. A. (2003) *J Biol Chem* **278**, 43008-43013
7. Pei, Z., Fraisl, P., Berger, J., Jia, Z., Forss-Petter, S., and Watkins, P. A. (2004) *J Biol Chem* **279**, 54454-54462
8. Zou, Z., DiRusso, C. C., Ctrnacta, V., and Black, P. N. (2002) *J Biol Chem* **277**, 31062-31071
9. Stuhlsatz-Krouper, S. M., Bennett, N. E., and Schaffer, J. E. (1999) *Prostaglandins Leukot Essent Fatty Acids* **60**, 285-289
10. Stuhlsatz-Krouper, S. M., Bennett, N. E., and Schaffer, J. E. (1998) *J Biol Chem* **273**, 28642-28650
11. Moulson, C. L., Martin, D. R., Lugus, J. J., Schaffer, J. E., Lind, A. C., and Miner, J. H. (2003) *Proc Natl Acad Sci U S A* **100**, 5274-5279
12. Herrmann, T., van der Hoeven, F., Grone, H. J., Stewart, A. F., Langbein, L., Kaiser, I., Liebisch, G., Gosch, I., Buchkremer, F., Drobnik, W., Schmitz, G., and Stremmel, W. (2003) *J Cell Biol* **161**, 1105-1115
13. Gimeno, R. E., Hirsch, D. J., Punreddy, S., Sun, Y., Ortegon, A. M., Wu, H., Daniels, T., Stricker-Krongrad, A., Lodish, H. F., and Stahl, A. (2003) *J Biol Chem* **278**, 49512-49516
14. Gertow, K., Bellanda, M., Eriksson, P., Boquist, S., Hamsten, A., Sunnerhagen, M., and Fisher, R. M. (2004) *J Clin Endocrinol Metab* **89**, 392-399
15. Gertow, K., Pietilainen, K. H., Yki-Jarvinen, H., Kaprio, J., Rissanen, A., Eriksson, P., Hamsten, A., and Fisher, R. M. (2004) *Diabetologia* **47**, 1118-1125

16. He, T. C., Zhou, S., da Costa, L. T., Yu, J., Kinzler, K. W., and Vogelstein, B. (1998) *Proc Natl Acad Sci U S A* **95**, 2509-2514
17. Wessel, D., and Flugge, U. I. (1984) *Anal Biochem* **138**, 141-143
18. Nagamatsu, K., Soeda, S., Mori, M., and Kishimoto, Y. (1985) *Biochim Biophys Acta* **836**, 80-88
19. Coe, N. R., Smith, A. J., Frohnert, B. I., Watkins, P. A., and Bernlohr, D. A. (1999) *J Biol Chem* **274**, 36300-36304
20. Kim, J. H., Lewin, T. M., and Coleman, R. A. (2001) *J Biol Chem* **276**, 24667-24673
21. Schaffer, J. E., and Lodish, H. F. (1994) *Cell* **79**, 427-436
22. Dirusso, C. C., Connell, E. J., Faergeman, N. J., Knudsen, J., Hansen, J. K., and Black, P. N. (2000) *Eur J Biochem* **267**, 4422-4433
23. Kim, J. K., Gimeno, R. E., Higashimori, T., Kim, H. J., Choi, H., Punreddy, S., Mozell, R. L., Tan, G., Stricker-Krongrad, A., Hirsch, D. J., Fillmore, J. J., Liu, Z. X., Dong, J., Cline, G., Stahl, A., Lodish, H. F., and Shulman, G. I. (2004) *J Clin Invest* **113**, 756-763

CHAPTER 3:

FATTY ACID METABOLISM IN ADIPOCYTES: FUNCTIONAL ANALYSIS OF FATTY ACID TRANSPORT PROTEINS 1 AND 4

This chapter is a reprint of the published manuscript of the same title with minor alterations. Lobo, S., **Wiczer, B. M.**, Smith, A. J., Hall, A. M., and Bernlohr, D. A. (2007) *J. Lipid Res.* **48**, 609-620

Brian Wiczer's contribution to this chapter was Table 1, and in the preparation of the text and discussion.

SUMMARY

The role of fatty acid transport protein 1 (FATP1) and fatty acid transport protein 4 (FATP4) in facilitating adipocyte fatty acid metabolism was investigated using stable FATP1 or FATP4 knockdown (kd) 3T3-L1 cell lines derived from retroviral-delivered shRNA. Decreased expression of FATP1 or FATP4 did not affect preadipocyte differentiation or the expression of FATP1 (in FATP4 kd), FATP4 (in FATP1 kd), CD36, ACSL1 and AFABP/aP2 but did lead to increased levels of PPARγ and C/EBPα. Both FATP1 and FATP4 kd adipocytes exhibited reduced triacylglycerol deposition and corresponding reductions in di-, and monoacylglycerol levels when compared to control cells. FATP1 kd adipocytes displayed a ~25% reduction in basal and a complete loss of insulin-stimulated [^{3}H]-fatty acid uptake compared to control adipocytes. In contrast, FATP4 kd adipocytes as well as HEK-293 cells over expressing FATP4 did not display any changes in fatty acid influx. FATP4 kd cells exhibited increased basal lipolysis whereas FATP1 kd cells exhibited no change in lipolytic capacity. Consistent with reduced triacylglycerol accumulation, FATP1 kd and FATP4 kd adipocytes exhibited enhanced 2-deoxyglucose uptake compared to control adipocytes. These findings define unique and distinct roles for FATP1 and FATP4 in adipose fatty acid metabolism.

INTRODUCTION

Dysregulation in adipose fatty acid metabolism is a significant contributing factor to the development of obesity and associated metabolic diseases such as type 2 diabetes, hypertension and cardiovascular disease (1-3). Central to this imbalance are differing rates of long-chain fatty acid (LCFA) influx, efflux and metabolism by adipose tissue. While appreciated for decades, the molecular mechanism(s) that control and mediate fatty acid flux in fat cells remain poorly defined from structural, mechanistic and regulatory viewpoints.

While diffusion may play a fundamental role in transbilayer movement of LCFA, molecular and genetic evidence from loss or gain of function studies have identified a number of proteins facilitating some component of the fatty acid influx process (4-8). Proteins implicated in fatty acid uptake are fatty acid translocase (CD36), acyl-CoA synthetases (FATP and ACSL family members), plasma membrane fatty acid binding protein (FABPpm) and caveolin-1. The relative contribution of each polypeptide to overall cellular fatty acid influx has not been quantitatively evaluated.

FATPs are a family of membrane bound proteins that catalyze the ATP-dependent esterification of long and very long-chain fatty acids to their acyl-CoA derivatives (9). The FATP proteins bear 20-40% sequence identity to the long-chain acyl-CoA synthetase (ACSL) class of proteins that function in long-chain acyl-CoA production. In mammals, six different isoforms of FATP (FATP1-6) have been identified with

tissue specific expression patterns (10). White adipose tissue predominantly expresses FATP1, FATP4 and ACSL1 while brown adipose tissue additionally expresses ACSL5.

FATP1 is a 63-kDa protein found to be localized primarily to high density membranes and to a lesser extent in the plasma and low density membrane fractions of murine adipocytes and 3T3-L1 cells (5). FATP1 (as well as ACSL1) was identified using an expression clone strategy designed to identify proteins that enhanced long-chain fatty acid uptake (11). Evidence for the role of FATPs in fatty acid transport has been qualitatively evaluated by various loss of function/gain of function model systems. Stable HEK-293 cell lines over expressing murine FATP1 demonstrate increased LCFA uptake and triacylglycerol accumulation (12). A transgenic mouse model with cardiac-specific expression of FATP1 demonstrated increased myocardial LCFA uptake (12,13). Disruption of the FATP1 homologue expressed in yeast, fat1p, markedly impaired LCFA uptake (14) and a murine FATP1 knockout mouse exhibited reduced muscle acyl-CoA levels and increased insulin sensitivity (15).

FATP4 is the closest homologue of FATP1 (60.3% identity) that is expressed in adipose tissue (16). It role in adipose tissue metabolism is largely unknown. However, FATP4 is also expressed in skeletal muscle, heart, skin, liver and is the principle fatty acid transporter in the small intestine localized to the apical side of enterocytes where it is though to mediate the uptake of dietary fatty acids (17). *FATP4* null mice displayed features of a human neonatally lethal restrictive dermopathy which has been associated with a disturbed function in the epidermal barrier (18-20). FATP4 encodes an acyl-

CoA synthetase with substrate specificity to very long-chain fatty acids that may be required for synthesis of lipids crucial in formation of a healthy epidermis (21,22). Polymorphisms in the human *FATP4* gene locus have identified this gene as a candidate for the insulin resistance syndrome (23). Moreover, FATP4 expression levels correlated with measures of acquired obesity and insulin resistance (23). These observations indicate the importance of the study of FATP4 function in adipocyte fatty acid uptake and metabolism.

Our long-term goal is to identify and define in quantitative terms the mechanisms controlling LCFA flux in mammalian cells and the roles of specific proteins implicated in the influx reaction. In this report, we evaluated the specific role(s) of FATP1 and FATP4 in mediating LCFA influx and efflux using FATP1/ FATP4 knockdown (FATP1 kd/ FATP4 kd) 3T3-L1 adipocytes produced using lentiviral delivery of shRNA targeted towards FATP1 or FATP4. We report herein that FATP1 facilitates the insulin-stimulated component of LCFA uptake, but only has a minor role in basal LCFA uptake in 3T3-L1 adipocytes. FATP4 does not play a rate-limiting role in either basal nor insulin-stimulated fatty acid uptake. FATP4 knockdown adipocytes exhibited increased basal lipolysis suggesting a role in fatty acid re-esterification in 3T3-L1 adipocytes.

MATERIALS AND METHODS

Materials- Cell culture reagents were obtained from Invitrogen. Porcine insulin, puromycin, cytocholasin B and deoxyglucose were obtained from Sigma-Aldrich. Geneticin was obtained from Gibco/BRL Life Technologies. Non-radiolabeled fatty acids were obtained from Nu-Chek Prep, Inc. (Elysian, MN). [^{3}H]-oleic and [^{3}H]-lignoceric acid was obtained from American Radiochemicals Company. [^{3}H]-palmitic, [^{3}H]-arachidonic acid and [^{14}C] 2-deoxy-D-glucose was obtained from Amersham Pharmacia Biotech.

Antibodies used: rabbit anti- CD36, rabbit anti-PPARγ, and rabbit anti-C/EBPα (obtained from Santa Cruz biotechnology. Inc.); rabbit anti-GLUT4 (gift of Dr. H. Haspel, Charles River Laboratory, Wilmington, MA); rabbit anti-ACSL1 (gift of Dr. Rosalind Coleman, University of North Carolina, Chapel Hill, NC); rabbit anti-FATP4 (gift of Dr. Paul Watkins, Kennedy Krieger Research Institute, Baltimore, MD); horseradish peroxidase (HRP)-coupled IgGs (obtained from Jackson ImmunoResearch Laboratories, Inc.). All other reagents were of analytical grade and obtained from Sigma.

Cell culture conditions- 3T3-L1 pre-adipocytes were cultured and differentiated into adipocytes as described previously (24). Briefly, preadipocytes were cultured in Dulbecco's modified Eagle's medium (DMEM) containing 10% calf serum. Two days after reaching confluence, cells were induced to differentiate in DMEM supplemented with 10% fetal bovine serum (FBS), 174 μM insulin, 0.5 mM methylisobutylxanthine, and 0.25 μM dexamethasone. Two days post initiation of differentiation,

dexamethasone and methylisobutylxanthine were withdrawn from the media, whereas insulin was withdrawn after four days. Differentiated adipocytes were maintained in DMEM and 10% FBS until mature (Day 8-12).

Generation of FATP1 kd and FATP4 kd 3T3-L1 adipocytes using lentiviral-delivered RNAi- A lentiviral-based RNAi vector pLKO1 (kindly provided by Sheila Stewart at the Whitehead institute, Cambridge, Massachusetts) was used for siRNA mediated FATP1 knockdown in cultured 3T3-L1 cells. This vector was shown to stably express shRNAs under the control of the RNA polymerase III promoter of the U6 gene in non-dividing cells (25). Oligomers 60 basepair in length containing a stem-loop structure directed against FATP1, FATP4 were synthesized and cloned into the AgeI/EcoRI site in pLKO1. Four siRNA sequence variants for each gene were synthesized and analyzed. Based on the ability of the lentiviral RNAi vector to effectively silence the expression of FATP1/FATP4 by 75 % or more in 293T cells transiently co-transfected with a FATP1/FATP4 expression vector and each of the four lentiviral RNAi vectors, one of the gene sequence variant constructs was selected for the generation of recombinant lentiviruses. The selected oligomer targeting the FATP1 nucleotide sequence was 5'-TGCTGTAGCCAACCTGTTCC-3' (nucleotide positions 342-361) and targeting the FATP4 nucleotide sequence was 5'-GGCACGAGCTCTCATCTT-3' (nucleotide positions 519-536). A construct expressing shRNA against a scrambled FATP1 sequence (5'- TAGGTCTTCAAGAGGGGATG-3') was used as a control. Recombinant lentiviruses were packaged in 293T cells and harvested 24, 48 and 72 hours later (4). 3T3-L1 fibroblasts were transduced with the lentiviruses for 4-6 hours

in the presence of 6 μg/ml polybrene at an m.o.i of approximately 50-100. Cells were allowed to recover for 48 hr post-transduction before addition of selection media containing 2 μg/ml of puromycin. Stable knockdown cell lines were generated from a heterogeneous pool of puromycin resistant 3T3-L1 fibroblasts.

Generation of stable HEK-293 cells expressing FATP4- FATP4 subcloned into pcDNA3.0 (Invitrogen) or vector control was linearized and introduced into 293 cells by electroporation. 293 cells are an excellent model system to evaluate FATP4 function in lipid metabolism for they are a well defined cell system, grow easily in culture, and have been shown to tolerate FATP expression (12). Dilutions of the electroporated cells were plated in DMEM containing 10% FBS and incubated at 37°C, 5% CO2. Selection was initiated after 48 hr with the addition of 400 μg/ml geneticin. After 8 days colonies were selected using cloning rings and individual lines developed. Once established, several lines were analyzed for FATP4 expression. The cell lines and vector control cells were maintained in 400 μg/ml geneticin. FATP4 over expressing cell lines were analyzed for total cellular lignoceroyl (C24:0) CoA synthetase activities and oleate (C18:1) uptake by a procedure similar to that used for 3T3-L1 adipocytes.

Immunoblot analysis- 3T3-L1 adipocytes were lysed in a buffer containing 50 mM Tris-HCl pH 7.5, 50 mM sodium fluoride, 5 mM sodium pyrophosphate, 1mM ethylenediamine tetraacetic acid, 1 mM dithiothreitol, 0.1 mM phenylmethyl sulfonyl fluoride, 10% glycerol and protease and phosphatase inhibitors. Crude cell extracts (50-100μg total protein) were separated by electrophoresis on a denaturing SDS-

polyacrylamide gel and transferred to nitrocellulose or PVDF membranes. The membranes were blocked with 5% non-fat milk in TBST (100 mM Tris pH 7.4, 0.9% sodium chloride, 0.05% Tween-20) for 1 hour at room temperature. Following incubation with primary antibodies, the membranes were incubated with secondary antibodies conjugated to horseradish peroxidase. Antibody reactivity was detected by chemiluminescence and protein abundance quantitated by densitometry using a FujiFilm FLA-5000 detector.

Analysis of cellular fatty acid uptake- 3T3-L1 adipocytes (day 8) were pre-incubated for 3 hours in Krebs–Ringer's Hepes (KRH) buffer (pH 7.4) containing 120 mM NaCl, 4.7 mM KCl, 2.2 mM $CaCl_2$, 10 mM HEPES, 1.2 mM KH_2PO_4, 1.2 mM MgSO4 and 5.4 mM glucose. Stock solutions (5 mM) of non-radioactive fatty acids were prepared as described (Hatch 1994). Radioactive [^{3}H]-fatty acids (1 mCi/ mmol) were added to achieve the final specific activity. Adipocytes were incubated either with or without insulin (50-100 nM) for 30 minutes and fatty acid uptake initiated by incubating cells in KRH buffer, pH 7.4, containing 5.4 mM glucose and 50 μM [^{3}H]-palmitic, oleic or arachidonic acid, each bound to fatty acid free BSA in a ratio adjusted to generate a free fatty acid concentration of 5 nM. The appropriate FA:BSA ratios for the different fatty acids used in the assay were calculated using LCFA binding constants for BSA as described by Kleinfeld and colleagues (26). After 5 minutes, the cells were rapidly washed three times in ice-cold KRH containing 0.1 % BSA and 200 μM phloretin. The cells were then incubated at room temperature in 0.5 % SDS for 30 minutes and the

cellular incorporated radioactive fatty acids was determined by liquid scintillation counting.

Lipid Analysis- Following cellular influx of radioactive fatty acids, fatty acyl-CoAs were extracted using Dole's reagent. The organic phase was dried down, taken up in a minimal volume of chloroform and bound to disposable primary aminopropyl bonded phase columns. The various polar and neutral classes of lipids were eluted off the column by organic fractionation using the procedures outlined by Kaluzny et al (27) and quantitated by liquid scintillation counting. Cellular tri-, di-, and monoacylglycerol lipids fractionated by the procedure described above were quantitated by alkaline hydrolysis and measurement of glycerol content using the glycerol determination kit (Sigma). Fatty acids were measured using a NEFA kit (Wako).

Fatty acyl-CoA synthetase assays- Cells were harvested in 150 mM Tris-HCl, 150 mM NaCl, 250 mM sucrose, pH 7.5 and lysed via sonication immediately prior to assaying activity. Extracts were assayed for acyl-CoA synthetase activity by the conversion of [^{3}H]-palmitic acid, [^{3}H]-oleic acid, [^{3}H]-arachidonic acid, or [^{3}H]-lignoceric acid to their CoA derivatives by a modified method from Nagamatsu et al. (28) as described by Hall et al (9). Briefly, samples were assayed for 2 minutes at pH 7.5 and 30 mM NaCl in 250 μL of a buffer containing 20 μM fatty acid delivered bound to α-cyclodextrin, 100 mM Tris-HCl (pH 7.5), 10 mM ATP, 5 mM $MgCl_2$, 200 μM CoA, and 200 μM dithiothreitol. Reactions were terminated with the addition of 1.25 mL of isopropanol:heptane:H_2SO_4 (40:10:1, v/v/v), 0.5 mL of H_2O and 0.75 mL of heptane to

facilitate organic phase separation. The aqueous phase was extracted three times with 0.75 mL of heptane to remove unreacted fatty acids and the radioactivity determined by liquid phase scintillation counting.

Immunofluorescence analysis of 3T3-L1 adipocytes- 3T3 L1 cells were plated on 13 mm optical glass coverslips and differentiated as described previously. On day 6 the cells were washed free of serum and maintained in DMEM for 2 hours. Insulin was added (50 ng/mL) and after 30 minutes the cells were washed in phosphate buffered saline (PBS) and fixed in 3% paraformaldehyde for 30 min at 25° C. Following fixation, the cells were rinsed in PBS containing 0.01% digitonin and incubated for 2 hours at 25° C in blocking buffer containing 0.01 M phosphate, 5% goat serum, 5% glycerol, 1.0% cold water fish gelatin, and 0.01% digitonin. The cells were subsequently incubated overnight at 4° C in a 1:50 dilution of rabbit-anti-FATP1 or anti-FATP4 antibody or in a 1:100 dilution of rabbit-anti-Glut 4 antibody in PBS containing 0.01% digitonin. After washing, the coverslips were incubated for 1 hour at 25° C in a 1:400 dilution of Alexa Fluor 488 conjugated donkey anti-rabbit IgG in PBS with 0.01% digitonin. After washing, the coverslips were incubated at 25° C in DMEM with 7.7 μM TOPRO3 (Molecular Probes) for nuclear staining, then washed, mounted, and visualized by confocal microscopy.

Confocal Microscopy- Monolayers were viewed using a Bio-Rad MRC-1024 confocal microscope attached to a Nikon Diaphot inverted microscope equipped with a 15-millwatt krypton/argon laser. Excitation filters allowing 488 and 647 nm were used

sequentially to visualize the Alexa 488 and TOPRO3 probes, respectively. The samples were viewed using either a 20 , 0.75 n.a. plan apo or a 40 , 1.0 n.a. plan apo objective. Digital images were collected using LaserSharp version 3.2 software (Bio-Rad) and analyzed using Image Pro Plus Version 4.5 software (Media Cybernetics, Silver Spring, MD 20910).

Analysis of 2-deoxyglucose uptake- Glucose uptake in 3T3-L1 adipocytes was carried out as described (29). Briefly, cells were serum starved in KRH buffer supplemented with 0.5 % BSA and 2 mM sodium pyruvate (pH 7.4) and incubated either with or without 100 nM insulin for 30 min at 37° C. Glucose uptake was initiated by the addition of [^{14}C] 2-deoxy-D-glucose to a final assay concentration of 100 μM at 37° C. After 5 min. 2-deoxyglucose uptake was terminated by three washes with ice-cold KRH buffer and the cells solubilized with 0.8 ml of KRH buffer containing 1% Triton X-100. The incorporated radioactivity was determined by scintillation counting. Nonspecific 2-deoxyglucose uptake was measured in the presence of 20 μM cytocholasin B and subtracted from the total glucose uptake assayed to obtain specific uptake.

RESULTS

To assess the role of FATP1 and FATP4 in fatty acid metabolism in adipocytes, we utilized stable 3T3-L1 adipocyte FATP1 kd and FATP4 kd cell lines derived from lentiviral delivered shRNA targeting either protein. Such knockdown preadipocytes grew at a normal rate and differentiated using the standard methylisobutylxanthine, dexamethasone and insulin protocol. An essentially complete loss of FATP1 protein expression was observed in cells expressing FATP1 sequence specific shRNA (FATP1 kd) indicating that the protein is not required for adipose conversion. Expression of shRNA directed towards FATP4 (FATP4 kd) produced a cell line exhibiting ~10% of the control FATP4 level (Figure 1). Immunoblotting of protein extracts from FATP1 kd, FATP4 kd and control (Scr) cells revealed that there was a ~50% increase in the expression of PPARγ and a ~20% increase in C/EBPα protein. Despite the increase in expression of key adipogenic transcription factors, the expression of proteins regulated by PPARγ and implicated in some facet of fatty acid influx (CD36, ACSL1, FATP4/FATP1) and/or the PPARγ target genes AFABP/aP2, CD36, FATP were unchanged in abundance in both cell lines (Figure 1).

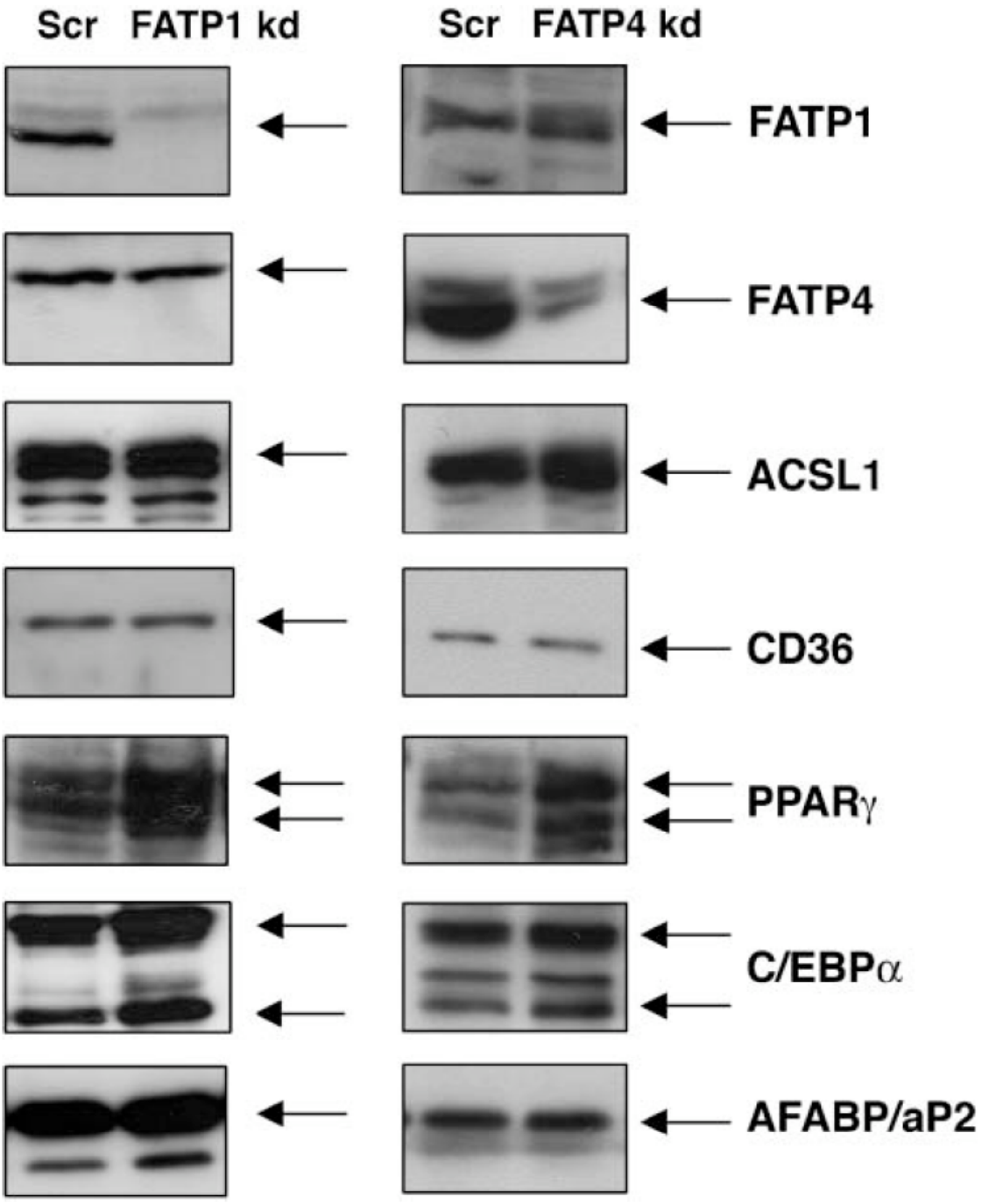

Figure 1. Immunoblot analysis of cell extracts from day 9 3T3-L1 adipocytes expressing FATP1 shRNA (FATP1 kd), FATP4 shRNA (FATP4 kd) or scrambled sequence shRNA (Scr) as a control. The blot is representative of 3 separate experiments.

Both FATP1 kd and FATP4 kd adipocytes exhibited reduced accumulation of triacylglycerol. Oil red O staining of triacylglycerol droplets was markedly reduced exhibiting smaller lipid droplet sizes in FATP1 kd and FATP4 kd 3T3-L1 adipocytes relative to the scrambled control (that was not different from uninfected or vector infected adipocytes, results not shown). Consistent with the reduced oil red O staining, FATP1 kd and FATP4 kd cells exhibited decreased triacylglycerol, diacylglycerol, and monoacylglycerol levels. FATP4 kd cells, but not FATP1 kd cells, exhibited a decrease in free fatty acid level (Figure 2).

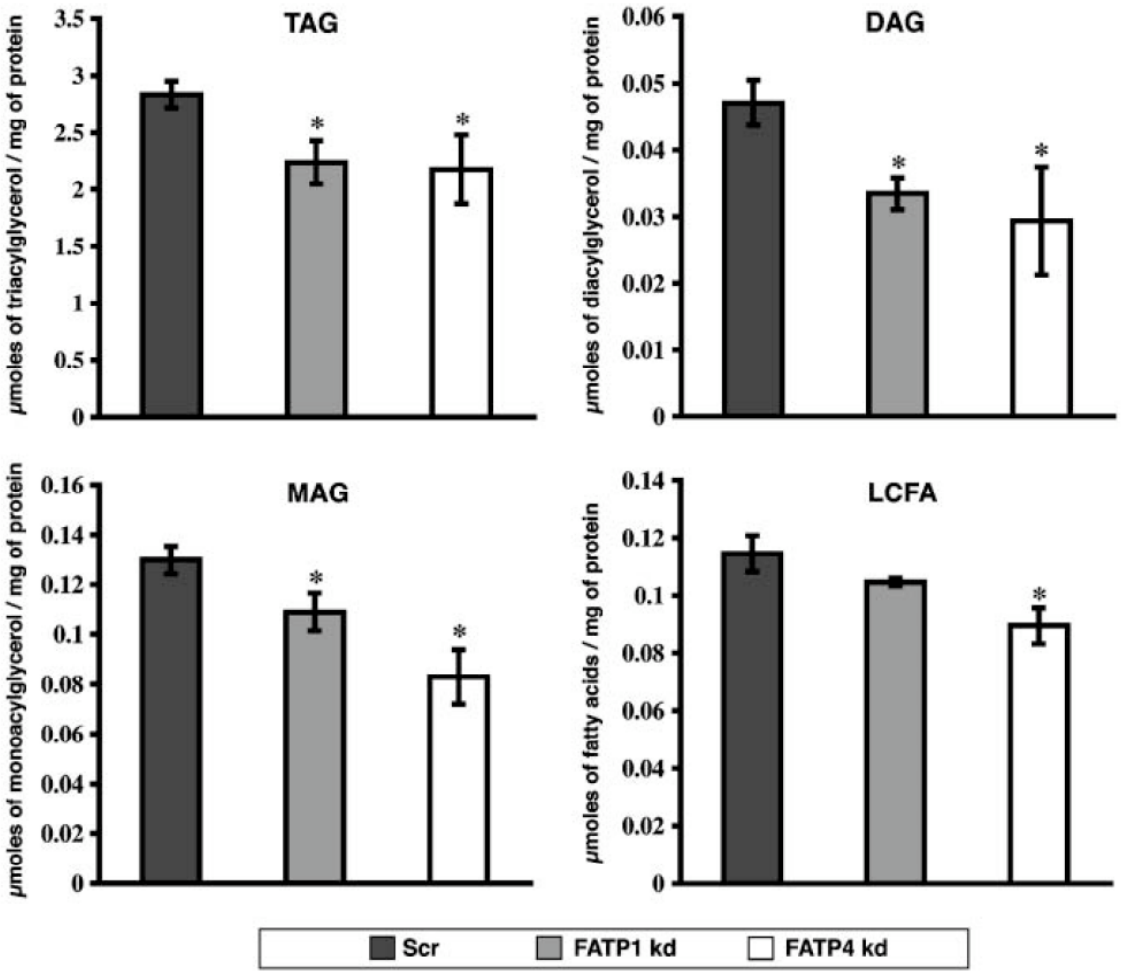

Figure 2. Quantitative determination of tri-, di-, monoacylglycerol and fatty acid content in FATP1 kd, FATP4 kd and control 3T3-L1 adipocytes. The data shown is representative of three separate experiments. *, $P < 0.05$ relative to Scr control cultures. Y-axis error bars = +/- standard deviation.

FATP1 is an acyl-CoA synthetase with broad substrate specificity (C16:0 vs. C24:0 esterification) but a rather low enzymatic reaction rate relative to other fatty acid CoA ligases. FATP4 conversely has a high acyl-CoA synthetase reaction rate relative to FATP1 and ACSL1 and has a substrate preference for very long-chain (C24:0) over long-chain (C16:0) fatty acids (21). To evaluate the effect of FATP1 kd and FATP4 kd on total cellular acyl-CoA synthetase activity, extracts were prepared and assayed for

fatty acid esterification using a variety of fatty acid substrates. As shown in Table 1, knockdown of FATP1 resulted in a ~10-15% decrease in cellular C16:0, C18:1 and C20:4 esterification activity respectively but essentially no change in total cellular C24:0 acyl-CoA synthetase activity. As compared to FATP1 kd adipocytes, FATP4 kd adipocytes displayed a 20-25% decrease in cellular C16:0, C18:1 and C20:4 acyl-CoA synthetase activities respectively and no change in total cellular C24:0 acyl-CoA synthetase activity. The decrease in total acyl-CoA synthetase activity for either knockdown cell line (10-25%) correlated well with the measured decrease in triacylglycerol, diacylglycerol and monoacylglycerol levels in the cell (Figure 2).

Table 1.
Analysis of acyl-CoA synthetase activity of cellular extracts from 3T3-L1 adipocytes expressing FATP1 shRNA and FATP4 shRNA compared to the scrambled control (Scr)

Acyl-CoA synthetase activities of cell extracts from day 8 differentiated 3T3-L1 adipocytes were assayed for esterification of palmitic acid (C16:0), oleic acid (C18:1), arachidonic acid (C20:4), lignoceric acid (C24:0) and expressed as nmol/min/mg of total protein. Data is representative of three independent experiments, *P < 0.05 comparing experimental to scrambled control.

	Acyl-CoA synthetase activity ± SD (*nmol/min/mg protein)*		
Substrate	**Scr**	**FATP1 kd**	**FATP4 kd**
C16:0	168.0 ± 2.5	140.3 ± 6.1*	134.1 ± 6.4*
C18:1	191.8 ± 5.2	155.8 ± 4.9*	149.6 ± 3.1*
C20:4	131.2 ± 2.7	118.6 ± 3.1*	106.3 ± 3.7*
C24:0	7.7 ± 1.2	8.7 ± 1.5	7.2 ± 1.7

Since there was a significant, albeit modest, decrease in total cellular acyl-CoA synthetase activities as well as triacylglycerol levels we assessed the role FATP1 and FATP4 may play in fatty acid uptake. Stahl and colleagues (5) have reported that

insulin stimulates the translocation of FATP1 from intracellular sites to the plasma membrane. To assess this, 3T3-L1 adipocytes were serum starved and then incubated with or without insulin for 30 minutes and the expression of FATP1, FATP4 and GLUT4 evaluated using secondary immunofluorescence. As shown in Figure 3, the majority of immunoreactive GLUT4 translocated to the plasma membrane as did some immunoreactive FATP1 (estimated to be 10%). In contrast to FATP1 and GLUT4, FATP4 did not appear to be localized to the plasma membrane under basal conditions and did not translocate to the plasma membrane in the presence of insulin.

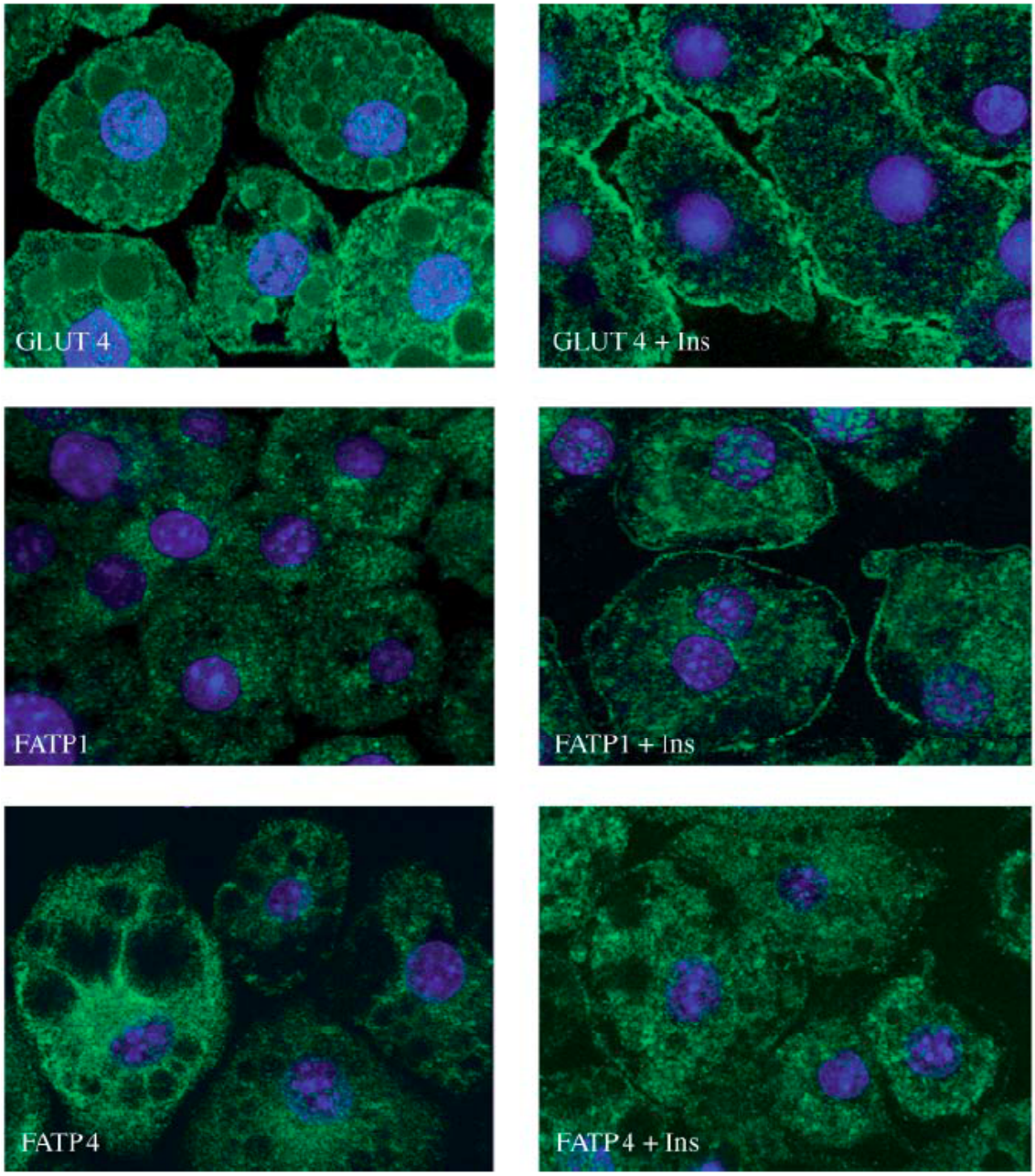

Figure 3. Immunolocalization by confocal microscopy of FATP1 and FATP4 compared to the glucose transporter, GLUT4 under basal and insulin-stimulatory condition in 3T3-L1 adipocytes. Serum-starved day 6 3T3-L1 adipocytes were treated with or without 50 ng/ml insulin for 30 minutes. Fluorescent detection was enabled by incubation with the secondary antibody Alexa Fluor 488 donkey anti-rabbit IgG (green) and subsequent nuclei staining with TOPRO3 (blue).

To parallel the translocation studies for FATP1 and FATP4 shown immunochemically with biochemical analysis, the cellular influx of [^{3}H]-fatty acids of different chain lengths was evaluated under basal and insulin-stimulated conditions. As shown in Figure 4A, under basal conditions, compared to control cells, FATP1 kd adipocytes displayed a ~25% decrease in fatty acid uptake for [^{3}H]-palmitic, -oleic acids and -arachidonic acid. Due to its poor solubility, influx studies with C24:0 were not performed. For control 3T3-L1 adipocytes insulin stimulation led to ~15-40% increase in fatty acid influx for [^{3}H]-palmitic, [^{3}H]-oleic acid and [^{3}H]-arachidonic acids. The increase in [^{3}H]-palmitic and [^{3}H]-oleic acid uptake in response to insulin was completely lost in FATP1 kd cells, indicating a crucial role of FATP1 in insulin-stimulated fatty acid influx. This is consistent with the translocation of FATP1 to the plasma membrane in response to insulin (Figure 3) and is indicative of the role of FATP1 in fatty acid uptake as a critical function of its cellular location. The increase in [^{3}H]-arachidonic acid uptake with insulin-stimulation in FATP1 kd cells is not completely lost but is decreased by ~20% compared to the response of control cells to insulin. This suggests that in addition to FATP1, another acyl-CoA synthetase with substrate specificity for arachidonic acid may facilitate its cellular uptake.

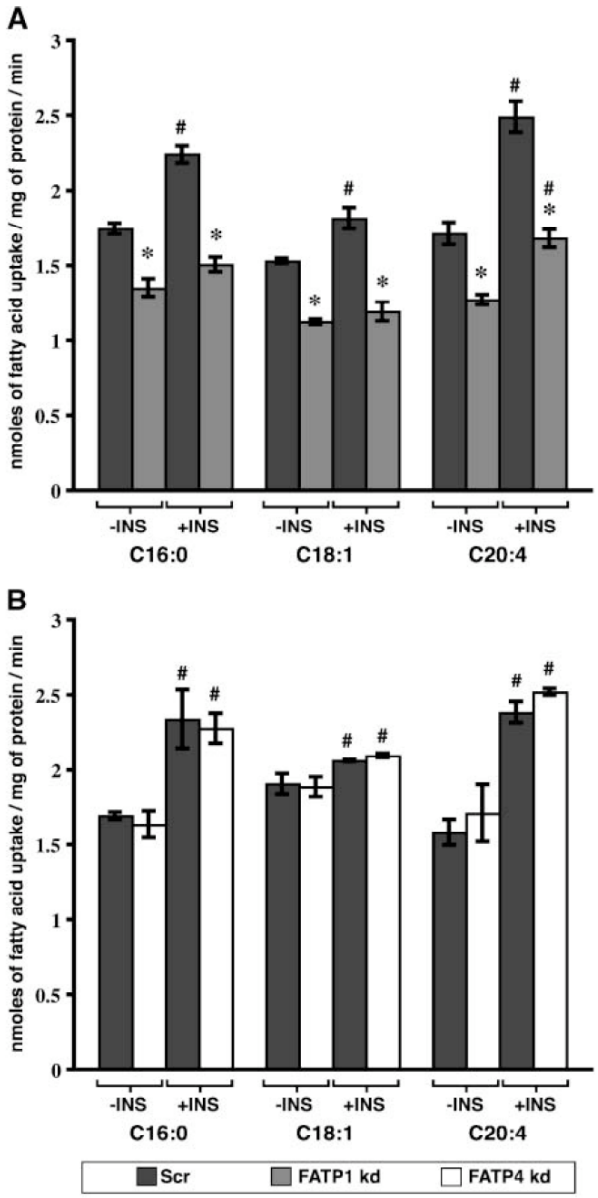

Figure 4. Fatty acid uptake in FATP1 and FATP4 knockdown adipocytes. Cellular uptake of different chain-length [^{3}H]-fatty acids in FATP1 kd (Panel A) and FATP4 kd (Panel B) 3T3-L1 adipocytes compared to the scrambled control. Day 9 differentiated serum starved 3T3-L1 adipocytes in the absence (-ins) and presence (+ins) of 50 nM insulin were incubated with 50 μM [^{3}H]-palmitic (C16:0), oleic (C18:1) or arachidonic acid (C20:4) bound to albumin to produce a free unbound concentration of LCFA of 5 nM. Influx reactions were terminated and the incorporated radioactivity determined as described in the "Experimental Procedures". Panel A; FATP1 kd (grey bars) compared to scrambled (control) adipocytes (black bars). Panel B; FATP4 kd adipocytes (white bars) compared to scrambled (control) adipocytes (black bars). The data shown is representative of three separate experiments. *, $P < 0.05$ relative to Scr control cultures; #, $P < 0.05$ relative to nonstimulatory basal conditions. Y-axis error bars = +/- standard deviation.

Despite FATP4 having the highest acyl-CoA synthetase enzyme reaction rates relative to other cellular acyl-CoA synthetases such as FATP1 and ACSL1, FATP4 kd adipocytes did not demonstrate any change in [^{3}H]-palmitic, -oleic or -arachidonic acid uptake relative to the control cells under both basal and insulin-stimulated conditions (Figure 4B). This is in agreement with the results of fatty acid influx studies carried out with different stable HEK-293 cell lines expressing varying amounts of FATP4 (Figure 5). The amounts of FATP4 expressed by each individual cell line was analyzed by immunoblotting and densitometric analysis and represented as arbitrary FATP4 units. As shown in Figure 5A, the acyl-CoA synthetase activity for a C24:0 fatty acid substrate analyzed with cell extracts from the different HEK-293 cell lines varied proportionately to the amount of FATP4 being expressed. However, the varying expression levels of FATP4 in HEK-293 cells did not affect the rate of cellular fatty acid influx for [^{3}H]-oleic acid (Figure 5B). Thus unlike FATP1, FATP4 is not translocated to the plasma membrane in response to insulin and is not rate-limiting for basal or insulin-stimulated fatty acid uptake.

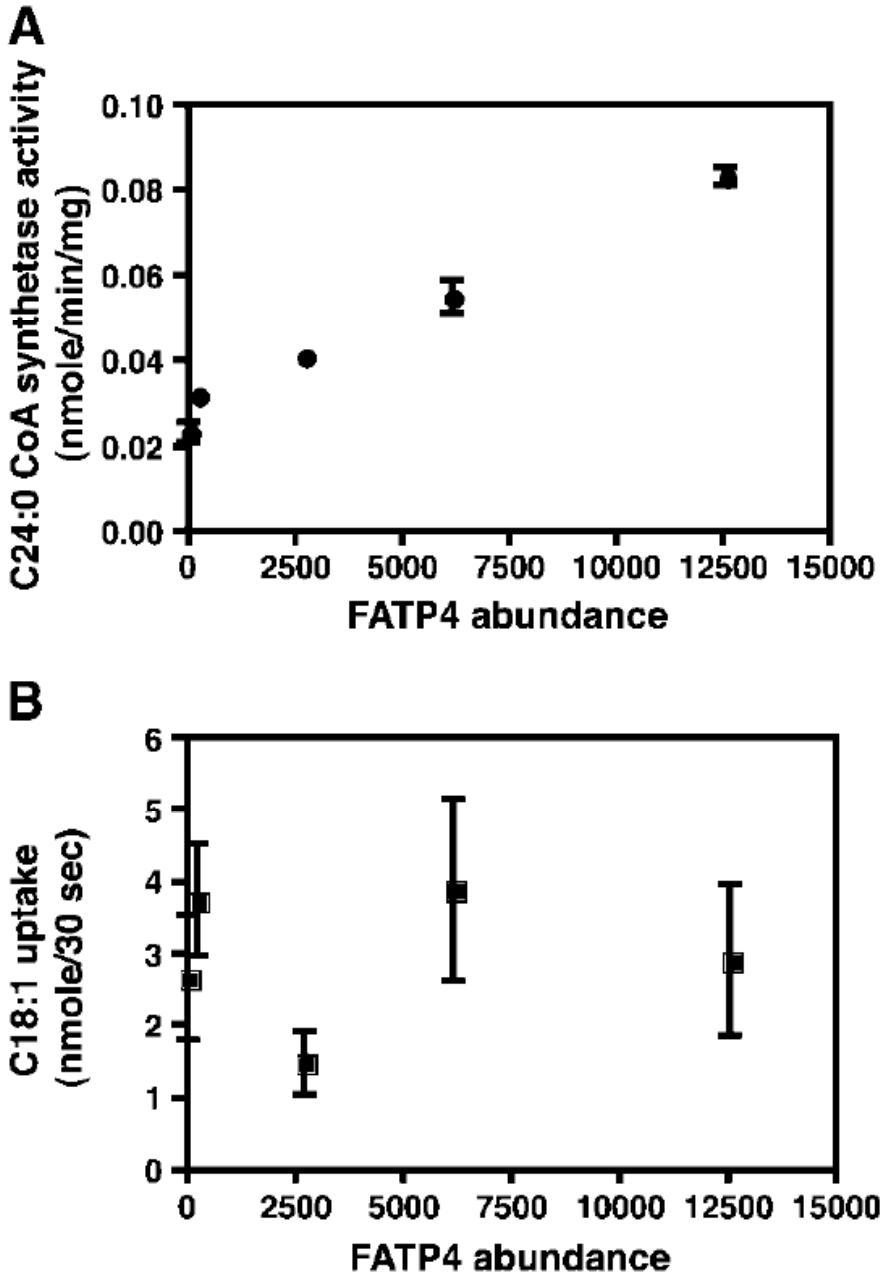

Figure 5. Acyl-CoA synthetase activity of HEK-293 cells overexpressing FATP4. Comparative analysis of cellular lignoceroyl (C24:0) CoA synthetase activity (Panel A) and oleic acid (C18:1) influx (Panel B) studies carried out with different stable HEK-293 cell lines expressing varying amounts of FATP4. The amounts of FATP4 expressed by each individual cell line were analyzed by immunoblotting and densitometry and represented as arbitrary FATP4 units. Y-axis error bars = +/- standard deviation.

To contrast the results of fatty acid influx observed in FATP1 kd and FATP4 kd adipocytes with measures of fatty acid efflux, control, FATP1 and FATP4 kd adipocytes were evaluated for their ability to carry out basal and forskolin-stimulated lipolysis. Lipolysis was measured as the amount of glycerol and fatty acids released from cells as a result of triglyceride hydrolysis. As shown in Figure 6, glycerol and fatty acid release in control, FATP1 kd and FATP4 kd adipocytes exhibited no significant differences between all cell types under forskolin-stimulated conditions. Consistent with the smaller droplet size, FATP1 knockdown adipocytes exhibited reduced basal fatty acid release. In contrast FATP4 kd adipocytes exhibited a ~ 30% increase in glycerol and a ~ 75% increase in fatty acid release during basal lipolysis.

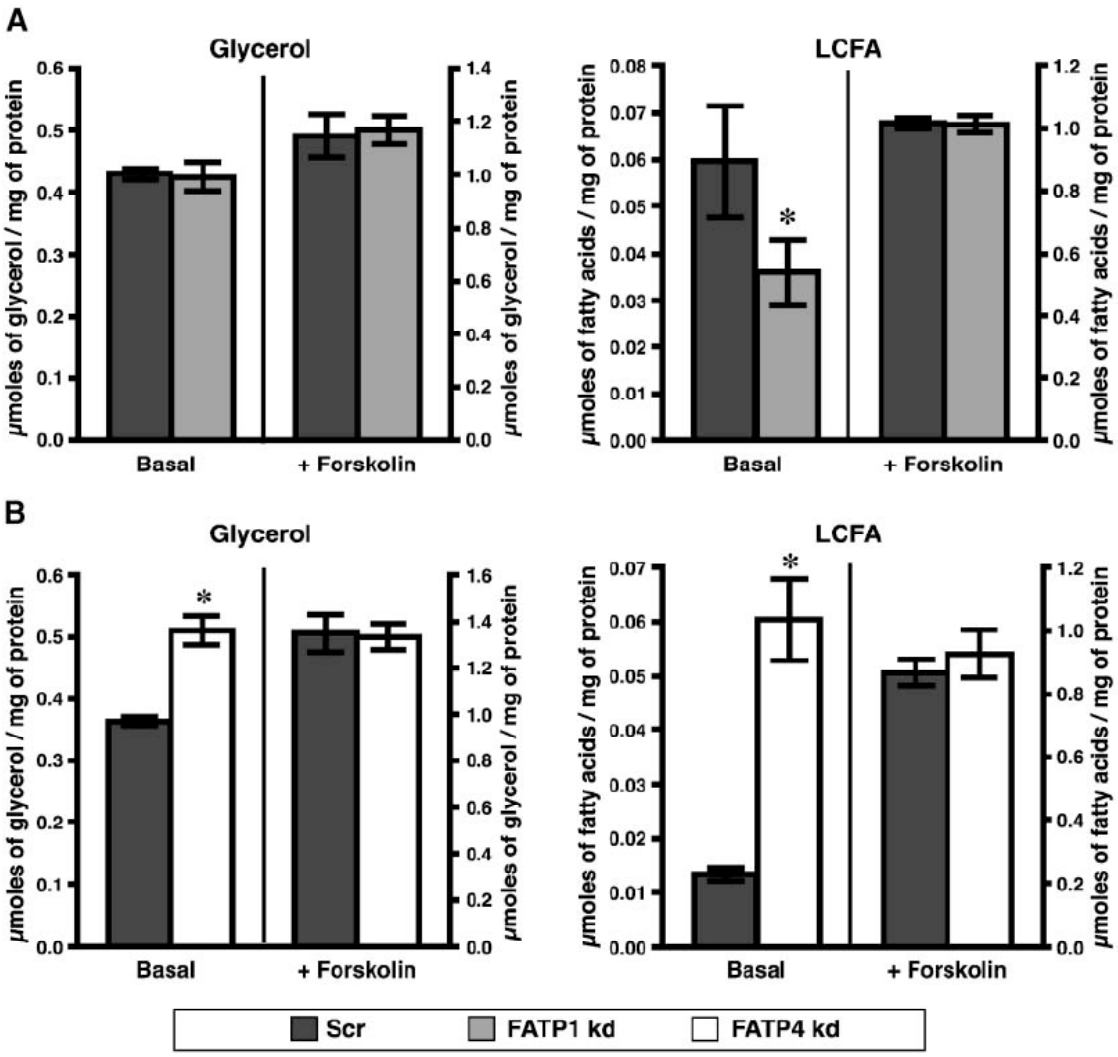

Figure 6. Analysis of basal and forskolin-stimulated lipolysis in FATP1 kd (Panel A) and FATP4 kd (Panel B) 3T3-L1 adipocytes compared to the scrambled control. Day 8 differentiated 3T3-L1 adipocytes were treated for 2 h in the absence or presence of 20 μM forskolin and aliquots of media withdrawn for measurement of glycerol and fatty acids release. The data shown is representative of three separate experiments. *, $P < 0.05$ relative to Scr control cultures. Y-axis error bars = +/- standard deviation

Insulin stimulated the translocation of FATP1 to the plasma membrane that correlated with the increase in fatty acid uptake observed in control adipocytes that was diminished in FATP1 kd adipocytes. As opposed to FATP1, FATP4 remained localized to intracellular membranes even with insulin-stimulation and did not affect fatty acid

uptake. To further understand the unique roles of these two fatty acid transporters in fat, we analyzed the differences in the metabolism of palmitate into various complex lipid pools following cellular influx in FATP1 kd, FATP4 kd and Scr adipocytes under basal and insulin-stimulatory condition. As shown in Table 2, under both basal and insulin-stimulated conditions, the vast majority of the fatty acid (greater than 90%) is activated to CoA esters and incorporated into neutral lipids, primarily triacylglycerol. A very small fraction (only 2%) of fatty acids are retained intracellularly without being metabolized (Table 2). Comparison of lipid profiles between FATP1 kd and Scr adipocytes indicated while there was an approximate ~15% decrease in total fatty acid uptake in the FATP1 kd adipocytes under basal conditions, there was essentially a 100% decrease in the insulin-stimulated fraction of uptake. A corresponding decrease in fatty acyl-CoA levels and triacylglycerol synthesis was observed in FATP1 kd adipocytes compared to the control. These results are consistent with a requirement for FATP1 in the insulin-stimulated component of LCFA influx and triacylglycerol synthesis in 3T3-L1 adipocytes. Although FATP4 did not play a role in fatty acid uptake under basal conditions, a ~40% decrease in the fatty acyl-CoA pools was observed in FATP4 kd adipocytes relative to the control (Table 3). The mechanistic basis for this is unclear but may suggest that other proteins may be rate-limiting for LCFA influx but that FATP4 plays a role in internalized lipid esterification. With insulin stimulation however, no change was observed in fatty acyl-CoA levels or in any other complex lipid class pool analyzed.

Table 2.

Complex lipid synthesis in FATP1 kd and scrambled (Scr) 3T3-L1 adipocytes

Serum starved 3T3-L1 adipocytes were incubated with [^{3}H]-palmitic acid bound to albumin for 5 minutes at 37° C in the absence (basal) and presence of 100 nM insulin. Cellular lipids were extracted, fractionated, and the incorporation of radiolabel into various lipid pools determined. The results are representative of three independent experiments, *P < 0.05 comparing experimental to the scrambled control.

	Basal		**Insulin**	
	Scr (nmoles/mg)	**FATP1 kd** (nmoles/mg)	**Scr** (nmoles/mg)	**FATP1 kd** (nmoles/mg)
Total incorporation	6.78 ± 0.25	5.83 ± 0.21*	9.00 ± 0.38	6.22 ± 0.26*
Cellular lipid class				
Fatty acids	0.09 ± 0.01	0.07 ± 0.003*	0.07 ± 0.01	0.04 ± 0.01*
Fatty acyl-CoA	0.71 ± 0.03	0.55 ± 0.03*	0.98 ± 0.07	0.78 ± 0.07*
Neutral lipids	4.32 ± 0.12	3.62 ± 0.10*	6.53 ± 0.24	4.38 ± 0.45*
Neutral lipid class				
Triacylglycerol	2.51 ± 0.13	2.13 ± 0.09*	4.69 ± 0.03	3.07 ± 0.24*
Diacylglycerol	0.13 ± 0.02	0.14 ± 0.01	0.53 ± 0.07	0.46 ± 0.02*
Monoacylglycerol	0.26 ± 0.02	0.28 ± 0.01	0.83 ± 0.09	0.71 ± 0.01*

Table 3

Complex lipid synthesis in FATP4 kd and scrambled (Scr) 3T3-L1 adipocytes

Serum starved 3T3-L1 adipocytes were incubated with [^{3}H]-palmitic acid bound to albumin in the absence (basal) and presence of 100 nM insulin. Cellular lipids were extracted, fractionated, the incorporation of radiolabel into various lipid pools determined. The results are representative of three independent experiments, *P < 0.05 comparing experimental to scrambled control.

	Basal		**Insulin**	
	Scr (nmoles/mg)	**FATP1 kd** (nmoles/mg)	**Scr** (nmoles/mg)	**FATP1 kd** (nmoles/mg)
Cellular lipid class				
Fatty acids	0.043 ± 0.01	0.047 ± 0.002	0.042 ± 0.01	0.032 ± 0.01
Fatty acyl-CoA	0.93 ± 0.04	0.59 ± 0.04*	1.01 ± 0.05	0.94 ± 0.06
Neutral lipids	3.06 ± 0.09	2.83 ± 0.25	4.13 ± 0.30	4.10 ± 0.21
Neutral lipid class				
Triacylglycerol	1.21 ± 0.05	1.31 ± 0.05	1.92 ± 0.08	1.68 ± 0.18
Diacylglycerol	0.09 ± 0.01	0.09 ± 0.01	0.07 ± 0.01	0.10 ± 0.03
Monoacylglycerol	0.21 ± 0.04	0.16 ± 0.03	0.62 ± 0.01	0.60 ± 0.02

Since both FATP1 kd and FATP4 kd adipocytes had a reduced lipid content compared to the control cells, and reduced triacylglycerol deposition is often correlated with increased hexose uptake (30,31), we evaluated the loss of each FATP isoform on basal and insulin-stimulated 2-deoxyglucose uptake. Interestingly, there was a ~30% increase in basal and insulin-stimulated glucose uptake in FATP1 kd adipocytes compared to the control (Figure 7). The increase in glucose uptake (~ 6 fold) upon insulin stimulation was the same in both adipocyte cell types. Similarly, when control and FATP4 knockdown cells were evaluated for 2-deoxyglucose uptake, cells lacking FATP4 exhibited a ~20% increase in insulin-stimulated but no change in basal glucose uptake.

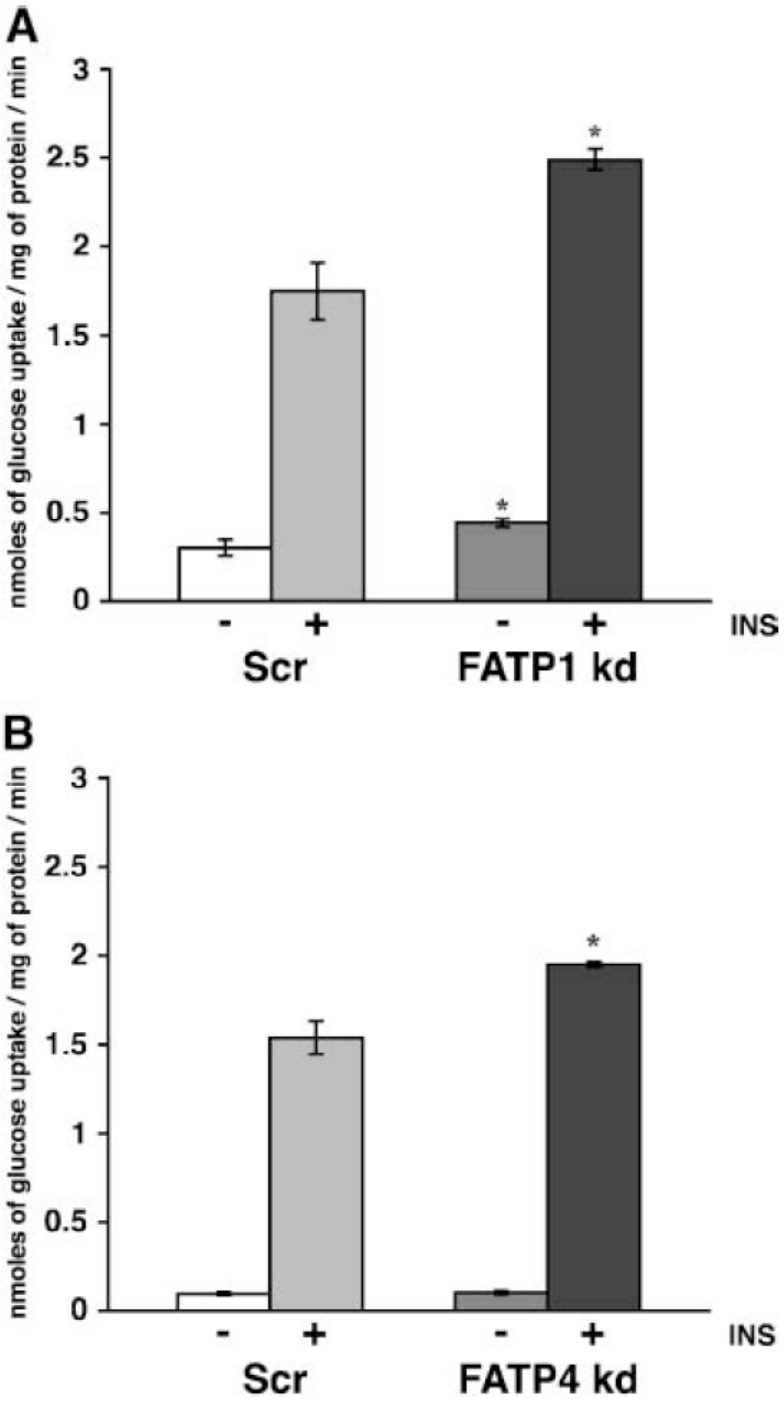

Figure 7. **Basal and insulin-stimulated 2-deoxyglucose uptake in FATP1 kd (Panel A) and FATP4 kd (Panel B) 3T3-L1 adipocytes compared to the scrambled control.** Day 9 differentiated serum-starved 3T3-L1 adipocytes were incubated with [^{14}C] 2-deoxy-D-glucose in the absence and presence of 100 nM insulin (INS) as described in "Experimental Procedures" and glucose influx determined. *, $P < 0.05$ relative to Scr control cultures. Y-axis error bars = +/- standard deviation.

DISCUSSION

Since its discovery in 1994, FATP1 has been investigated for its role in fatty acid transport and regulation. Various over expression systems and a knockout mouse model have implicated FATP1 in fatty acid uptake (13,15). FATP1 transcription is regulated by multiple systems; negatively by insulin and positively by a PPARγ-dependent mechanism (32,33). Consistent with this, FATP1 expression in muscle and fat is increased in obese diabetic animals and mice null for FATP1 exhibit reduced skeletal muscle LCFA uptake and resistance to high-fat diet induced insulin-resistance (15,34). In fat cells rosiglitazone, a PPARγ agonist increases the expression of both CD36 and FATP1 suggesting that the lipid lowering effects of this insulin-sensitizing drug may be exerted at the level of adipose LCFA influx (35). Thus the identification of a precise role for FATP1 in fatty acid influx maybe crucial to understanding the mechanism of the beneficial insulin-sensitizing effects of this widely used class of drugs.

Although loss and gain of function model systems have defined a role of FATP4 as a major intestinal fatty acid transporter and in the maintenance of the skin's epidermal barrier function, its role in adipocyte fatty acid uptake and lipid metabolism is less well defined. FATP4 expression in primary human placental trophoblasts is regulated by PPARγ and retinoid X receptor (36). Genetic polymorphisms in humans support a role of FATP4 in insulin sensitivity (23). Indeed, heterozygotes for a G209S polymorphism (Ser frequency 5%) exhibited lower body mass index, lower serum fatty acids and triglycerides, reduced systolic blood pressure and diminished insulin levels. FATP4

expression levels correlate with acquired obesity that is independent of genetic background (23).

Using a lentiviral-delivered RNAi knockdown technique, we have succeeded in suppressing the FATP1/FATP4 protein expression levels in 3T3-L1 adipocytes. Interestingly, loss of FATP1 and FATP4 independently led to an increase in the expression of both C/EBPα and PPARγ. The mechanistic basis for the increase is not clear but may be related to reduced PPARγ degradation affecting negative feedback regulation of the receptor as opposed to changes in activating factors (37). Despite the increased expression of these key transcription factors, other PPARγ targets were not increased in expression including aP2/AFABP, ACSL1 and CD36. Knockdown of FATP1 or FATP4 in 3T3-L1 adipocytes affected small changes in total cellular long-chain acyl-CoA synthetase activities without influencing any change in cellular very long-chain acyl-CoA synthetase activity.

Depletion of FATP1 expression resulted in an essentially quantitative loss in insulin-stimulated oleic and palmitic acid uptake and a ~20% decrease in insulin-stimulated arachidonic acid influx. Significant reduction in FATP1 expression levels however caused only a small ~25% decrease in basal LCFA influx for all fatty acids analyzed. Depletion of FATP4 on the other hand did not affect either basal nor insulin-stimulated fatty acid uptake and over expression of FATP4 in HEK-293 cells did not affect cellular fatty acid influx rates. We (Figure 3) and others (5) have shown that in 3T3-L1 adipocytes insulin can stimulate translocation of FATP1 from intracellular membranes

to the plasma membrane. However as opposed to GLUT4, only a small fraction (estimated to be less than 10%) of total FATP1 translocated. As such, the increase in the relative abundance of the enzyme at the plasma membrane, correlates with increased LCFA influx and may be crucial to regulation of the fatty acid transport function of FATP1. Our results with FATP4 knockdown adipocytes indicate that although FATP4 has a high acyl-CoA synthetase reaction rate relative to FATP1 and ACSL1, it is localized to internal membranes and not the plasma membrane, which could be the reason why it does not contribute to either insulin-stimulated or basal fatty acid uptake. In contrast to our studies, FATP4 over expressed in COS cells (which too was localized to the endoplasmic reticulum) did result in a net increase in LCFA influx (38). It is not clear if the contradictory findings are the result of differences in the absolute level of FATP4 expression, differences in experimental assay conditions or simply a difference in the cell culture system utilized.

Our results do not eliminate the possibility of other proteins functioning in insulin-stimulated LCFA influx. Indeed, insulin-stimulated arachidonic acid uptake is not completely lost in FATP1 kd adipocytes suggesting that another acyl-CoA synthetase could participate in insulin-stimulated arachidonic acid fatty acid influx. ACSL1, which has been suggested to form a complex with FATP1 (6), could participate in some facet of insulin-stimulated or basal LCFA influx. What is not clear in the present study is what facilitates basal LCFA influx in adipocytes. Insulin stimulation of LCFA influx is fatty acid specific and is quantitatively modest (~15-40%) relative to insulin-

stimulated hexose uptake (5-20 fold). Other factors (caveolin-1, CD36, ACSL1, diffusion) are likely contributors to basal LCFA influx.

Fatty acid re-esterification within the adipocyte can vary within 30-70% during periods of basal lipolysis affecting the net output of lipid from the adipocyte (39). The basal lipolytic rate is proportional to triacylglycerol deposition and in general, larger fat cells have greater rates of basal lipolysis than do small fat cells (40). However, the mechanism and the components involved in basal lipolysis are less well characterized. Herein we show that under basal lipolytic conditions, FATP4 kd adipocytes exhibited an increase in the amount of glycerol and fatty acid released relative to a control scrambled cell line. One explanation for this is that the acyl-CoA synthetase activity of FATP4 may facilitate some component of the CoA-dependent re-esterification of fatty acids derived from basal lipolysis of the triacylglycerol droplet. Other acyl-CoA synthetases such as ACSL1 that is found to be associated with the lipid droplet may also play a role in fatty acid re-esterification during basal lipolysis (41). However, alternate explanations also exist.

Experiments analyzing the distribution of [H^3]-palmitate into various complex lipids indicate that in 3T3-L1 adipocytes, the vast majority of incoming fatty acids are converted into their acyl-CoA derivatives and preferentially shunted into the triacylglycerol synthesis pathway. In FATP1 kd adipocytes, a decrease in LCFA influx was coupled with reduced acyl-CoA levels as well as tri-, di- and monoacylglycerol pools. Importantly, the LCFA pool was not elevated but also similarly reduced,

consistent with the model that the acyl-CoA synthetase activity of FATP1 is critical for facilitating LCFA influx. These results are in agreement with the observations of Schaffer and colleagues who have shown that mutation of FATP1 serine 250 to alanine, not only reduced the catalytic activity of the enzyme, but also eliminated LCFA influx, implying that catalysis is functionally linked to uptake (42). In contrast to FATP1 kd adipocytes, FATP4 kd adipocytes revealed no change in basal or insulin stimulated cellular fatty acid influx. Under basal conditions FATP4 kd adipocytes revealed a decrease in the incorporation of [^{3}H]-palmitate into acyl-CoA pools but not triglyceride pools. The mechanistic basis for this is undetermined but may suggest that under basal conditions FATP4 functions in LCFA esterification but other proteins may mediate the rate-controlling steps in internalization. With insulin-stimulation however, no changes in the fatty acyl-CoA pools incorporating [^{3}H]-palmitate was observed which is consistent with the anti-lipolytic effects of the hormone insulin and the proposed role of FATP4 in basal lipolysis. Stalfors and colleagues (43) have recently reported that the conversion of fatty acids to triacylglycerol occurs on or around the plasma membrane of rat adipocytes. Our results herein are consistent with this view and imply that acyl-CoA production at the plasma membrane may be mechanistically linked to triacylglycerol synthesis via some type of organized lipid synthesis machinery.

Both FATP1 as well as FATP4 knockdown adipocytes exhibited increased insulin stimulated glucose uptake. FATP1 knockout mice exhibit a similar increase in insulin-stimulated glucose uptake in soleus muscle compared to wild-type mice (44). Although the increase in glucose uptake may be quantitatively modest, over time small changes in

glucose uptake have important metabolic consequences with insulin sensitivity such as those observed in FATP1 KO mice and humans expressing either the S209 or G209 polymorphism of the *FATP4* gene. In both FATP1 kd and FATP4 kd cells, the abundance of several potential lipid regulators (DAG, LCFA) (45) of insulin signaling is altered. Consequently, the development of FATP1/FATP4 kd adipocytes may provide an opportunity to identify lipid-derived signaling pathways that originate from altered triacylglycerol levels that affect insulin resistance in adipocytes.

In summary, although FATP1 and FATP4 both possess acyl-CoA synthetase enzyme activities and share a 60.3% sequence identity, they each have unique functional roles in the adipocyte. FATP1 plays a minor role in basal fatty acid uptake and by virtue of its translocation to the plasma membrane from intracellular membrane in response to insulin, plays a major role in insulin-stimulated fatty acid uptake. FATP4, is an intracellular acyl-CoA synthetase that does not play a rate-limiting role in either basal or insulin-stimulated fatty acid uptake and may be involved in fatty acid re-esterification following lipolysis. FATP1 and FATP4 by virtue of their distinctive cellular locations and roles affect triglyceride lipid droplet size and other complex lipid pools both of which have been implicated in the development of obesity and insulin resistance.

ACKNOWLEDGEMENTS

The authors would like to thank Dr. Paul Watkins for advice on selection of FATP1 and FATP4 siRNA sequences. Supported by NIH DK053189, ADA RA12 and the Minnesota Obesity Center.

REFERENCES

1. Frayn, K. N., Fielding, B. A., and Karpe, F. (2005) *Curr Opin Lipidol* **16**, 409-415
2. Lazar, M. A. (2005) *Science* **307**, 373-375
3. Zhang, J., Phillips, D. I., Wang, C., and Byrne, C. D. (2004) *Am J Physiol Endocrinol Metab* **286**, E168-175
4. Coburn, C. T., Knapp, F. F., Jr., Febbraio, M., Beets, A. L., Silverstein, R. L., and Abumrad, N. A. (2000) *J Biol Chem* **275**, 32523-32529
5. Stahl, A., Evans, J. G., Pattel, S., Hirsch, D., and Lodish, H. F. (2002) *Dev Cell* **2**, 477-488
6. Richards, M. R., Harp, J. D., Ory, D. S., and Schaffer, J. E. (2006) *J Lipid Res* **47**, 665-672
7. Zhou, S. L., Stump, D., Kiang, C. L., Isola, L. M., and Berk, P. D. (1995) *Proc Soc Exp Biol Med* **208**, 263-270
8. Trigatti, B. L., Anderson, R. G., and Gerber, G. E. (1999) *Biochem Biophys Res Commun* **255**, 34-39
9. Hall, A. M., Smith, A. J., and Bernlohr, D. A. (2003) *J Biol Chem* **278**, 43008-43013
10. Stahl, A. (2004) *Pflugers Arch* **447**, 722-727
11. Schaffer, J. E., and Lodish, H. F. (1994) *Cell* **79**, 427-436
12. Hatch, G. M., Smith, A. J., Xu, F. Y., Hall, A. M., and Bernlohr, D. A. (2002) *J Lipid Res* **43**, 1380-1389
13. Chiu, H. C., Kovacs, A., Blanton, R. M., Han, X., Courtois, M., Weinheimer, C. J., Yamada, K. A., Brunet, S., Xu, H., Nerbonne, J. M., Welch, M. J., Fettig, N. M., Sharp, T. L., Sambandam, N., Olson, K. M., Ory, D. S., and Schaffer, J. E. (2005) *Circ Res* **96**, 225-233
14. Faergeman, N. J., DiRusso, C. C., Elberger, A., Knudsen, J., and Black, P. N. (1997) *J Biol Chem* **272**, 8531-8538
15. Kim, J. K., Gimeno, R. E., Higashimori, T., Kim, H. J., Choi, H., Punreddy, S., Mozell, R. L., Tan, G., Stricker-Krongrad, A., Hirsch, D. J., Fillmore, J. J., Liu, Z. X., Dong, J., Cline, G., Stahl, A., Lodish, H. F., and Shulman, G. I. (2004) *J Clin Invest* **113**, 756-763

16. Herrmann, T., Buchkremer, F., Gosch, I., Hall, A. M., Bernlohr, D. A., and Stremmel, W. (2001) *Gene* **270**, 31-40
17. Stahl, A., Hirsch, D. J., Gimeno, R. E., Punreddy, S., Ge, P., Watson, N., Patel, S., Kotler, M., Raimondi, A., Tartaglia, L. A., and Lodish, H. F. (1999) *Mol Cell* **4**, 299-308
18. Gimeno, R. E., Hirsch, D. J., Punreddy, S., Sun, Y., Ortegon, A. M., Wu, H., Daniels, T., Stricker-Krongrad, A., Lodish, H. F., and Stahl, A. (2003) *J Biol Chem* **278**, 49512-49516
19. Herrmann, T., van der Hoeven, F., Grone, H. J., Stewart, A. F., Langbein, L., Kaiser, I., Liebisch, G., Gosch, I., Buchkremer, F., Drobnik, W., Schmitz, G., and Stremmel, W. (2003) *J Cell Biol* **161**, 1105-1115
20. Moulson, C. L., Martin, D. R., Lugus, J. J., Schaffer, J. E., Lind, A. C., and Miner, J. H. (2003) *Proc Natl Acad Sci U S A* **100**, 5274-5279
21. Hall, A. M., Wiczer, B. M., Herrmann, T., Stremmel, W., and Bernlohr, D. A. (2005) *J Biol Chem* **280**, 11948-11954
22. Herrmann, T., Grone, H. J., Langbein, L., Kaiser, I., Gosch, I., Bennemann, U., Metzger, D., Chambon, P., Stewart, A. F., and Stremmel, W. (2005) *J Invest Dermatol* **125**, 1228-1235
23. Gertow, K., Bellanda, M., Eriksson, P., Boquist, S., Hamsten, A., Sunnerhagen, M., and Fisher, R. M. (2004) *J Clin Endocrinol Metab* **89**, 392-399
24. Student, A. K., Hsu, R. Y., and Lane, M. D. (1980) *J Biol Chem* **255**, 4745-4750
25. Stewart, S. A., Dykxhoorn, D. M., Palliser, D., Mizuno, H., Yu, E. Y., An, D. S., Sabatini, D. M., Chen, I. S., Hahn, W. C., Sharp, P. A., Weinberg, R. A., and Novina, C. D. (2003) *Rna* **9**, 493-501
26. Richieri, G. V., Anel, A., and Kleinfeld, A. M. (1993) *Biochemistry* **32**, 7574-7580
27. Kaluzny, M. A., Duncan, L. A., Merritt, M. V., and Epps, D. E. (1985) *J Lipid Res* **26**, 135-140
28. Nagamatsu, K., Soeda, S., Mori, M., and Kishimoto, Y. (1985) *Biochim Biophys Acta* **836**, 80-88
29. Jiang, Z. Y., Zhou, Q. L., Coleman, K. A., Chouinard, M., Boese, Q., and Czech, M. P. (2003) *Proc Natl Acad Sci U S A* **100**, 7569-7574
30. Yamauchi, T., Kamon, J., Waki, H., Murakami, K., Motojima, K., Komeda, K., Ide, T., Kubota, N., Terauchi, Y., Tobe, K., Miki, H., Tsuchida, A., Akanuma, Y., Nagai, R., Kimura, S., and Kadowaki, T. (2001) *J Biol Chem* **276**, 41245-41254
31. de Souza, C. J., Eckhardt, M., Gagen, K., Dong, M., Chen, W., Laurent, D., and Burkey, B. F. (2001) *Diabetes* **50**, 1863-1871
32. Hui, T. Y., Frohnert, B. I., Smith, A. J., Schaffer, J. E., and Bernlohr, D. A. (1998) *J Biol Chem* **273**, 27420-27429
33. Frohnert, B. I., Hui, T. Y., and Bernlohr, D. A. (1999) *J Biol Chem* **274**, 3970-3977
34. Berk, P. D., Zhou, S. L., Kiang, C. L., Stump, D., Bradbury, M., and Isola, L. M. (1997) *J Biol Chem* **272**, 8830-8835

35. Coort, S. L., Coumans, W. A., Bonen, A., van der Vusse, G. J., Glatz, J. F., and Luiken, J. J. (2005) *J Lipid Res* **46**, 1295-1302
36. Schaiff, W. T., Bildirici, I., Cheong, M., Chern, P. L., Nelson, D. M., and Sadovsky, Y. (2005) *J Clin Endocrinol Metab* **90**, 4267-4275
37. Hauser, S., Adelmant, G., Sarraf, P., Wright, H. M., Mueller, E., and Spiegelman, B. M. (2000) *J Biol Chem* **275**, 18527-18533
38. Milger, K., Herrmann, T., Becker, C., Gotthardt, D., Zickwolf, J., Ehehalt, R., Watkins, P. A., Stremmel, W., and Fullekrug, J. (2006) *J Cell Sci* **119**, 4678-4688
39. Reshef, L., Olswang, Y., Cassuto, H., Blum, B., Croniger, C. M., Kalhan, S. C., Tilghman, S. M., and Hanson, R. W. (2003) *J Biol Chem* **278**, 30413-30416
40. Hellstrom, L., Langin, D., Reynisdottir, S., Dauzats, M., and Arner, P. (1996) *Diabetologia* **39**, 921-928
41. Brasaemle, D. L., Dolios, G., Shapiro, L., and Wang, R. (2004) *J Biol Chem* **279**, 46835-46842
42. Stuhlsatz-Krouper, S. M., Bennett, N. E., and Schaffer, J. E. (1998) *J Biol Chem* **273**, 28642-28650
43. Ost, A., Ortegren, U., Gustavsson, J., Nystrom, F. H., and Stralfors, P. (2005) *J Biol Chem* **280**, 5-8
44. Wu, Q., Ortegon, A. M., Tsang, B., Doege, H., Feingold, K. R., and Stahl, A. (2006) *Mol Cell Biol* **26**, 3455-3467
45. Chavez, J. A., Knotts, T. A., Wang, L. P., Li, G., Dobrowsky, R. T., Florant, G. L., and Summers, S. A. (2003) *J Biol Chem* **278**, 10297-10303

CHAPTER 4:

A NOVEL ROLE FOR FATTY ACID TRANSPORT PROTEIN 1 IN THE REGULATION OF TRICARBOXYLIC ACID CYCLE AND MITOCHONDRIAL FUNCTION IN 3T3-L1 ADIPOCYTES

This chapter is a reprint of the published manuscript of the same title with minor alterations. **Wiczer, B. M.** and Bernlohr, D. A. (2009) *J. Lipid Res*. In press.

Brian Wiczer's contribution to this chapter was development of all the figures and writing the entire text.

SUMMARY

Fatty acid transport proteins are integral membrane acyl-CoA synthetases implicated in adipocyte fatty acid influx and esterification. While some FATP1 translocates to the plasma membrane in response to insulin, the majority of FATP1 remains within intracellular structures, and bioinformatic and immunofluorescence analysis of FATP1 suggests that the protein primarily resides in the mitochondrion. To evaluate potential roles for FATP1 in mitochondrial metabolism we utilized a proteomic approach following immunoprecipitation of endogenous FATP1 from 3T3-L1 adipocytes and identified mitochondrial 2-oxoglutarate dehydrogenase. To assess the functional consequence of the interaction, purified FATP1 was reconstituted into phospholipid-containing vesicles and its effect on purified 2-oxoglutarate dehydrogenase evaluated. Surprisingly, FATP1 enhanced the activity of 2-oxoglutarate dehydrogenase independently of its acyl-CoA synthetase activity while silencing of FATP1 in 3T3-L1 adipocytes resulted in decreased activity of 2-oxoglutarate dehydrogenase. FATP1-silenced 3T3-L1 adipocytes exhibited decreased tricarboxylic acid (TCA) cycle activity, increased cellular NAD^+/NADH, increased fatty acid oxidation, and increased lactate production indicative of altered mitochondrial energy metabolism. These results reveal a novel role for FATP1 as a regulator of TCA cycle activity and mitochondrial function.

INTRODUCTION

Long-chain fatty acid (LCFA) flux in tissues such as cardiac and skeletal muscle, liver, and adipose is a highly regulated and complex process involving both diffusional and protein-mediated components (1-3). A number of proteins have been identified and shown to play roles in LCFA influx (2, 4-7) including fatty acid translocase/CD36, plasma membrane fatty acid-binding protein, caveolin-1, as well as fatty acid transport proteins (FATPs). Members of the FATP family are integral membrane proteins and exhibit CoA- and ATP-dependent long-chain and very long-chain fatty acyl-CoA synthetase activity (8-12). FATPs facilitate LCFA influx, at least in part, by coupling the diffusion of LCFA through the plasma membrane with CoA-esterification on the inner leaflet of the membrane in a process termed vectoral acylation (13-15).

Mammals possess six FATP isoforms (FATP1-6) that have varying tissue expression and subcellular localization (3, 16, 17). Over expression of FATPs in mammalian cells results in increased LCFA influx (9, 18-21) and several isoforms, though not all, can rescue the decrease in LCFA influx in yeast lacking the FATP homologue, Fat1p (11). In contrast, functional studies using primary adipocytes and skeletal muscle from FATP1 null mice (22) or FATP1 knockdown 3T3-L1 adipocytes (3) have shown FATP1 has only a minor role in basal LCFA influx (3, 5). Rather, consistent with the insulin-stimulated translocation of FATP1 to the plasma membrane (5), FATP1 is required for insulin-stimulated LCFA uptake (3, 5). Functional studies of FATP4 have shown that the protein does not play a role in LCFA uptake in either enterocytes (23) or

adipocytes (3) but in fat cells may function in fatty acid re-esterification following lipolysis (3).

Interestingly, the majority of FATP1 remains on intracellular structures even under insulin-stimulated conditions (3, 5), leading to the possibility of additional roles for FATP1. In this report we used a proteomic approach to identify novel FATP1-interacting proteins in 3T3-L1 adipocytes and identified mitochondrial 2-oxoglutarate dehydrogenase (OGDH), a kinetically rate-limiting step in the tricarboxylic acid (TCA) cycle, as a binding partner. Using a reconstituted FATP1 proteoliposome system we find that FATP1 enhances the activity of OGDH *in vitro* that is independent of FATP1 acyl-CoA synthetase activity. Consistent with this, OGDH activity is decreased in 3T3-L1 adipocytes stably expressing shRNA directed at FATP1. These observations are coincident with altered mitochondrial TCA cycle metabolism in the FATP1 knockdown adipocytes indicating that FATP1 is a novel regulator of mitochondrial function.

MATERIALS AND METHODS

Reagents and cell culture—Cell culture reagents were obtained from Invitrogen. Cell culture-grade porcine insulin, puromycin, methylisobutylxanthine, and dexamethasone were obtained from Sigma-Aldrich. Non-radiolabeled fatty acids were obtained from Nu-Chek Prep, Inc (Elsyian, MN). [^{3}H]-lignoceric acid was obtained from American Radiochemicals Co. [9,10-^{3}H]- and [1-^{14}C]-palmitate and [2-^{14}C]-pyruvate were obtained from GE Healthcare Life Sciences. *n*-dodecyl-β-D-maltoside was obtained

from MBL International Corp. Dioleoylphosphatidylcholine (DOPC), dioleoylphosphatidylethanolamine (DOPE), dioleoylphosphatidyl-L-serine (DOPS), and cholesterol were obtained from Avanti Polar Lipids, Inc. Antibodies were obtained as follows: Alexa Fluor 488-conjugated goat anti-rabbit IgG (Invitrogen); IRDye 700-conjugated goat anti-rabbit IgG (Li-Cor Biosciences). All other reagents were of analytical grade and obtained from Sigma-Aldrich. Differentiation and maintenance of 3T3-L1 cell lines expressing either a shRNA targeting FATP1 or a scrambled sequence was previously described (3).

3T3-L1 adipocyte cross-linking, immunoprecipitation and proteomic analysis— Formaldehyde cross-linking performed as described (24), with modifications. Briefly, day 8 3T3-L1 adipocytes were cross-linked with 0.5% formaldehyde for 10 min at room temperature and quenched with 1.5-fold molar excess Tris-HCL pH 7.5. Monolayers were lysed into RIPA buffer (50 mM Tris, pH 7.5, 100 mM NaCl, 50 mM sodium fluoride, 5 mM sodium pyrophosphate, 1% Triton X-100, 1% sodium deoxycholate, 0.1% SDS) containing protease and phosphatase inhibitors, sonicated and centrifuged at 13,000 x g for 10 min at 4 °C to prepare a detergent soluble extract. FATP1 was immunoprecipitated overnight at 4° C using rabbit anti-FATP1 with rabbit preimmune IgG used as a negative control at the same concentration; 20 μg/mL. Immune complex were incubated with protein A-agarose beads for 1 h and washed in RIPA buffer. The immune complex beads were transferred to new tubes and boiled in SDS-loading buffer for 20 min to reverse the cross-linking. The supernatant was subjected to SDS-PAGE and stained for total protein using Sypro Ruby gel stain (Millipore).

Proteomic analysis was applied to either isolated gel bands or the entire sample lane. To analyze the sample lane, the gel segments containing the immunoglobulin heavy chain and light chain bands were excised and discarded. The remaining lane fragments were divided into 10 fractions, reduced and cysteine residues alkylated with iodoacetic acid. Samples were subjected to trypsin digestion for 24 hr at 37 °C and peptides were extracted from the gel and applied to a C18 Zip-Tip (Millipore), washed and eluted in 80% acetonitrile/0.1% TFA. Recovered peptides were subjected to μLC-MS/MS analysis on a LTQ-Orbitrap mass spectrometer. MS/MS spectra were searched using SEQUEST (version 27, rev. 12, ThermoFinnigan, San Jose, CA) against a non-redundant mouse proteome sequence database assuming a maximum of two missed tryptic cleavages per peptide and the results were validated and organized using Scaffold (version Scaffold_2_02_00, Proteome Software Inc., Portland, OR). Reported peptide sequence matches meet the following criteria: 1) all peptides were multiply charged, 2) the parent mass tolerance was 7 ppm, 3) two tryptic termini per peptide, and 4) a minimum of two unique peptides per match, with a minimum peptide probability of 70% as specified by the Peptide Prophet algorithm (25). Peptide sequence matches were considered positive interactions if enriched a minimum of 60-fold over the negative control based on normalized spectrum counts.

Immunofluorescence and confocal microscopy—Immunofluorescence analysis of 3T3-L1 adipocytes was performed as described (3), with minor modifications. 3T3-L1 adipocytes grown on glass cover slips were incubated with 100 nM Mitotracker Red

CMXRos (Invitrogen) for 20 min at 37 °C and fixed in pre-warmed 3.7% formaldehyde for 15 min at room temperature. Cells were permeabilized with ice-cold 75% methanol in water for 10 min at -20 °C, washed in PBS and treated with Image IT-FX enhancer (Invitrogen) for 30 min at room temperature. The cover slips were washed and incubated in blocking buffer containing 0.3% Triton X-100 then stained with the rabbit anti-FATP1 antibody and Alexa Fluor 488-conjugated goat anti-rabbit IgG sequentially, each diluted in PBS and 0.3% Triton X-100, and incubated for 1 h at room temperature. Nuclei were stained with 0.2 μg/mL DAPI in PBS for 1 minute and viewed using an Olympus FluoView FV1000 inverted confocal microscope. The images were acquired and analyzed using FluoView software.

Purification and reconstitution of FATP into small unilamellar vesicles (SUVs)— Purification of murine FATP1-Myc/His was performed as previously described (8, 10). Purified FATP1 was buffer exchanged into buffer A (100 mM Tris, pH 7.5, 150 mM NaCl, 20% (v/v) glycerol) using a desalting column (Zeba Desalt Spin Columns, Thermo Scientific). For reconstitution, lipids dissolved in chloroform were mixed, dried under nitrogen, and buffer A was added for 1 h at room temperature. The lipid solution was vortexed briefly and sonicated until the solution changed from milky to clear. The resulting small unilamellar vesicles (SUVs) were stored at 4 °C until used. Purified FATP1 was reconstituted into SUVs at a protein:lipid molar ratio of 1:1000. SUVs were detergent destabilized at room temperature via the addition of dodecylmaltoside to a final concentration of 3.8 mM (0.195% w/v) that lead to the onset of vesicle solubilization (26). The dodecylmaltoside concentration of purified FATP

was adjusted to 0.195%, added to the lipid-detergent solution, and allowed to incubate with gentle stirring for 10 min at 4 °C. Excess dodecylmaltoside was removed by adding CALBIOSORB adsorbent resin (Calbiochem) equilibrated in buffer A. The resin was incubated with the protein-lipid-detergent solution at 4 °C with gentle stirring and after 90 min additional resin was added to remove residual detergent. The FATP1 proteoliposomes were kept on ice and used immediately.

To analyze the orientation of reconstituted FATP1, detergent-purified or reconstituted FATP samples were incubated in the presence of trypsin (Promega) (1:50 trypsin:protein) for various lengths of time and the reaction stopped by boiling in the presence of reducing and denaturing SDS-PAGE loading buffer containing 4% SDS for 10 min. The samples were separated via SDS-PAGE using a 5-15% SDS-polyacrylamide gel and analyzed via immunoblot analysis as previously described (3). Purified or reconstituted FATP were assayed for acyl-CoA synthetase activity by the conversion of [^{3}H]-palmitic acid or [^{3}H]-lignoceric acid to their CoA derivatives by a modified method from Nagamatsu et al. (27) as previously described (3, 10).

In situ and in vitro oxoglutarate dehydrogenase activity assay—In situ oxoglutarate dehydrogenase activity was measured as described (28), with modifications. Briefly, cells were washed in HBSS (Invitrogen) and the assay was initiated upon addition of OGDH reaction buffer containing 50 mM Tris, pH 7.6, 5 mM $MgCl_2$, 0.3 mM thiamine pyrophosphate, 3 mM α-ketoglutarate, 3 mM NAD, 0.2 mM CoA, 0.1 mM $CaCl_2$, 0.05 mM EDTA, 0.5 μg/mL rotenone, 0.2% Triton X-100, 3.5% polyvinyl alcohol (MW 7,000-10,000), 0.75 mM nitrotetrazolium blue, 0.05 mM phenazine methosulfate. After

10 min at room temperature, cells were aspirated and washed in HBSS. Cells were incubated in 5% NP-40 in HBSS overnight at 37 °C and sonicated to dissolve the formazan product. Samples were centrifuged at 8,000 x g for 10 min to remove lipid and absorbance was measured at 555 nm.

For the *in vitro* activity assay, purified 2-oxoglutarate dehydrogenase complex (Sigma) (or purified pyruvate dehydrogenase complex (Sigma)) was buffer exchanged into 20 mM potassium phosphate, pH 7.3, 20% glycerol. 10 mU of dehydrogenase was assayed for 15 min at 37 °C in 250 μL of a modified reaction buffer containing 50 μM fatty acid-free BSA, 50 mM Tris, pH 7.6, 5 mM $MgCl_2$, 0.3 mM thiamine pyrophosphate, 3 mM α-ketoglutarate or 3 mM pyruvate, 3 mM NAD, 0.2 mM CoA, 0.1 mM $CaCl_2$, 0.05 mM EDTA, 5 mM potassium phosphate, 0.75 mM nitrotetrazolium blue, 0.05 mM phenazine methosulfate. The reaction was placed on ice for 5 min and centrifuged at 16,000 x g for 30 min at 4° C. The formazan pellet was dissolved by sonication and the absorbance at 555 nm measured.

Analysis of cellular and mitochondrial fatty acid oxidation—Cellular fatty acid oxidation was performed as described (29). Briefly, 3T3-L1 adipocytes were incubated in growth medium containing 50 μM L-carnitine overnight and serum-starved for 1 h in KRH containing 5.4 mM glucose, 1 mM L-carnitine, and 0.1% fatty acid-free BSA. Palmitate oxidation was initiated upon addition of 400 μM [1-^{14}C]-palmitate (2 μCi/μmol palmitate) buffered with fatty acid-free BSA (4:1 fatty acid:BSA) and incubated for 1 h at 37 °C and 5% CO_2. Media and cells were transferred to glass vials

and acidified with 70% perchloric acid. Volatilized $^{14}CO_2$ was absorbed in 1 M NaOH and transferred to liquid scintillation vials for counting. The remaining acidified sample was centrifuged at 2,000 x g at 4 °C and the radioactivity in the supernatant (acid soluble metabolites) determined by liquid scintillation counting.

For mitochondrial fatty acid oxidation, mitochondria were isolated as described (30). 100 μL isolated mitochondria were added to 1 mL fatty acid oxidation buffer (150 μM [1-^{14}C]-palmitate (4 μCi/μmole palmitate), 20 mM Tris, pH 7.4, 100 mM sucrose, 10 mM potassium phosphate, 100 mM KCl, 1 mM $MgCl_2$, 1 mM L-carnitine, 0.1 mM malate, 2 mM ATP, 0.1 mM CoA, 1 mM DTT, 0.3% fatty acid-free BSA) and incubated for 30 min at 37 °C. Reactions were acidified to terminate the reaction and the released $^{14}CO_2$ and ^{14}C-acid soluble metabolites determined by scintillation counting.

Analysis of mitochondrial pyruvate oxidation—Pyruvate oxidation was performed as described (31), with modifications. 3T3-L1 adipocytes were incubated in growth medium containing 50 μM L-carnitine overnight and isolated mitochondria were added to 1 mL pyruvate oxidation buffer (1 mM [2-^{14}C]-pyruvate (0.5 μCi/μmole pyruvate), 20 mM Tris, pH 7.4, 100 mM sucrose, 10 mM potassium phosphate, 100 mM KCl, 1 mM $MgCl_2$, 2 mM ADP, 0.1 mM CoA, 1 mM DTT) and incubated for 30 min at 37 °C. Reactions were terminated with injection of 200 μL 9 M sulfuric acid and $^{14}CO_2$ was assessed as described previously.

Metabolite quantitation—To measure lactate production, cells were incubated overnight in low-serum DMEM (high-glucose DMEM, 0.5% FBS, 50 μM L-carnitine) and the medium was collected for lactate quantitation. To measure levels of cellular NAD^+ and NADH, cells were grown as above under normal serum conditions and washed twice in PBS before nucleotide extraction. Lactate and NAD^+/NADH levels were assessed using their respective kits (BioVision) according to the manufacture's instructions.

Statistical analysis—The data are represented as the mean ± standard deviation (SD) or as the mean ± standard error of the mean (SEM) as indicated. Statistical significance was determined using the two-tail Student's *t*-test and one-way ANOVA where appropriate. $p < 0.05$ was considered to be statistically significant.

RESULTS

Previous studies on FATP1 have focused on its role in mediating long- and very long-chain fatty acid influx into adipocytes and muscle cells. As shown originally by Stahl and colleagues (5) and subsequently by Lobo et al. (3) FATP1 translocates from intracellular sites to the plasma membrane in response to insulin and such translocation mediates, in part, insulin-stimulated fatty acid influx. However, immunolocalization analysis by Lobo et al. indicated that as opposed to GLUT4 translocation, only a small percentage of FATP1 migrated to the plasma membrane, the vast majority of all FATP1 remained intracellular. Moreover, the appearance of punctate regions of immunofluorescence suggested that FATP1 may be organellar. These observations

suggested that FATP1 may play a role independent of mediating plasma membrane fatty acid influx.

Inspection of the FATP1 primary sequence and bioinformatic analysis predicted that the protein may be associated with the mitochondrion. To assess this, each of the FATP family members was evaluated using MitoProt II (32) to identify putative mitochondrial targeting sequences and the probability of mitochondrial import (Table 1). The analysis predicts with a probability greater than 95% that FATPs 1, 2, and 4 may be imported into the mitochondrion. Work by Stahl and colleagues have previously shown that FATP1 fractionates with mitochondria (5) and we were able to confirm that observation through a combination of differential centrifugation and immunoblotting (results not shown). As an independent method to demonstrate FATP1 localization with the mitochondrion, immunofluorescence microscopy was used in conjunction with the mitochondrion-specific dye, Mitotracker Red. Figure 1 shows that FATP1 co-localized with Mitotracker Red and taken together, confirms that FATP1 is, in part, localized to the adipocyte mitochondrion.

TABLE 1

Probability of murine FATP import into mitochondria.

FATP family member	Probability of mitochondrial import (%)
FATP1	**95.3**
FATP2	**99.6**
FATP3	1.9
FATP4	**97.6**
FATP5	77.7
FATP6	21.9

Peptide sequences of FATP family members were analyzed for mitochondrial targeting sequences and the probability of mitochondrial import was calculated using MitoProt II.

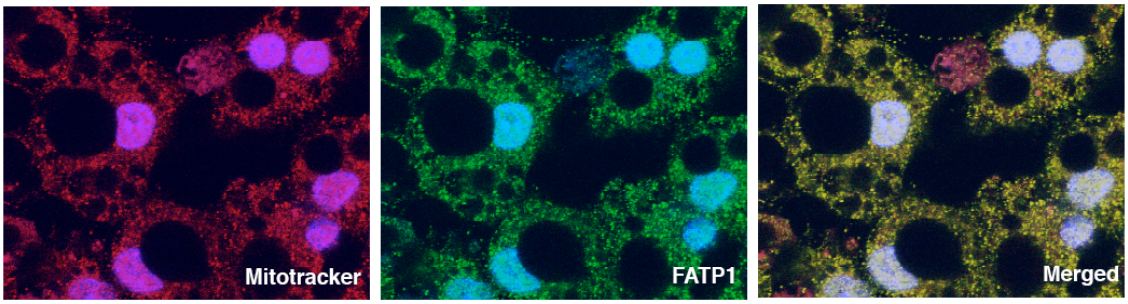

Figure 1. FATP1 co-localizes with mitochondria in 3T3-L1 adipocytes. 3T3-L1 adipocytes (day 8) were stained with Mitotracker Red and nuclei with DAPI (blue). FATP1 was detected using rabbit anti-FATP1 antibody and Alexa Fluor 488-conjugated goat anti-rabbit IgG (green).

If FATP1 resides in the mitochondrion, it is likely that it functions in conjunction with other proteins. To test this hypothesis, we undertook a proteomics approach to identify such FATP1-interacting partners. To that end, endogenous FATP1 was immunoprecipitated from detergent-solubilized 3T3-L1 adipocytes. The immune complex and associated polypeptides were subjected to SDS-PAGE (Figure 2) and

Sypro Ruby staining. A protein at ~100 kDa that was routinely observed in multiple experiments but not present in control immunoprecipitates was excised from the gel, trypsin digested and the resultant peptides analyzed via μLC-MS/MS. The peptides identified matched the E1 subunit of mitochondrial 2-oxoglutarate dehydrogenase complex (OGDH), a rate-limiting step in the TCA cycle (Figure 2, Table 2). A 90 kDa band was also observed and processed in parallel, however, its identity was not determined.

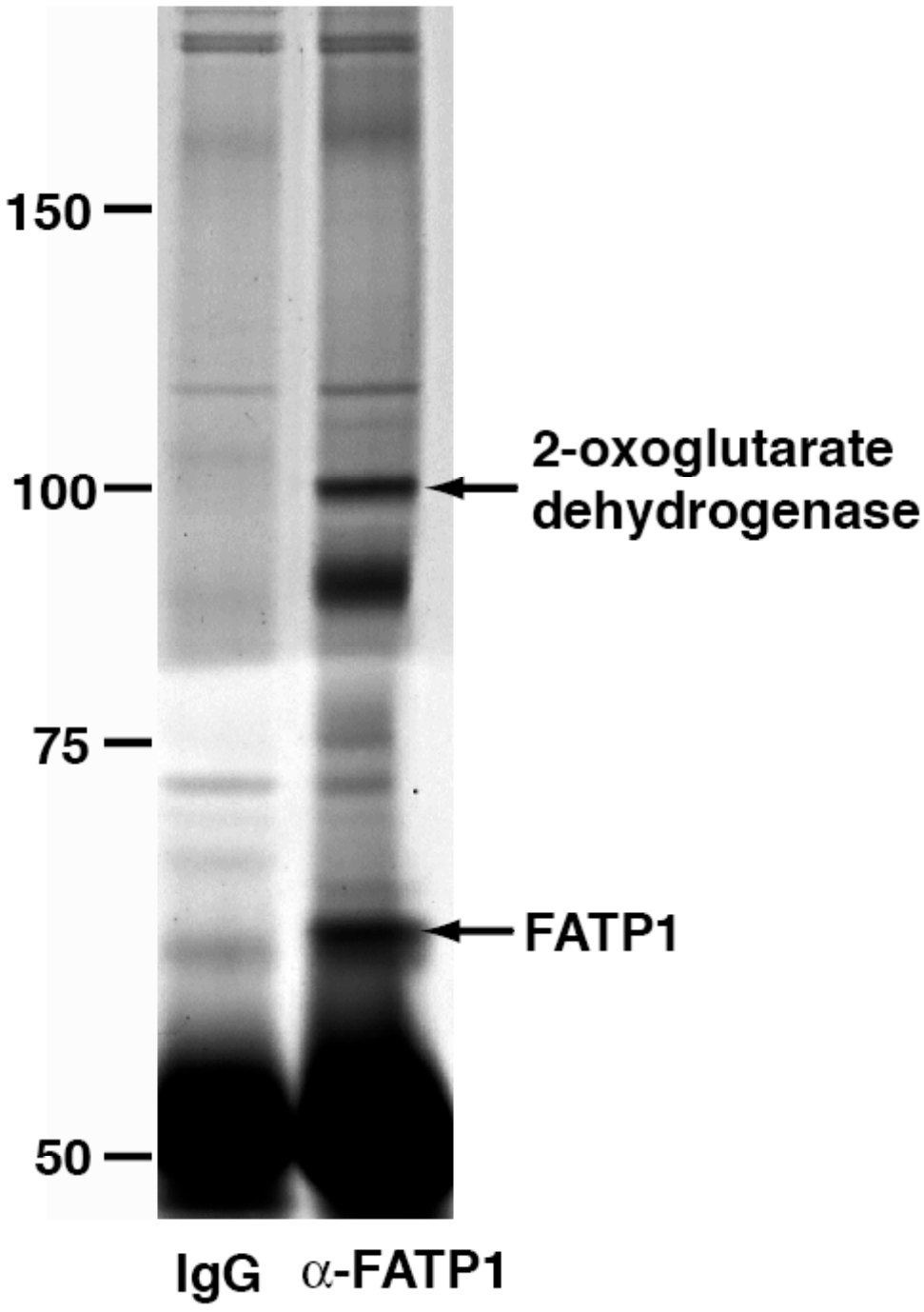

Figure 2. Immunoprecipitation of FATP1 and association with 2-oxoglutarate dehydrogenase. Control IgG or anti-FATP1 antibody was incubated with detergent-solubilized proteins from 3T3-L1 cells, immunoprecipitated, subjected to SDS-PAGE and stained with Sypro Ruby. The 100 kDa and FATP1 bands were excised and subjected to MS/MS analysis as described in Materials and Methods.

TABLE 2

Identification of ~100 kDa protein from FATP1 immunoprecipitate of 3T3-L1 adipocytes

Protein ID	Accession No.	Mass (kDa)	Seq. Cov.	Peptide Sequence	Xcorr	DCn	-log(e)
oxoglutarate dehydrogenase (E1o subunit)	NP_035086.2	116	19.1 %	(K)AEQFYCGDTEGK(K)	0	0	3
				(K)FETPGIMQFTNEEK(R)	0	0	3.85
				(R)FLDTAFDLDAFKK(F)	3.49	0.491	2.64
				(K)ICEEAFTR(S)	2.76	0.238	0
				(R)KPLIVFTPK(S)	2.69	0.201	1.47
				(K)LVEDHLAVQSLIR(A)	4.42	0.492	2.09
				(R)NITLSLVANPSHLEAADPVVMGK(T)	4.51	0.534	6.33
				(R)NMEEEVAITR(I)	3.88	0.296	0
				(K)NQGYYDYVKPR(L)	0	0	2.19
				(R)NTNAGAPPGTAYQSPLSLSR(S)	0	0	5.96
				(R)SSLATMAHAQSLVEAQPNVDK(L)	4.9	0.343	0
				(K)TKAEQFYCGDTEGKK(V)	4.93	0.529	2.72
				(K)VASSVPVENFTIHGGLSR(I)	2.94	0.38	3.2
				(K)VFHLPTTTFIGGQEPALPLR(E)	3.19	0.193	3.3

The 100 kDa band in Figure 2 was excised and subjected to MS/MS analysis as described in Materials and Methods using the X! Tandem search engine (v2007.01.01.1) in addition. Xcorr and DCn scores generated from SEQUEST and –log(e) scores generated from X! Tandem.

Because the association between FATP1 and OGDH could have formed following detergent extraction, we used formaldehyde cross-linking as an additional method to evaluate FATP1-OGDH interaction. Mild formaldehyde cross-linking of cells has been used previously to stabilize protein-protein interactions while minimizing non-specific interactions (33). In this analysis, proteins that directly associate with FATP1 plus secondary interactions between other associated proteins are revealed through the cross-

linking. Experimentally, 3T3-L1 adipocyte proteins were cross-linked with formaldehyde, immunoprecipitated with anti-FATP1 antibodies, heated to reverse the cross-links and the resultant proteins resolved by SDS-PAGE. The regions corresponding to the heavy and light chains were discarded and the remaining segment of the gel divided into 10 sections. Protein in each segment was digested with trypsin and the peptides recovered and analyzed via μLC-MS/MS sequencing. The resulting matches included the target protein FATP1 and the 2-oxoglutarate dehydrogenase complex (OGDH) (i.e., the E1, E2, and E3 subunits) (Table 3), as well as proteins involved in fatty acid synthesis and oxidation, glucose metabolism, TCA cycle and branched-chain amino acid metabolism. The level of each protein determined from the FATP1 immunoprecipitation was estimated to be at least 60-fold greater than in the control immunoprecipitates based on normalized spectral counts.

TABLE 3

Identification of proteins found in FATP1 immunoprecipitation from formaldehyde cross-linked 3T3-L1 adipocytes

Proteins Identified	Accession No.	Mol. Mass	Seq. Cov.	Unique Peptides (#)
Target Protein				
solute carrier family 27, member 1 (FATP1)	NP_036107.1	71 kDa	28.0%	17
Tricarboxylic Acid Cycle				
oxoglutarate dehydrogenase (E1o subunit)	NP_035086.2	116 kDa	50.0%	48
dihydrolipoamide S-succinyltransferase (E2o subunit)	NP_084501.1	49 kDa	41.0%	10
dihydrolipoamide dehydrogenase (E3 subunit)	NP_031887.2	54 kDa	18.0%	7
citrate synthase	NP_080720.1	52 kDa	11.0%	4
isocitrate dehydrogenase 3 (NAD+) alpha	NP_083849.1	40 kDa	7.9%	3
aconitase 2, mitochondrial	NP_542364.1	85 kDa	2.9%	2
Glycerogenesis and Glycolysis				
aldolase A, fructose-bisphosphate	NP_031464.1	39 kDa	9.3%	3
hexokinase 2	NP_038848.1	103 kDa	3.6%	3
glycerol-3-phosphate dehydrogenase 1 (soluble)	NP_034401.1	38 kDa	8.6%	2
Fatty Acid Metabolism				
acetyl-Coenzyme A acyltransferase 1	NP_570934.1	44 kDa	21.0%	8
acetyl-Coenzyme A acyltransferase 1B	NP_666342.1	44 kDa	28%	6
ATP citrate lyase	NP_598798.1	120 kDa	5.1%	5
plasma membrane associated protein, S3-12	NP_065593.2	139 kDa	4.2%	5
sterol carrier protein 2, liver	NP_035457.1	59 kDa	7.7%	4
acetyl-Coenzyme A acetyltransferase 1 precursor	NP_659033.1	45 kDa	14.0%	4
acyl-Coenzyme A dehydrogenase, medium chain	NP_031408.1	46 kDa	11.0%	4
dodecenoyl-Coenzyme A delta isomerase	NP_034153.2	32 kDa	19.0%	4
acyl-Coenzyme A dehydrogenase, long-chain	NP_031407.2	48 kDa	5.8%	2
acyl-Coenzyme A dehydrogenase, short chain	NP_031409.2	45 kDa	6.1%	2
2,4-dienoyl-CoA reductase 1, mitochondrial	NP_080448.1	36 kDa	5.1%	2
acyl-CoA synthetase long-chain family member 1	NP_032007.2	78 kDa	3.4%	2
acyl-Coenzyme A dehydrogenase family, member 11	NP_780533.2	87 kDa	2.6%	2
carnitine acetyltransferase	NP_031786.2	71 kDa	3.0%	2
Amino Acid Metabolism				
branched chain ketoacid dehydrogenase E1, beta	NP_954665.1	36 kDa	14.0%	4
branched chain ketoacid dehydrogenase E1, alpha	NP_031559.3	51 kDa	9.2%	4
branched chain aminotransferase 2, mitochondrial	NP_033867.1	44 kDa	8.9%	3
glutamate oxaloacetate transaminase 2, mitochondrial	NP_034455.1	47 kDa	8.4%	3
3-hydroxyisobutyrate dehydrogenase precursor	NP_663542.1	35 kDa	9.9%	2
Miscellaneous				
peroxisomal lon protease	NP_080103.1	95 kDa	35.0%	23
oxoglutarate dehydrogenase-like	NP_001074599.1	117 kDa	16.0%	11
unc-84 homolog B	NP_919323.2	78 kDa	13.0%	7
missing oocyte, meiosis regulator, homolog	NP_663349.2	98 kDa	11.0%	7
heat shock protein 1 (chaperonin)	NP_034607.3	61 kDa	5.2%	3
SCY1-like 1	NP_076401.1	89 kDa	3.8%	3
desmoplakin	NP_076331.2	333 kDa	1.0%	3

protein arginine N-methyltransferase 5	NP_038796.2	73 kDa	8.3%	4
adenosine monophosphate deaminase 2 (isoform L)	NP_083055.1	92 kDa	5.8%	4
epoxide hydrolase 2, cytoplasmic	NP_031966.2	63 kDa	12.0%	5
plakophilin 1	NP_062619.1	81 kDa	4.0%	3
nucleoside diphosphate kinase 4	NP_062705.1	21 kDa	31.0%	4
TANK-binding kinase 1	NP_062760.2	83 kDa	8.2%	5
stratifin	NP_061224.2	28 kDa	9.3%	3
heat shock protein 1, beta	NP_032328.2	83 kDa	3.6%	2
mitochondrial ribosomal protein S36	NP_079645.1	11 kDa	34.0%	3
glutamyl-prolyl-tRNA synthetase	NP_084011.1	170 kDa	2.1%	2
G protein, beta polypeptide 2 like 1	NP_032169.1	35 kDa	8.2%	2
ubiquitin A-52 residue ribosomal protein fusion product 1	NP_001098627.1	15 kDa	23.0%	2
mitochondrial carrier, adenine nucleotide translocator	NP_031476.3	33 kDa	8.4%	2
sec13-like protein isoform a	NP_001034177.1	40 kDa	6.1%	2
actin, gamma, cytoplasmic 1	NP_033739.1	42 kDa	10.0%	2
poly(rC) binding protein 1	NP_035995.1	37 kDa	7.0%	2
ATP synthase, mitochondrial F1 complex, gamma subunit	NP_001106209.1	30 kDa	7.7%	2
trimethyllysine hydroxylase, epsilon	NP_620097.1	50 kDa	5.5%	2
mitochondrial carrier, citrate transporter	NP_694790.1	34 kDa	5.1%	2

Differentiated 3T3-L1 adipocytes were cross-linked with 0.5% formaldehyde, and FATP1 immunoprecipitated. The resultant proteins were separated by SDS-PAGE and subjected to MS/MS analysis as described in Methods and Materials. All identified proteins were enriched at least 60-fold compared to control IgG immunoprecipitate.

To address the association between FATP1 and OGDH directly, we evaluated the influence of FATP1 on the activity of purified OGDH. We previously reported that the activity of purified FATP1 in dodecylmaltoside (DDM)-micelles is unstable at 37 °C and is rapidly lost within minutes while being stable for several hours at 4° C (10). Since many integral membrane proteins are unstable unless reconstituted into lipid bilayers, we produced FATP1-containing proteoliposomes and evaluated the effects of reconstitution on FATP1 activity. FATP1 was reconstituted using glycerophospholipids that contained oleoyl side chains at the *sn*-1 and *sn*-2 positions since these phospholipids exhibit gel-to-liquid crystal transition temperatures below 4 °C, keeping the lipid bilayer fluid during the reconstitution. Preformed small unilamellar vesicles (SUVs) were detergent-destabilized prior to the addition of purified protein and were

successfully reconstituted into mixed DOPC:DOPE (3:1) vesicles based on the migration of FATP1 in a 15-60% sucrose gradient (results not shown).

FATP1 is predicted to have a single transmembrane domain separating a 4-10 amino acid N-terminal domain from the catalytic region (34). This suggested that limited tryptic proteolysis could be used to determine the fraction of FATP1 orientated toward the outside of the vesicle versus that orientated inside of the vesicle. Using trypsin sensitivity and an antibody directed towards the catalytic region (amino acids 192-215), FATP1 in DDM-micelles was rapidly proteolyzed producing an immunoreactive stable core peptide of 25 kDa (Figure 3A). Reconstituted FATP1 was also rapidly and completely proteolyzed generating an immunoreactive stable core peptide of 15 kDa. These results suggested that FATP1 was orientated essentially unidirectionally in an inside-out manner with the catalytic domain located on the exofacial side of the SUV. This characteristic allowed subsequent assessment of acyl-CoA synthetase activity as previously performed in DDM-micelles. Reconstituted FATP1 exhibited a slightly altered structural conformation resulting in the increased accessibility of at least one trypsin cleavage site as observed by the appearance of a core 15 kDa cleavage product, rather than the 25 kDa product found for trypsinized FATP1 in DDM-micelles. To compare the thermostability of reconstituted FATP1 in SUVs to that purified in DDM, the acyl-CoA synthetase activity of FATP1 at 37 °C was monitored as a function of time (Figure 3B). The acyl-CoA synthetase activity of FATP1 in DDM-micelles was lost rapidly with a half-life ($t_{1/2}$) of ~1 min. In contrast, reconstituted FATP1 exhibited increased thermostability at 37 °C with a half-life of 30-60 min. The activity of

reconstituted FATP1 was essentially unaffected by changes in the phospholipid composition or addition of cholesterol (results not shown).

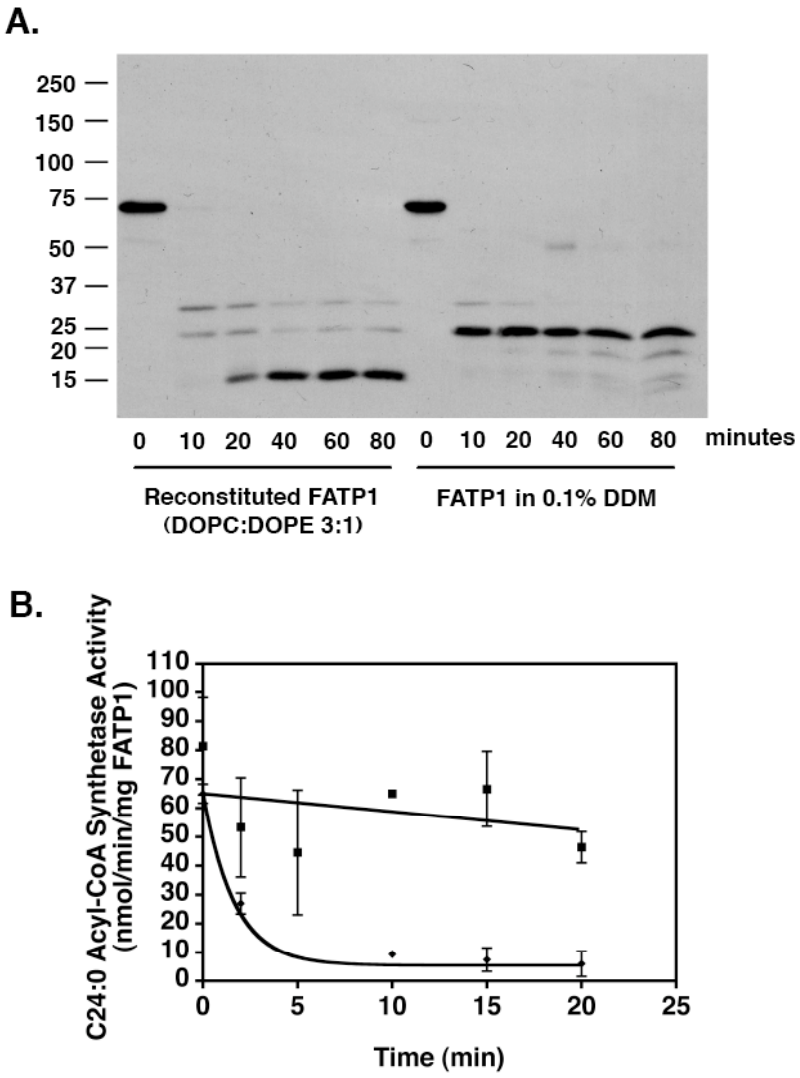

Figure 3. Reconstitution of FATP1 into small unilamellar vesicles and increased thermostability. A. Reconstituted FATP1 in lipid vesicles comprised of DOPC:DOPE (3:1) or purified FATP1 in DDM-micelles were subjected to trypsin cleavage (1:50 trypsin:protein) for the times indicated, aliquots were removed, added to 4% SDS, subjected to SDS-PAGE and immunoblot analysis using the anti-FATP1 antibody. Numbers on the y-axis represent M_r in kilodaltons. B. Samples of purified FATP1 in DDM-micelles (♦) or reconstituted FATP1 (■) were incubated at 37 °C for 0-20 min. After incubation for the indicated times, the acyl-CoA synthetase activity of the samples was assessed using lignoceric acid (C24:0) as the substrate. Data points are represented as the mean ± SD. The data shown are representative of three independent experiments.

OGDH activity is inhibited *in vitro* by fatty acyl-CoAs at micromolar levels (35-40). Because of this, we hypothesized that FATP1 would potentially act as an OGDH inhibitor via it's acyl-CoA synthetase activity. Having established functional and stable FATP1 proteoliposomes, we assessed the activity of OGDH in the absence or presence of FATP1. Surprisingly, FATP1 enhanced OGDH activity over two-fold and was independent of ATP and fatty acids (Figure 4A). Additionally, the increase in OGDH activity was dependent on the concentration of FATP1 (Figure 4B). Taken together, these results indicate that FATP1 is an OGDH activator independently of acyl-CoA production.

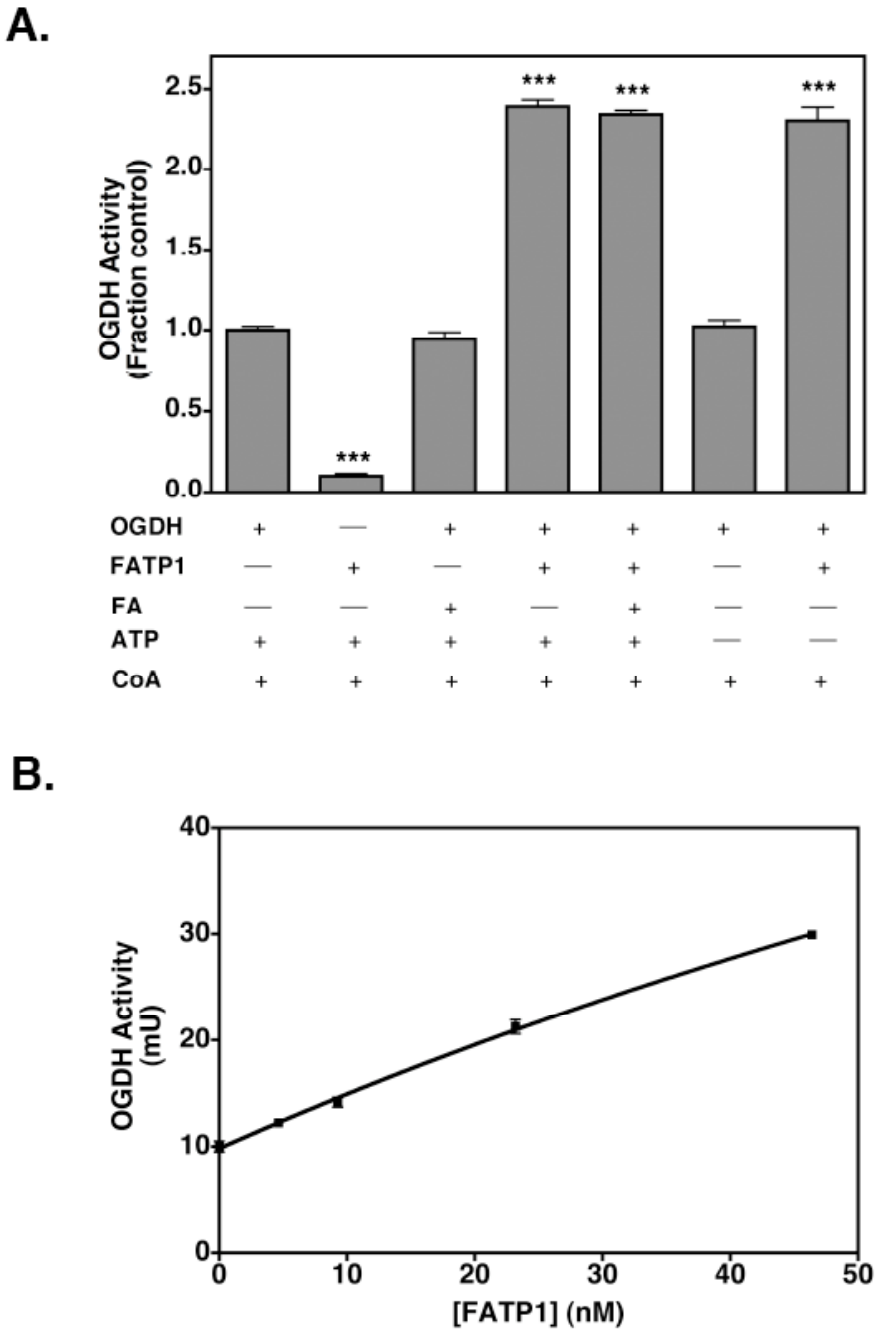

Figure 4. FATP1 enhances activity of OGDH *in vitro*. A. The activity of purified OGDH (10 mU) was assessed in the presence or absence of FATP1 proteoliposomes (20 nM FATP1), 250 μM palmitate (FA), or 3 mM ATP. An equivalent amount of lipid vesicles were added when FATP1 was absent. n = 3, mean ± SEM. Statistical analysis using one-way ANOVA with Newman-Keuls post-hoc analysis. B. The activity of OGDH was assessed in the absence of ATP and palmitate with increasing concentrations of reconstituted FATP1. Amount of lipid vesicles present was constant. n = 3, mean ± SEM. ***, $p < 0.001$ relative to OGDH alone.

To determine if the ability of FATP1 to enhance OGDH activity occurred in a cellular context we took advantage of a 3T3-L1 adipocyte cell line stably expressing shRNA directed against FATP1 that we had previously established (Figure 5A, (3)) and accessed OGDH activity. Corroborating the *in vitro* data, OGDH activity was decreased 20% in the FATP1 knockdown adipocytes compared to the scramble shRNA-expressing adipocytes (Figure 5B). This suggests that FATP1 is a physiological regulator of OGDH.

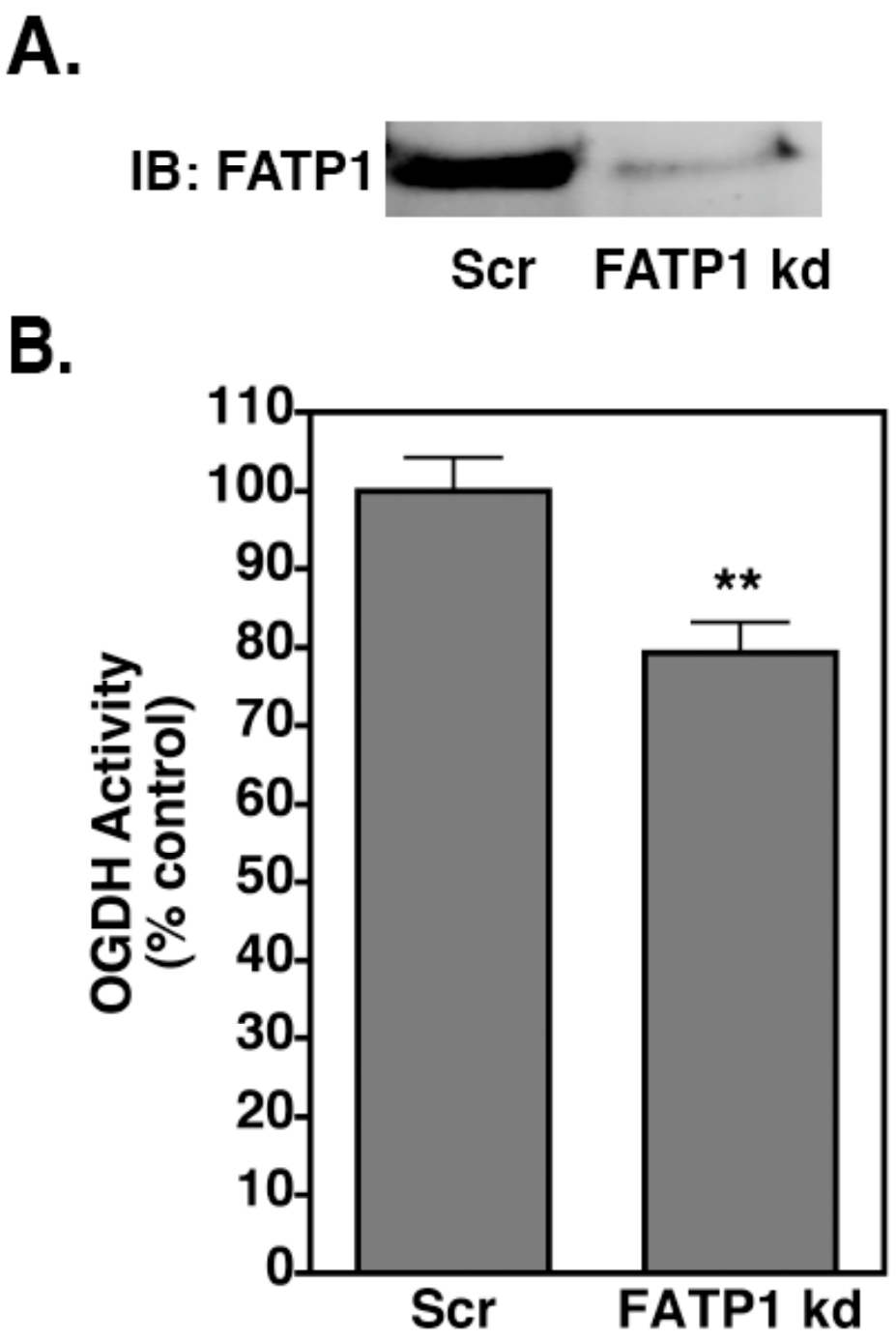

Figure 5. Analysis of OGDH activity in FATP1-silenced adipocytes. Expression of FATP1 in 3T3-L1 adipocytes stably expressing a scrambled (Scr) or FATP1 shRNA (FATP1 kd) (A) were assayed for OGDH activity for 10 min (B) as described in Materials and Methods. n = 6, mean ± SEM. **, $p < 0.01$ relative to Scr.

Because OGDH is a rate-limiting step in the TCA cycle, the decrease in OGDH activity in the FATP1 knockdown adipocytes could also result in decreased TCA cycle activity. To assess this, the rate of [2-^{14}C]-pyruvate oxidation was evaluated as a measure of TCA cycle activity (31). As shown in Figure 6A, mitochondria isolated from FATP1 knockdown adipocytes exhibited a 60% reduction in the rate of [2-^{14}C]-pyruvate oxidation compared to that in the control mitochondria indicating a decrease in TCA cycle activity that is consistent with the decrease in OGDH activity.

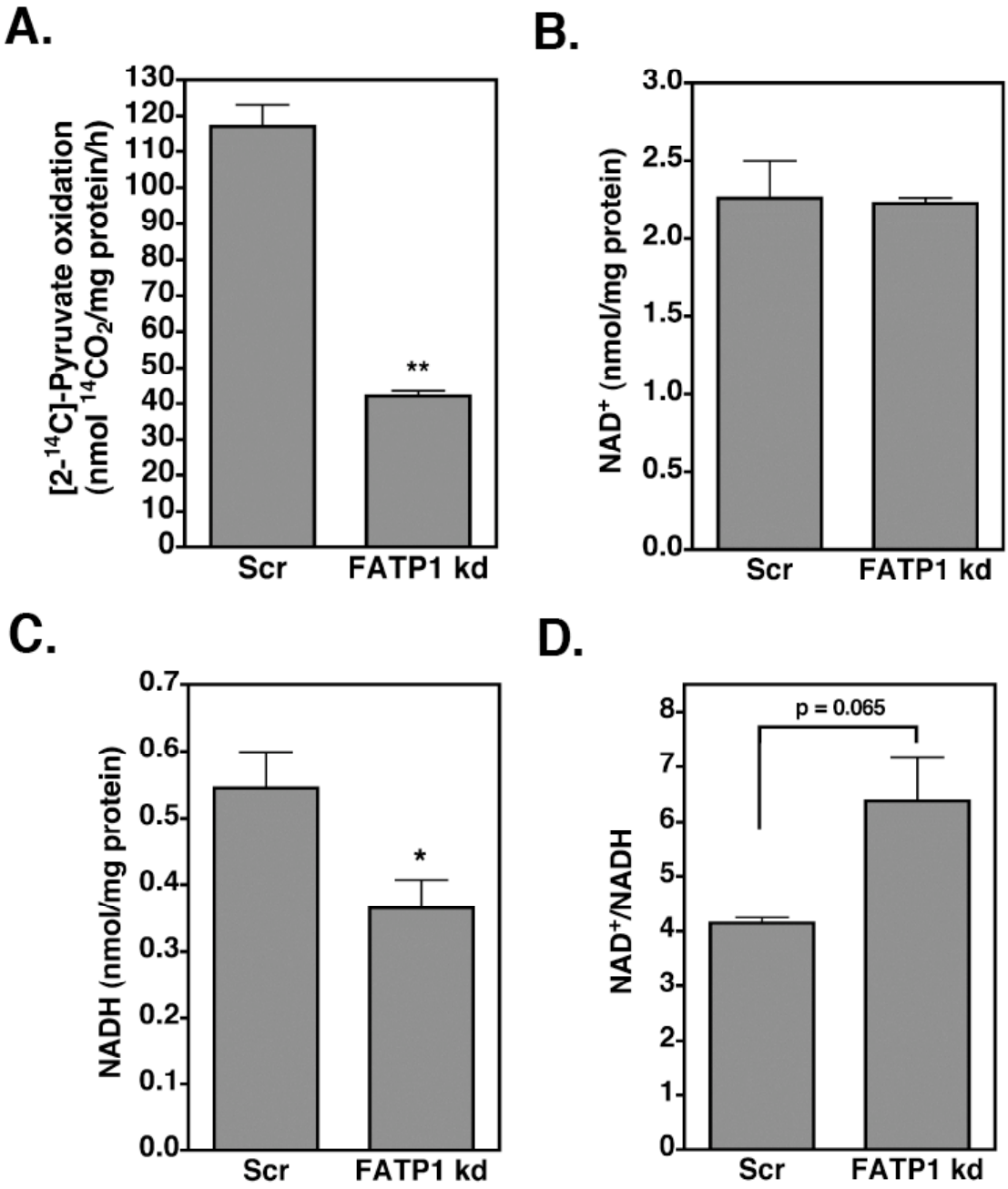

Figure 6. TCA cycle activity is decreased in the FATP1 knockdown adipocytes. A. Mitochondria from 3T3-L1 Scr or FATP1-silenced adipocytes pretreated with 50 μM L-carnitine overnight were isolated and incubated with 1 mM [2-^{14}C]-pyruvate for 30 min in pyruvate oxidation buffer and $^{14}CO_2$ determined. n = 3, mean ± SEM. B-D. 3T3-L1 Scr or FATP1 knockdown adipocytes were treated similarly and NAD^+ (B), NADH (C) and the NAD^+/NADH ratio determined (D). n = 4, mean ± SEM. *, $p < 0.05$; **, $p < 0.01$ relative to Scr.

Because TCA cycle function plays an important role in the cellular redox status, we measured the NAD^+ and NADH levels in the FATP1 knockdown cells. NAD^+ levels were unchanged in the FATP1-silenced adipocytes compared to scramble adipocytes, while NADH levels were decreased 33% (Fig. 6B, 6C). There was no statistical change in total NAD levels, however (data not shown). This resulted in a 50% increase in the cellular NAD^+/NADH ratio (Figure 6D) and is consistent with decreased TCA cycle activity.

The inability to derive energy from mitochondrial metabolism is frequently accompanied by increased metabolism of glucose and fatty acids to compensate for the energy deficiency. This suggests that the FATP1-silenced adipocytes may exhibit increased glucose metabolism and lactate production. Consistent with this view, lactate production was increased 2.4-fold in the FATP1 knockdown adipocytes (Figure 7A). Similar metabolic changes were seen in cellular fatty acid oxidation, where total fatty acid oxidation increased 13% (Figure 7B). This was due to a 24% increase in the acid soluble metabolites (ASM) produced, while complete oxidation of fatty acids (i.e., fatty acids oxidized to CO_2) decreased 30%, consistent with a defect in TCA cycle activity. To eliminate the possibility that the change in fatty acid oxidation is due to other peripheral changes in lipid and glucose metabolism, fatty acid oxidation was measured in isolated mitochondria from the FATP1-silenced cells (Figure 7C). Similarly, total fatty acid oxidation in isolated mitochondria was increased 17% compared to scramble adipocytes and predominantly due to a 17% increase in ASM. However, unlike what was measured for cellular fatty acid oxidation, complete fatty acid oxidation in isolated

mitochondria was increased 11% compared to the scramble adipocytes. This difference may arise from the absence of glucose metabolism in the isolated mitochondria. Consistent with this, the presence of pyruvate attenuates CO_2 production from fatty acids without effecting total fatty acid oxidation (data not shown).

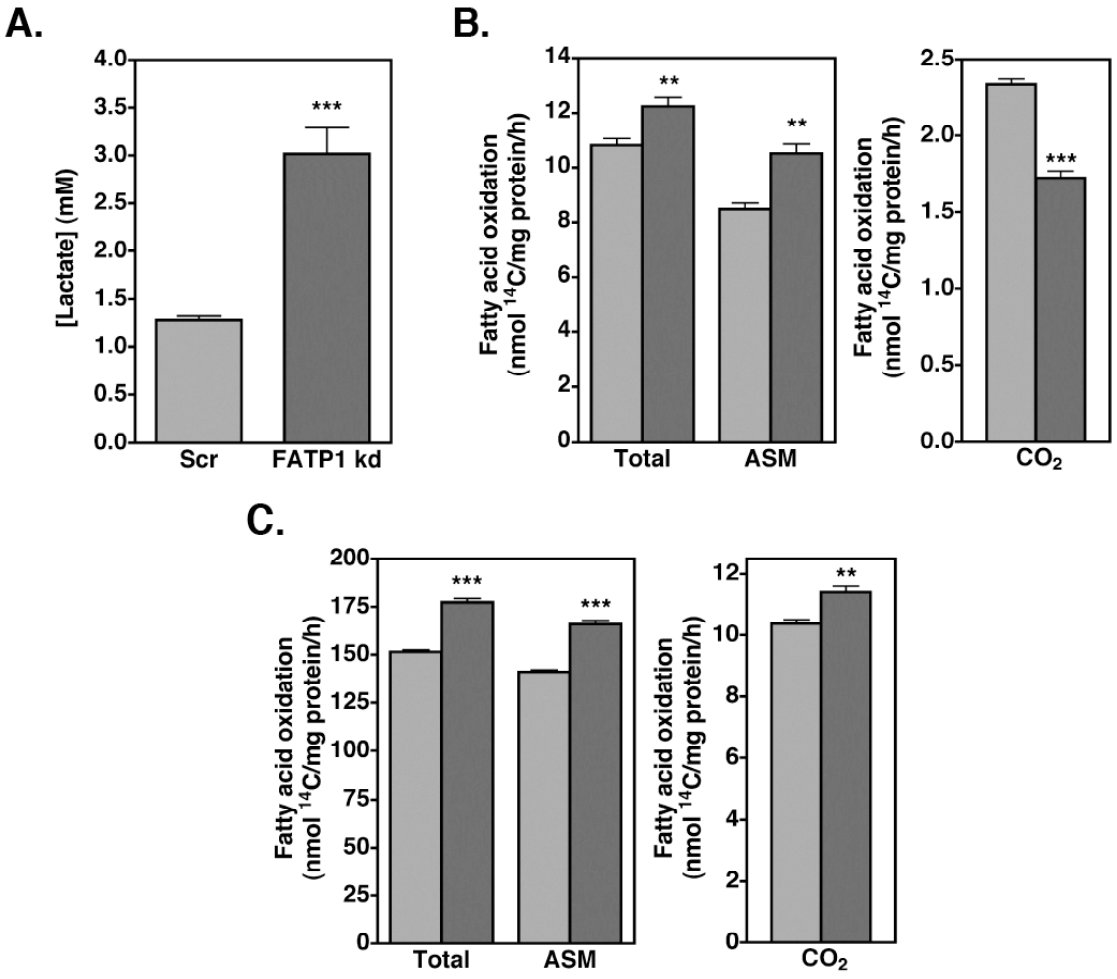

Figure 7. Lactate production and fatty acid oxidation are increased in the FATP1-silenced adipocytes. A. Lactate in the culture media. n = 6, mean ± SEM. B & C. 3T3-L1 Scr (*light gray*) or FATP1 knockdown (*dark gray*) adipocytes were pretreated with 50 μM L-carnitine overnight and fatty acid oxidation assessed in the adipocytes (B) or isolated mitochondria (C) using [1-^{14}C]-palmitate. B. n = 6, mean ± SEM. C. n = 4, mean ± SEM. ASM, acid soluble metabolites; Total, ASM + CO_2. **, $p < 0.01$; ***, $p < 0.001$ relative to Scr.

DISCUSSION

FATP1 has been previously demonstrated to play a vital role in insulin-stimulated LCFA influx, both in adipocytes (3, 5) and skeletal muscle (5). Consistent with the role of FATP1 in LCFA uptake, FATP1 translocates from intracellular membranes to the plasma membrane upon insulin-stimulation, however a large fraction of FATP1 remains on intracellular structures (3, 5). Several reports have noted the wide subcellular distribution of FATP1 in adipocytes and muscle (3, 5, 41, 42), implying that FATP1 has additional roles in these tissues. Using 3T3-L1 adipocytes as a model system, we took a multidimensional approach to elucidate additional functions of FATP1. Using a combination of immunoprecipitation of endogenous FATP1 and mild formaldehyde cross-linking to stabilize protein-protein interactions, we identified proteins of the 2-oxoglutarate dehydrogenase complex (OGDH) as a likely binding partner for FATP1. In the absence of cross-linking, the E1 subunit of OGDH was identified as the major FATP1 associated protein (Figure 2, Table 2). Using cross-linking, a large number of mitochondrial and mitochondrially associated proteins were identified consistent with a large supramolecular complex of multiple proteins and functional activities. Amongst those identified in the cross-linking experiment was long-chain acyl-CoA synthetase 1 (ACSL1). Schaffer and colleagues previously co-immunoprecipitated epitope-tagged FATP1 and ACSL1 using lentiviral over expression in 3T3-L1 adipocytes (15). Recent work has shown that ACSL1 is not involved in LCFA influx in adipocytes but may be linked to re-esterification of fatty acids following lipolysis (43). Therefore, the true function of the FATP1-ACSL1 interaction is still unknown. These results in sum conclude that FATP1 is a mitochondrially-associated protein. Consistent with this, both

bioinformatic analysis and immunofluorescence microscopy indicated that FATP1 is localized to mitochondria in 3T3-L1 adipocytes (Table 1, Figure 1). Moreover, during the preparation of this manuscript, Garcia-Martinez and colleagues published work demonstrating that FATP1 localizes to mitochondria in both cultured myotubes and human skeletal muscle (44). As such, findings in multiple systems conclude that FATP1 has additional functions beyond facilitating fatty acid influx.

In order to determine whether the proposed FATP1-OGDH interaction is functionally significant, we developed detergent-free FATP1 proteoliposomes for *in vitro* analysis. FATP1 purified in DDM-micelles is unstable at 37 °C (Figure 3B). However, reconstitution of FATP1 into SUVs resulted in the surprising finding that the enzyme activity was markedly stabilized when maintained at 37 °C. Characterization of FATP1 proteoliposomes revealed an approximately 30-fold increase in thermostability compared to FATP1 in DDM-micelles (Figure 3B). These changes in protein function may be explained by an altered structural conformation in the N-terminal catalytic domain. Consistent with this view tryptic cleavage of reconstituted FATP1 resulted in a stable 15 kDa protein fragment containing amino acids 192-215 of the N-terminal catalytic domain in contrast to the stable 25 kDa protein fragment generated from FATP1 in DDM-micelles (Figure 3A). Because the lipid vesicles represent a more physiological environment and result in increased thermostability of FATP1, the altered structure of FATP1 is believed to represent the natural conformation found *in vivo*. This suggests that FATP1 proteoliposomes could be used in subsequent *in vitro* studies.

Using FATP1 proteoliposomes and purified OGDH, we found that FATP1 enhanced OGDH activity in a concentration-dependent manner that was independent of ATP and fatty acids and, therefore, independent of the acyl-CoA synthetase activity of FATP1 (Figure 4). This observation was corroborated in the FATP1 knockdown adipocytes where OGDH activity was decreased 20% (Figure 5). Because we were unable to measure OGDH protein levels due to lack of a functional commercial antibody, we cannot rule out the possibility that OGDH levels are altered in the FATP1-silenced adipocytes. However, because FATP1 was able to enhance purified OGDH activity *in vitro*, it is strongly suggestive that the interaction is direct and that the loss of FATP1 in the silenced cells is at least in part directly responsible for the observed decrease in the OGDH activity. Fatty acyl-CoAs have been previously shown to attenuate OGDH activity *in vitro* at low micromolar levels (35-40). While we were unable to observe any OGDH inhibition in the presence of 6 μM palmitoyl-CoA (data not shown), it is likely that the lipid vesicles in this study act as a sink for fatty acyl-CoAs due to their amphiphilic nature. We therefore cannot exclude the possibility that FATP1 acyl-CoA synthetase activity influences OGDH *in vivo*.

OGDH catalyzes one of the rate-limiting steps in the TCA cycle (45, 46) and uses NAD^+ for the oxidative decarboxylation of α-ketoglutarate to succinyl-CoA, producing NADH. The NADH produced at this step and subsequent steps in the TCA cycle provide the electrons necessary for maintaining the mitochondrial membrane potential. Because TCA cycle activity is intimately linked to the cellular redox state and energy homeostasis (47-51), we hypothesized that the decrease in OGDH activity in the FATP1

knockdown adipocytes would manifest in decreased TCA cycle activity and further lead to alterations in other energy-producing pathways. We demonstrated that TCA cycle activity is decreased substantially (60%) in the FATP1 knockdown adipocyte mitochondria as measured by [2-^{14}C]-pyruvate oxidation (Figure 6A). This is consistent with the decrease in the NADH levels and, hence, increases in the NAD^+/NADH ratio (Figure 6C, D), indicating altered mitochondrial energy metabolism. Attenuated TCA cycle activity has also been linked to increases in compensatory glycolysis in the cytoplasm (52-55), in part due to the decrease flux of pyruvate through the TCA cycle, as well as increases in fatty acid oxidation (56). Accordingly, lactate production was increased over two-fold (Figure 7A) and total mitochondrial fatty acid oxidation increased 17% in the FATP1-silenced cells (Figure 7B, C). Previous work from Lobo et al. has shown that FATP1 knockdown adipocytes have a 10% increase in basal glucose uptake (3). While this would in part contribute to an increase in lactate production (57, 58), the magnitude of this increase correlates with the magnitude of the decrease in TCA cycle activity. Further work is needed to explore the mechanistic links between FATP1, TCA activity, and alterations in mitochondrial function.

The work of Garcia-Martinez and colleagues also linked FATP1 to glucose oxidation in skeletal myotubes (44). In their studies FATP1 over expression in myotubes resulted in enhanced glucose oxidation while fatty acid oxidation was decreased. These results mirror our own observations in the FATP1 knockdown adipocytes. Garcia-Martinez and colleagues also found that the increase in glucose oxidation was consistent with an increase in the activity of the pyruvate dehydrogenase complex (PDH) although the

mechanism through which FATP1 increases the activity of PDH remained unknown. PDH belongs to the 2-oxo acid dehydrogenase superfamily and includes OGDH and the branched-chain keto acid dehydrogenase complex (BCKDH). All three of these dehydrogenase complexes are structurally similar and are comprised of 3 subunits (E1, E2, and E3), where the E1 and E2 subunits are unique to each of the dehydrogenases while sharing the same E3 (59). While assessing FATP1 activation of purified OGDH using our FATP1 proteoliposome system, we found that purified PDH was similarly activated by FATP1 in a concentration-dependent manner (data not shown). This suggests that the enhancing ability of FATP1 on OGDH activity also pertains to PDH activity. Furthermore, BCKDH was also identified as a candidate FATP1-protein interaction (Table 3). Together, our data suggest the ability of FATP1 to enhance dehydrogenase activity may be conserved for all 2-oxo acid dehydrogenase superfamily members. It is unclear as to why none of the unique PDH subunits were identified as candidate FATP1-protein interactions. One explanation is that the proteins were simply excluded when the IgG gel bands were excised and discarded. Another possibility is that endogenous FATP1 interacts with PDH at relatively low stoichiometry in adipocytes, making it difficult to detect the interaction. While our current study correlates the decrease in OGDH activity with the decrease in TCA cycle activity in the FATP1 knockdown adipocytes, PDH activity within the knockdowns was not assessed. Therefore, it is possible that a decrease in PDH activity exists in the FATP1 knockdowns and may be contributing to the decreased TCA cycle activity. Further studies are needed to better understand the nature of the physical interactions between

FATP1 and the dehydrogenases and the contribution of each of the dehydrogenases to TCA cycle activity in adipocytes.

Interestingly, cardiomyocyte-specific over expression of FATP1 results in cardiac lipotoxicity (19), while *Fatp1*$^{-/-}$ mice maintain insulin sensitivity even on a high-fat diet (7). While the effects of FATP1 in these systems has been solely considered with regard to fatty acid influx, it is possible that the changes in mitochondrial FATP1 levels and the associated modulation of TCA cycle function are also contributing to these phenotypes. *Fatp1*$^{-/-}$ mice are also cold intolerant due to a defect in nonshivering thermogenesis in brown adipose tissue (60). Wu et al. indicated that FATP1 plays an important role in the early phase of thermogenesis as indicated by a decrease in oxygen consumption and CO_2 production, prior to the increase in FATP1 protein expression during the late phase of thermogenesis (60). These observations are also consistent with the decreases in TCA cycle activity and NADH levels we observed in the FATP1 knockdowns and may even result in attenuation of mitochondrial membrane potential in brown adipocytes (61). This would retard the rate of electron transport uncoupling, and, in part, attenuate thermogenesis. Additional studies are needed to confirm the role of mitochondrial FATP1 in these systems.

In summary, we demonstrate that FATP1 is localized to mitochondria and enhances OGDH activity *in vitro*. This is consistent with an attenuation of OGDH activity in cultured FATP1 knockdown adipocytes and correlates with a decrease in TCA cycle activity. Furthermore, the FATP1 knockdown adipocytes have an increased

NAD^+/NADH ratio due to decreased NADH levels. These changes in the cellular redox status correlate with the observed increase in lactate production and fatty acid oxidation in the FATP1 knockdowns. This work, along with the work of Garcia-Martinez and colleagues, reveals a novel role for FATP1 in the regulation of TCA cycle function and energy homeostasis via its protein interactions with key proteins in the TCA cycle.

ACKNOWLEDGEMENTS

We would like to thank Dr. Matthew Stone and the Minnesota Center for Mass Spectrometry and Proteomics for their assistance, the Biomedical Image Processing Lab, the University of Minnesota Supercomputer Institute, and members of the Bernlohr laboratory for their comments and discussions. Supported by 7-06-RA-12 from the American Diabetes Association to DAB.

REFERENCES

1. Kampf, J. P., and Kleinfeld, A. M. (2004) *J Biol Chem* **279**, 35775-35780
2. Coburn, C. T., Knapp, F. F., Jr., Febbraio, M., Beets, A. L., Silverstein, R. L., and Abumrad, N. A. (2000) *J Biol Chem* **275**, 32523-32529
3. Lobo, S., Wiczer, B. M., Smith, A. J., Hall, A. M., and Bernlohr, D. A. (2007) *J Lipid Res* **48**, 609-620
4. Zhou, S. L., Stump, D., Kiang, C. L., Isola, L. M., and Berk, P. D. (1995) *Proc Soc Exp Biol Med* **208**, 263-270
5. Stahl, A., Evans, J. G., Pattel, S., Hirsch, D., and Lodish, H. F. (2002) *Dev Cell* **2**, 477-488
6. Trigatti, B. L., Anderson, R. G., and Gerber, G. E. (1999) *Biochem Biophys Res Commun* **255**, 34-39
7. Kim, J. K., Gimeno, R. E., Higashimori, T., Kim, H. J., Choi, H., Punreddy, S., Mozell, R. L., Tan, G., Stricker-Krongrad, A., Hirsch, D. J., Fillmore, J. J., Liu, Z. X., Dong, J., Cline, G., Stahl, A., Lodish, H. F., and Shulman, G. I. (2004) *J Clin Invest* **113**, 756-763
8. Hall, A. M., Smith, A. J., and Bernlohr, D. A. (2003) *J Biol Chem* **278**, 43008-43013
9. Gimeno, R. E., Ortegon, A. M., Patel, S., Punreddy, S., Ge, P., Sun, Y., Lodish, H. F., and Stahl, A. (2003) *J Biol Chem* **278**, 16039-16044
10. Hall, A. M., Wiczer, B. M., Herrmann, T., Stremmel, W., and Bernlohr, D. A. (2005) *J Biol Chem* **280**, 11948-11954
11. DiRusso, C. C., Li, H., Darwis, D., Watkins, P. A., Berger, J., and Black, P. N. (2005) *J Biol Chem* **280**, 16829-16837
12. DiRusso, C. C., Darwis, D., Obermeyer, T., and Black, P. N. (2008) *Biochim Biophys Acta* **1781**, 135-143
13. Zou, Z., Tong, F., Faergeman, N. J., Borsting, C., Black, P. N., and DiRusso, C. C. (2003) *J Biol Chem* **278**, 16414-16422
14. Tong, F., Black, P. N., Coleman, R. A., and DiRusso, C. C. (2006) *Arch Biochem Biophys* **447**, 46-52
15. Richards, M. R., Harp, J. D., Ory, D. S., and Schaffer, J. E. (2006) *J Lipid Res* **47**, 665-672
16. Ortegren, U., Yin, L., Ost, A., Karlsson, H., Nystrom, F. H., and Stralfors, P. (2006) *Febs J* **273**, 3381-3392
17. Watkins, P. A. (2008) *J Biol Chem* **283**, 1773-1777
18. Stahl, A., Hirsch, D. J., Gimeno, R. E., Punreddy, S., Ge, P., Watson, N., Patel, S., Kotler, M., Raimondi, A., Tartaglia, L. A., and Lodish, H. F. (1999) *Mol Cell* **4**, 299-308
19. Chiu, H. C., Kovacs, A., Blanton, R. M., Han, X., Courtois, M., Weinheimer, C. J., Yamada, K. A., Brunet, S., Xu, H., Nerbonne, J. M., Welch, M. J., Fettig, N. M., Sharp, T. L., Sambandam, N., Olson, K. M., Ory, D. S., and Schaffer, J. E. (2005) *Circ Res* **96**, 225-233
20. Schaffer, J. E., and Lodish, H. F. (1994) *Cell* **79**, 427-436

21. Hatch, G. M., Smith, A. J., Xu, F. Y., Hall, A. M., and Bernlohr, D. A. (2002) *J Lipid Res* **43**, 1380-1389
22. Wu, Q., Ortegon, A. M., Tsang, B., Doege, H., Feingold, K. R., and Stahl, A. (2006) *Mol Cell Biol* **26**, 3455-3467
23. Shim, J., Moulson, C. L., Newberry, E. P., Lin, M. H., Xie, Y., Kennedy, S. M., Miner, J. H., and Davidson, N. O. (2009) *J Lipid Res* **50**, 491-500
24. Thompson, B. R., Muzurkiewicz-Munoz, A. M., Suttles, J., Carter-Su, C., and Bernlohr, D. A. (2009) *J Biol Chem*
25. Keller, A., Nesvizhskii, A. I., Kolker, E., and Aebersold, R. (2002) *Anal Chem* **74**, 5383-5392
26. Knol, J., Veenhoff, L., Liang, W. J., Henderson, P. J., Leblanc, G., and Poolman, B. (1996) *J Biol Chem* **271**, 15358-15366
27. Nagamatsu, K., Soeda, S., Mori, M., and Kishimoto, Y. (1985) *Biochim Biophys Acta* **836**, 80-88
28. Park, L. C., Calingasan, N. Y., Sheu, K. F., and Gibson, G. E. (2000) *Anal Biochem* **277**, 86-93
29. Koves, T. R., Ussher, J. R., Noland, R. C., Slentz, D., Mosedale, M., Ilkayeva, O., Bain, J., Stevens, R., Dyck, J. R., Newgard, C. B., Lopaschuk, G. D., and Muoio, D. M. (2008) *Cell Metab* **7**, 45-56
30. Koves, T. R., Noland, R. C., Bates, A. L., Henes, S. T., Muoio, D. M., and Cortright, R. N. (2005) *Am J Physiol Cell Physiol* **288**, C1074-1082
31. Willems, H. L., de Kort, T. F., Trijbels, F. J., Monnens, L. A., and Veerkamp, J. H. (1978) *Clin Chem* **24**, 200-203
32. Claros, M. G., and Vincens, P. (1996) *Eur J Biochem* **241**, 779-786
33. Sutherland, B. W., Toews, J., and Kast, J. (2008) *J Mass Spectrom* **43**, 699-715
34. Lewis, S. E., Listenberger, L. L., Ory, D. S., and Schaffer, J. E. (2001) *J Biol Chem* **276**, 37042-37050
35. Bunik, V. I., Raddatz, G., Wanders, R. J., and Reiser, G. (2006) *FEBS Lett* **580**, 3551-3557
36. Smith, C. M., Bryla, J., and Williamson, J. R. (1974) *J Biol Chem* **249**, 1497-1505
37. Garland, P. B. (1964) *Biochem J* **92**, 10C-12C
38. Gomazkova, V. S., and Krasovskaia, O. E. (1979) *Biokhimiia* **44**, 1126-1136
39. Hamada, M., Koike, K., Nakaula, Y., Hiraoka, T., and Koike, M. (1975) *J Biochem* **77**, 1047-1056
40. Kornfeld, S., Benziman, M., and Milner, Y. (1977) *J Biol Chem* **252**, 2940-2947
41. Gargiulo, C. E., Stuhlsatz-Krouper, S. M., and Schaffer, J. E. (1999) *J Lipid Res* **40**, 881-892
42. Garcia-Martinez, C., Marotta, M., Moore-Carrasco, R., Guitart, M., Camps, M., Busquets, S., Montell, E., and Gomez-Foix, A. M. (2005) *Am J Physiol Cell Physiol* **288**, C1264-1272
43. Lobo, S., Wiczer, B. M., and Bernlohr, D. A. (2009) *J Biol Chem*
44. Guitart, M., Andreu, A. L., Garcia-Arumi, E., Briones, P., Quintana, E., Gomez-Foix, A. M., and Garcia-Martinez, C. (2009) *Mitochondrion*

45. Huang, H. M., Zhang, H., Xu, H., and Gibson, G. E. (2003) *Biochim Biophys Acta* **1637**, 119-126
46. Naveri, H. K., Leinonen, H., Kiilavuori, K., and Harkonen, M. (1997) *Eur Heart J* **18**, 1937-1945
47. Pan, Y., Mansfield, K. D., Bertozzi, C. C., Rudenko, V., Chan, D. A., Giaccia, A. J., and Simon, M. C. (2007) *Mol Cell Biol* **27**, 912-925
48. Mailloux, R. J., Beriault, R., Lemire, J., Singh, R., Chenier, D. R., Hamel, R. D., and Appanna, V. D. (2007) *PLoS ONE* **2**, e690
49. Fernie, A. R., Carrari, F., and Sweetlove, L. J. (2004) *Curr Opin Plant Biol* **7**, 254-261
50. Hausler, N., Browning, J., Merritt, M., Storey, C., Milde, A., Jeffrey, F. M., Sherry, A. D., Malloy, C. R., and Burgess, S. C. (2006) *Biochem J* **394**, 465-473
51. Wlodek, D., and Gonzales, M. (2003) *J Theor Biol* **225**, 33-44
52. Durkot, M. J., De Garavilla, L., Caretti, D., and Francesconi, R. (1995) *Int J Sports Med* **16**, 167-171
53. Dienel, G. A., and Hertz, L. (2001) *J Neurosci Res* **66**, 824-838
54. Weiss, R. G., Chacko, V. P., Glickson, J. D., and Gerstenblith, G. (1989) *Proc Natl Acad Sci U S A* **86**, 6426-6430
55. Southam, A. D., Easton, J. M., Stentiford, G. D., Ludwig, C., Arvanitis, T. N., and Viant, M. R. (2008) *J Proteome Res* **7**, 5277-5285
56. Randle, P. J., Garland, P. B., Hales, C. N., and Newsholme, E. A. (1963) *Lancet* **1**, 785-789
57. Gaidhu, M. P., Fediuc, S., and Ceddia, R. B. (2006) *J Biol Chem* **281**, 25956-25964
58. Hwang, D. Y., and Ismail-Beigi, F. (2002) *Arch Biochem Biophys* **399**, 206-211
59. Bunik, V. I., and Degtyarev, D. (2008) *Proteins* **71**, 874-890
60. Wu, Q., Kazantzis, M., Doege, H., Ortegon, A. M., Tsang, B., Falcon, A., and Stahl, A. (2006) *Diabetes* **55**, 3229-3237
61. Talbot, J., Barrett, J. N., Barrett, E. F., and David, G. (2007) *J Physiol* **579**, 783-798

CHAPTER 5:

FATP1 MEDIATES LONG-CHAIN FATTY ACID-INDUCED ACTIVATION OF AMP-ACTIVATED PROTEIN KINASE IN 3T3-L1 ADIPOCYTES

This chapter is a reprint of the published manuscript of the same title with minor alterations. **Wiczer, B. M.**, Lobo S., Machen, G. L., Graves, L. M., and Bernlohr, D. A. (2009) *Biochem. Biophys. Res. Comm*. In press.

Luke Machen and Lee Graves performed the HPLC analysis of AMP and ATP levels. Brian Wiczer's contribution to this chapter was development of all the figures and writing the entire text.

SUMMARY

Fatty acid transport proteins are integral membrane acyl-CoA synthetases implicated in adipocyte fatty acid influx and esterification. FATP-dependent production of AMP was evaluated using FATP4 proteoliposomes, and fatty acid-dependent activation of AMP-activated protein kinase (AMPK) was assessed in 3T3-L1 adipocytes. Insulin-stimulated fatty acid influx (palmitate or arachidonate) into cultured adipocytes resulted in an increase in the phosphorylation of AMPK and its downstream target acetyl-CoA carboxylase. Consistent with the activation of AMPK, palmitate uptake into 3T3-L1 adipocytes resulted in an increase in intracellular [AMP]/[ATP]. The fatty acid-induced increase in AMPK activation was attenuated in a cell line expressing shRNA targeting FATP1. Taken together, these results demonstrate that, in adipocytes, insulin-stimulated fatty acid influx mediated by FATP1 regulates AMPK and provides a potential regulatory mechanism for balancing *de novo* production of fatty acids from glucose metabolism with influx of preformed fatty acids via phosphorylation of acetyl-CoA carboxylase.

INTRODUCTION

Long-chain fatty acid (LCFA) flux in tissues such as cardiac and skeletal muscle, liver, and adipose is a highly regulated and complex process involving both diffusional and protein-mediated components (1-3). A number of proteins have been identified and shown to play roles in LCFA influx (2,4-7) including fatty acid translocase/CD36, plasma membrane fatty acid-binding protein, caveolin-1, as well as fatty acid transport proteins (FATPs). Members of the FATP family are integral membrane proteins and have been shown to exhibit coenzyme A (CoA) and ATP-dependent long-chain and very long-chain fatty acyl-CoA synthetase activity (8-12). FATPs facilitate LCFA influx, at least in part, by coupling the diffusion of LCFA through the plasma membrane with CoA-esterification on the inner membrane in a process termed vectoral acylation, producing a fatty acyl-CoA, AMP, and pyrophosphate (13-15).

Mammals possess six FATP isoforms (FATP1-6) that have varying tissue expression and subcellular localization (3,16). Overexpression of FATPs in mammalian cells results in increased LCFA influx (9,17-20) and several isoforms, though not all, can rescue the decrease in LCFA influx in yeast lacking the FATP homologue, Fat1p (11). Functional studies using primary adipocytes from FATP1 null mice (21) and FATP1 knockdown 3T3-L1 adipocytes (3) have shown FATP1 is required for insulin-stimulated LCFA uptake but has only a minor role in basal LCFA influx, consistent with the insulin-stimulated translocation of FATP1 to the plasma membrane (3,5). Consistent with its localization to internal membranes functional studies of FATP4 have shown that the protein does not play a role in LCFA uptake in adipocytes (3).

AMP-activated protein kinase (AMPK) has been described as the cellular fuel gauge, regulating glucose and fatty acid metabolism (22-25). In terms of fatty acid metabolism, AMPK activation decreases *de novo* fatty acid and triacylglycerol synthesis and increases β-oxidation. Fatty acid influx has been shown in cardiac, skeletal muscle and liver to induce phosphorylation and activation of AMPK (26-29). However, the mechanistic linkage between LCFA influx and AMPK activation has not been addressed in adipocytes.

In this report, we analyze FATP1-dependent production of AMP both in vitro and in 3T3-L1 cells. We demonstrate that in 3T3-L1 adipocytes, fatty acid influx temporally increases the intracellular [AMP]/[ATP]. This increase in [AMP]/[ATP] occurred coincident with an increase in AMPK phosphorylation and an increase in the phosphorylation of AMPK's downstream target, acetyl-CoA carboxylase (ACC), indicating increased AMPK activity. Activation of AMPK was attenuated in cell lines expressing shRNA targeting FATP1. These results demonstrate that insulin-stimulated fatty acid influx increases [AMP]/[ATP] that in turn regulates AMPK in an FATP1-dependent manner and serves as a possible regulatory mechanism to balance *de novo* lipogenesis with fatty acid influx in adipocytes.

EXPERIMENTAL PROCEDURES

Reagents and cell culture—Cell culture reagents were obtained from Invitrogen. Cell culture-grade porcine insulin, puromycin, methylisobutylxanthine, and dexamethasone were obtained from Sigma-Aldrich. Non-radiolabeled fatty acids were obtained from Nu-Chek Prep, Inc (Elsyian, MN). [^{3}H]lignoceric acid was obtained from American Radiochemicals Co. [^{3}H]palmitate and [α-^{32}P]ATP were obtained from GE Healthcare Life Sciences. *n*-dodecyl-β-D-maltopyranoside was obtained from MBL International Corp. Dioleoylphosphatidylcholine (DOPC), dioleoylphosphatidylethanolamine (DOPE), dioleoylphosphatidyl-L-serine (DOPS), and cholesterol were obtained from Avanti Polar Lipids, Inc. Antibodies used were obtained as follows: rabbit anti-FATP4 (a gift from Dr. Paul Watkins, Kennedy Krieger Research Institute, Baltimore, MD); rabbit anti-phospho-acetyl-CoA carboxylase (Ser79) (Millipore); rabbit anti-phospho-AMPKα (Thr172) mAb and rabbit anti-AMPKα (Cell Signaling Technology); HRP-conjugated goat anti-rabbit IgG (Jackson ImmunoResearch Laboratories, Inc); and IRDye 700-conjugated goat anti-rabbit IgG (Li-Cor Biosciences). All other reagents were of analytical grade and obtained from Sigma-Aldrich. Differentiation and maintenance of stable 3T3-L1 cell lines expressing shRNA targeting FATP1, FATP4, or a scrambled sequence were previously described (3).

Purification and reconstitution of purified FATP into small unilamellar vesicles (SUVs)—Purification of murine FATP1-Myc/His and murine FATP4-Flag was performed as previously described (8,10). Purity of elution fractions was determined by Coomassie Blue staining and quantitation was performed using densitometry.

Reconstitution of FATP1 was performed as described in Chapter 4 of this thesis. Reconstituted FATP was kept on ice and used immediately.

Adenine nucleotide formation and separation using thin layer chromatography—Fatty acyl-CoA synthetase assay was initiated as above except that the final reaction volume contained 2 mM ATP, 70 μCi/mL [α-^{32}P]ATP and was assayed for 1 h at 37 °C. 5 μL of the reaction was subsequently spotted onto a PEI-cellulose thin-layer plate, dried, and developed as described (30). The thin-layer plate was air-dried, exposed in a PhosphorImager cassette (FujiFilm) and scanned using a Fuji FLA-5000. Adenine nucleotide migration was determined by spotting standards of non-radioactive ATP, ADP, and AMP in parallel with samples.

Analysis of intracellular AMP and ATP by HPLC—Nucleotide analysis was performed as described by Huang et al. (31). Briefly, cells were lysed in 10% trichloroacetic acid, the acid was removed by diethyl ether extraction, and the samples concentrated using a SpeedVac. HPLC analyses were performed using 70 μL of sample injected onto a SAX column at a flow rate of 0.750 mL/min. After 5 minutes of isocratic separation in buffer A (7 mM H_2PO_4, pH 3.8), a linear gradient of 0-80% buffer B (250 mM $NH_4H_2PO_4$, pH 4.7) was applied over 30 minutes followed by a 10 minutes of isocratic buffer B. Prior to analyzing the nucleotides, standard solutions of ATP, AMP, and UMP were chromatographed in order to determine their elution times and peak areas. AMP and ATP nucleotide concentrations were obtained by integrating the area under each peak.

Analysis of cellular fatty acid uptake—Fatty acid uptake was performed essentially as described (3). Briefly, cells were serum starved for 2 h using Kreb-Ringers's HEPES (KRH) buffer (20 mM HEPES, 120 mM NaCl, 4.7 mM KCl, 1.2 mM $MgSO_4$, 1.3 mM $CaCl_2$, 5 mM $NaHCO_3$), pH 7.4 containing 5.4 mM glucose and 0.1% fatty acid-free BSA prior to a 20 min pre-treatment with 100 nM insulin. Fatty acids were complexed to fatty acid-free BSA so that the free fatty acid concentration was ~100 nM as calculated using the equations described by Richieri, et al. (32). After addition of LCFA:BSA complex to cells for various times, cells were washed three times in ice-cold KRH containing 0.1% BSA and 200 μM phloretin and solubilized in 0.5% SDS. Samples were analyzed for total lipid influx via liquid scintillation counting.

Evaluation of AMPK activation during insulin-stimulated fatty acid uptake in 3T3-L1 adipocytes—Cells were rapidly washed in ice-cold PBS twice and immediately scraped into lysis buffer (50 mM Tris-HCl, pH 7.5, 50 mM NaF, 5 mM sodium pyrophosphate, 1 mM EDTA, 1 mM DTT, 10% (v/v) glycerol, 1% (v/v) Triton X-100, 2 μM pepstatin A, Complete-Mini Protease Inhibitor cocktail (Roche), and phosphatase inhibitors). Lysates were precipitated by the addition of PEG-8000 (10% final). Pellets were re-solubilized in 2% SDS and total protein concentration was determined by bicinchoninic acid assay. Protein was separated by SDS-PAGE on an 8.5% SDS-polyacrylamide gel and subjected to immunoblot analysis.

Statistical analysis—The data are represented as the mean ± standard deviation (SD) or as the mean ± standard error of the mean (SEM) as indicated. Statistical significance

was determined using the two-tail Student's *t*-test and two-way ANOVA where appropriate. $p < 0.05$ was considered to be statistically significant.

RESULTS

In addition to the formation of long-chain fatty acyl-CoA, AMP and pyrophosphate are also predicted to form as acyl-CoA synthetase reaction products. We took advantage of the FATP proteoliposomes established in Chapter 4 of this thesis to experimentally demonstrate that AMP is a product. FATP4 displays the greatest specific activity (Chapter 2) and therefore was used as a FATP family representative to assess AMP formation (Figure 1). Using [α-^{32}P]ATP, CoA, and palmitate as substrates, the products of the reaction were subjected to thin-layer chromatography and confirmed that AMP was produced as a product of the long-chain acyl-CoA synthetase reaction.

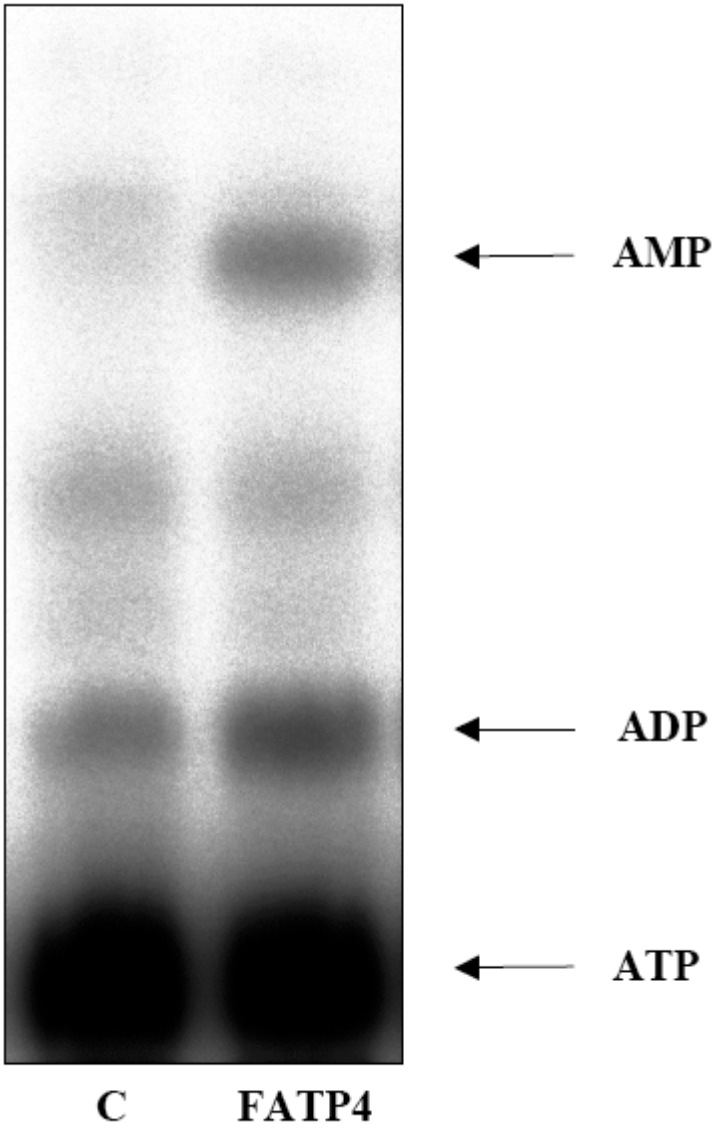

Figure 1. Analysis of AMP production by FATP. Reconstituted FATP4 was assayed for AMP formation using a modified version of the acyl-CoA synthetase activity assay using [α-^{32}P]ATP as described in Experimental Procedures. After 1 h, 5 μL was spotted onto a PEI-cellulose thin layer plate and developed. The (C) lane represents the no enzyme control. Adenine nucleotide separation was determined by spotting adenine nucleotide standards in parallel with samples. The data shown is representative of three independent experiments.

Based on the vectoral acylation hypothesis, LCFA influx is predicted to increase the intracellular [AMP]/[ATP] ratio and activate the AMP-activated protein kinase (AMPK). Since LCFA influx is greatest during insulin stimulation (5), we measured

intracellular [AMP] and [ATP] during insulin-stimulated LCFA influx using palmitate as a model fatty acid. Insulin treatment led to a marked reduction in intracellular [AMP]/[ATP], consistent with increases in glucose uptake and metabolism, while subsequent insulin-stimulated palmitate influx temporally increased intracellular [AMP]/[ATP] compared to insulin alone (Figure 2B). While palmitate influx increases linearly during the 20 min incubation (Figure 2A), intracellular [AMP]/[ATP] increased during the first 5-10 min of palmitate influx then returned to basal levels. (Figure 2B). Consistent with the changes in intracellular [AMP]/[ATP], AMPK phosphorylation on the catalytic α-subunit on Thr172 decreased 75% upon insulin treatment while palmitate influx transiently increased AMPK phosphorylation 60% compared to insulin alone (Figure 2C), paralleling changes in [AMP]/[ATP]. AMPK activation was manifest in the paralleled phosphorylation changes of the AMPK protein substrate, acetyl-CoA carboxylase (ACC) (Figure 2D). Following insulin-stimulated translocation of FATP1 to the plasma membrane, arachidonate addition led to a statistically significant increase in AMPK activation (Figure 3A, 3B) while oleate addition exhibited a trend towards increased AMPK phosphorylation.

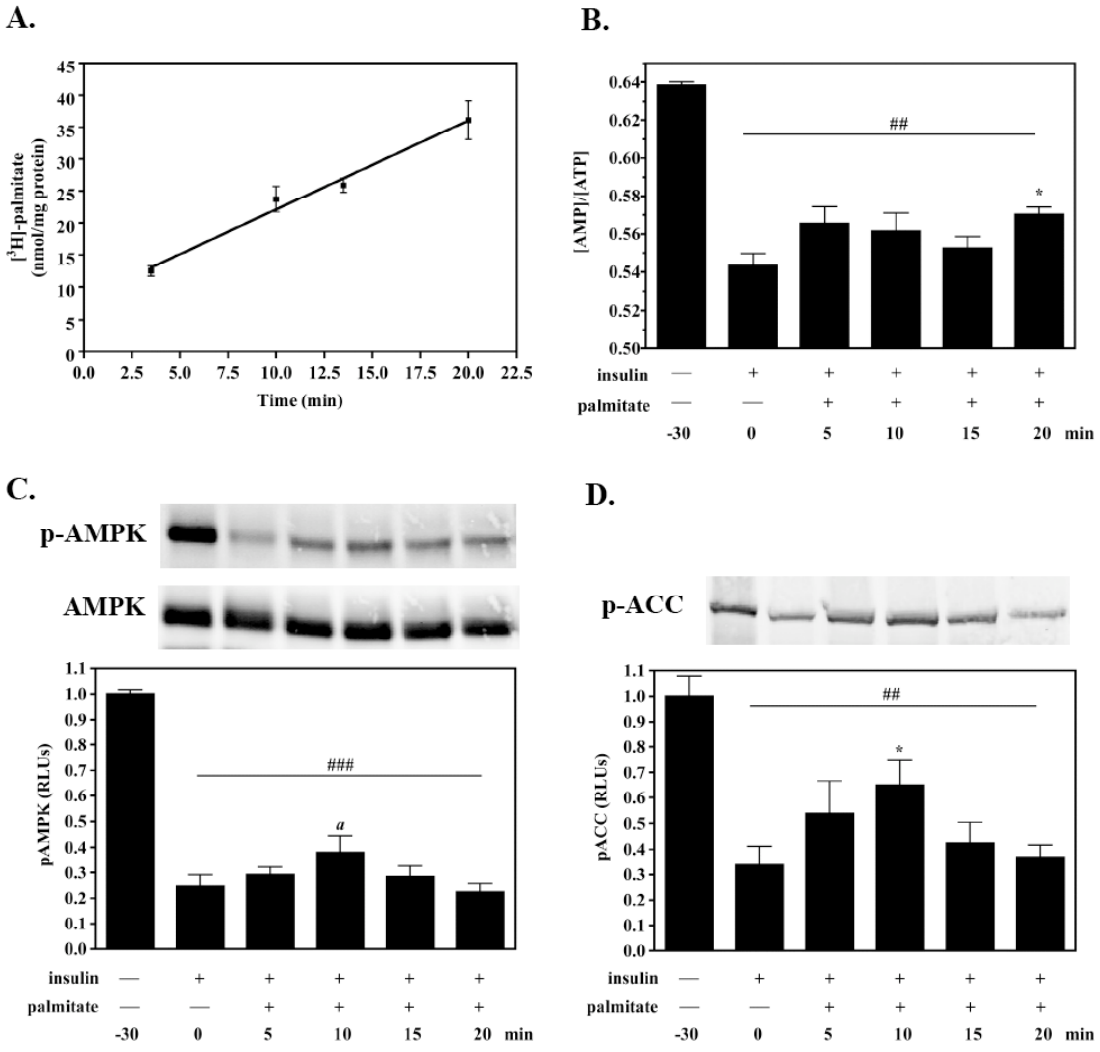

Figure 2. Insulin-stimulated palmitate influx into 3T3-L1 adipocytes increases the intracellular [AMP]/[ATP] ratio and AMPK activation. *A.* Time course of insulin-stimulated palmitate influx. Serum-starved 3T3-L1 adipocytes were insulin treated for 30 min and palmitate influx was initiated upon addition of [^{3}H]palmitate (palmitate:BSA 5:1). n = 3, mean ± SEM. *B.* Intracellular [AMP]/[ATP] during insulin-stimulated palmitate influx. 3T3-L1 adipocytes were incubated with palmitate:BSA (5:1) and at various times, the [AMP] and [ATP] levels were determined by HPLC. n = 4, mean ± SEM. *C & D.* p-AMPK and p-ACC levels during insulin-stimulated palmitate influx. Blots shown are representative of three independent experiments. The blots of were quantitated and graphically represented as the mean ± SEM., n = 6. For *B-D, a,* $p = 0.10$; *, $p < 0.05$ relative to absence of palmitate; ##, $p < 0.01$; ###, $p < 0.001$ relative to absence of insulin.

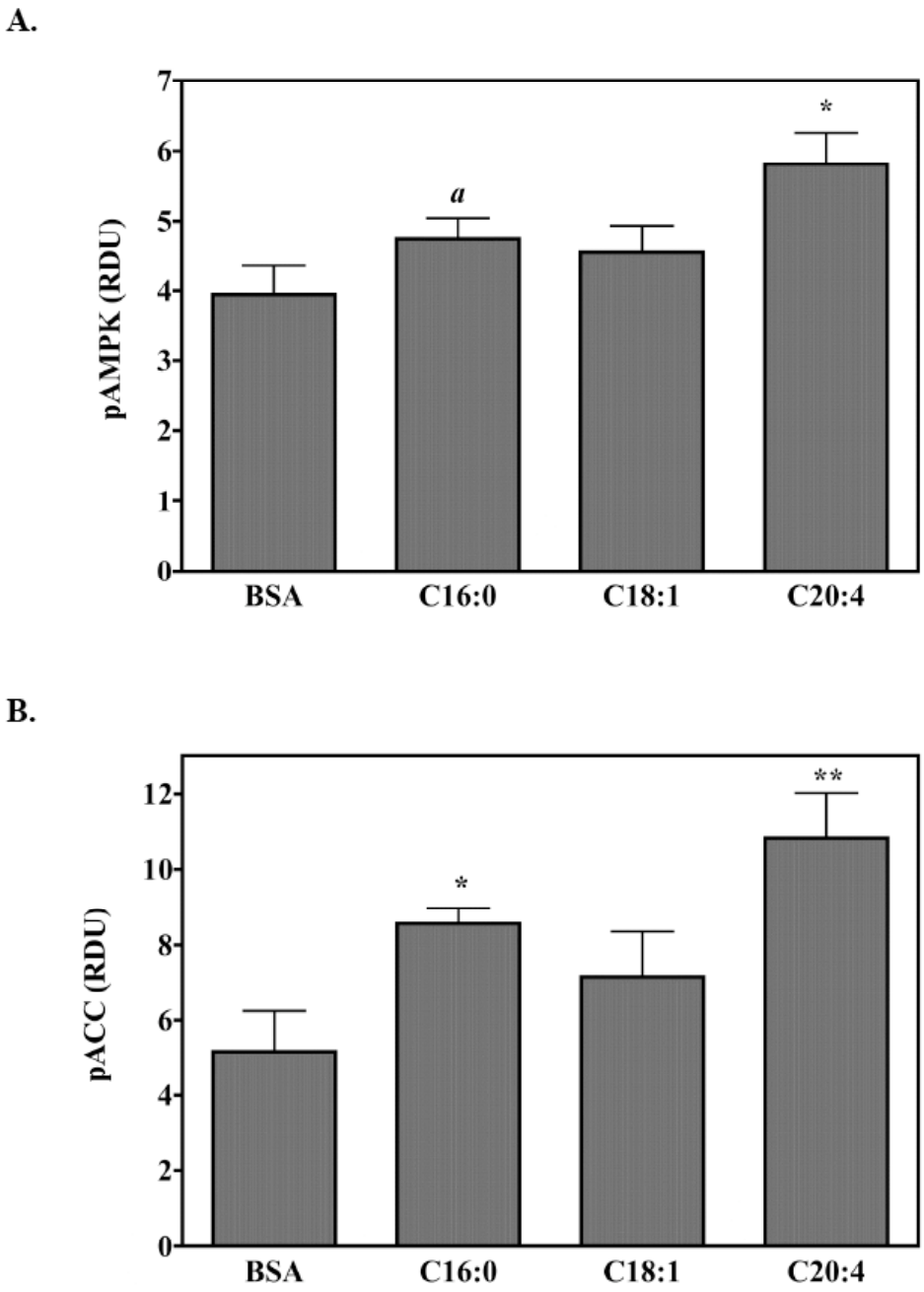

Figure 3. Exogenous long-chain fatty acids induce AMPK phosphorylation in 3T3-L1 adipocytes. Serum-starved 3T3-L1 adipocytes were pretreated with 100 nM insulin for 30 min and then incubated with fatty acid-free BSA or BSA-buffered palmitate (*C16:0*), oleate (*C18:1*), or arachidonate (*C20:4*) plus insulin for 10 min such that the free fatty acid concentration was 100 nM. 30 μg of protein was subjected to SDS-PAGE and immunoblot analysis using anti-p-AMPK (*A*) and anti-p-ACC (*B*) antibodies. The blots were quantitated via densitometry and graphically represented as the mean ± SEM, n = 6. Relative to BSA alone: *a*, $p = 0.15$; *, $p < 0.05$; **, $p < 0.01$.

The increase in intracellular [AMP]/[ATP] observed during insulin-stimulated palmitate influx is consistent with the reaction mechanism for FATPs. FATP1, but not FATP4, facilitates the insulin-stimulated component of fatty acid uptake into 3T3-L1 adipocytes (3). These observations together with the increase in [AMP]/[ATP] led us to hypothesize that the AMPK activation during insulin-stimulated fatty acid influx in adipocytes would be dependent on FATP1. To that end, we evaluated the fatty acid-dependent activation of AMPK in 3T3-L1 adipocytes stably expressing a lentiviral-directed shRNA targeting FATP1 or a control scrambled shRNA (3). When insulin-treated FATP1 knockdown and control 3T3-L1 adipocytes were incubated with palmitate for 10 minutes and AMPKα phosphorylation assessed, the control cells exhibited an increase of 2.5-fold compared to the absence of palmitate (Figure 4A). Consistent with AMPKα activation, phosphorylated ACC levels correlated with the levels of AMPKα phosphorylation and increased 8-fold compared to the absence of palmitate (Figure 4B). In contrast, insulin-treated FATP1-silenced adipocytes exhibited only a 1.6-fold increase in phosphorylated AMPKα and a 2.3-fold increase in ACC phosphorylation in response to palmitate influx (Figure 4A, 4B). These results suggest that the fatty acid-induced activation of AMPK during insulin-stimulation is dependent on FATP1 and is consistent with the vectoral acylation model for LCFA influx.

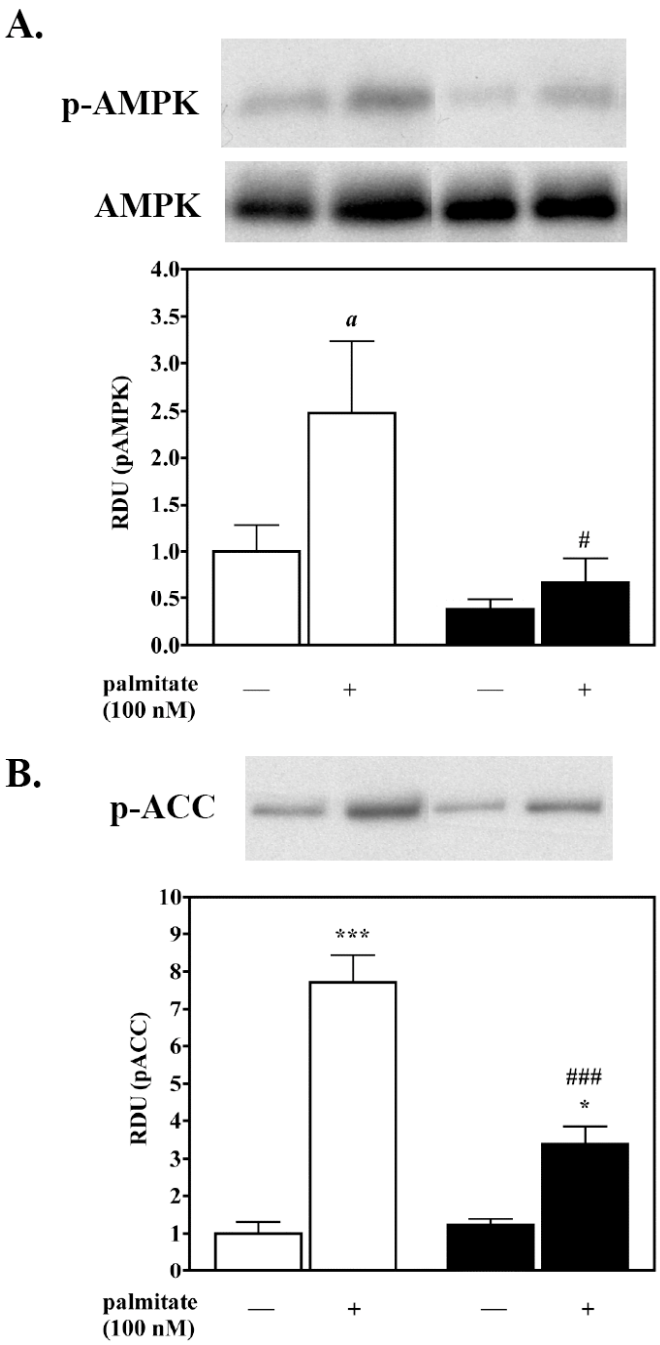

Figure 4. Adipocyte AMPK activation during insulin-stimulated fatty acid uptake is dependent on FATP1. *A & B.* Serum starved, 3T3-L1 Scr (*white bars*) or FATP1 (*black bars*) knockdown adipocytes were pretreated with 100 nM insulin for 20 min and incubated in the absence or presence of 100 nM free palmitate for 10 min. Cells were washed, lysed, and proteins analyzed by immunoblotting using the anti-AMPK, anti-p-AMPK (*B*), or anti-p-ACC (*C*) antibodies. Blots shown are representative of three independent experiments. The blots of each of the experiments were quantitated and graphically represented as the mean ± SEM, n = 6. Relative to the absence of palmitate: *a*, $p = 0.065$; *, $p < 0.05$; ***, $p < 0.001$. Relative to Scr: #, $p < 0.05$; ###, $p < 0.001$.

DISCUSSION

Taking advantage of the increased enzymatic stability (Chapter 4), FATP proteoliposomes were used to show for the first time that AMP is formed during the FATP acyl-CoA synthetase reaction (Figure 1), giving further evidence that FATPs share the same reaction mechanism as other long-chain acyl-CoA synthetases. This result, taken together with the requirement of FATP1 in adipocyte insulin-stimulated LCFA influx (3,21), is consistent with the observed increase in intracellular [AMP]/[ATP] and increase in AMPK activation during insulin-stimulated LCFA influx (Figure 2 & 3). Furthermore, reducing FATP1 expression via lentivirus mediated gene silencing attenuated LCFA-induced AMPK activation during insulin stimulation (Figure 4).

While the increase in intracellular [AMP]/[ATP] is consistent with AMPK activation in adipocytes, it does not rule out the possibility that additional mechanisms are involved. In skeletal myocytes, Watt et al. showed that LCFA-induced AMPK activation was AMP-independent and suggested that LCFA influx led to a change in the interaction of the AMPKβ and γ regulatory subunits with the catalytic α-subunit, allowing LKB1 to phosphorylate AMPKα more effectively (28). Therefore, it is possible that in adipocytes fatty acyl-CoAs produced by FATP1 or downstream lipid metabolites potentiate the AMPK activation in addition to changes in intracellular [AMP]/[ATP]. However, Taylor et al. demonstrated that long-chain fatty acyl-CoAs inhibit AMPK activity *in vitro* through prevention of Thr172 phosphorylation by LKB1 (33), suggesting that increasing levels of fatty acyl-CoAs could antagonize the fatty acid-

induced AMPK activation and prevent hyperactivation of AMPK. It is unclear whether such regulation is manifest under the conditions of the current study.

Whereas FATP1 mediates insulin-stimulated LCFA influx, it is likely that other proteins participate in the influx process. Ample evidence links CD36 to LCFA influx in adipocytes (2,34-37), suggesting the possibility of a functional synergy between FATP1 and CD36 in insulin-stimulated LCFA uptake. CD36 may function as a LCFA "receptor" while FATP1 catalyzes the esterification reaction trapping the fatty acid internally. Linking the two functions, Kleinfeld and colleagues have suggested that a "true" LCFA transporter exists in adipocytes and mediates transit across the plasma membrane. Taken together, the results suggest that a complex of proteins mediate basal and/or insulin-stimulated LCFA influx leading to increased acyl-CoA formation, increased intracellular [AMP]/[ATP] and AMPK activation that could result in an attenuation of *de novo* lipogenesis via the phosphorylation of ACC (Figure 5). Such a regulatory mechanism in adipocytes would provide for molecular control between the *de novo* fatty acid synthetic and fatty acid influx pathways. The molecular linkage between acyl-CoA synthetase activity and activation of AMPK need not be limited to reactions of LCFA influx. Indeed, Gauthier et al. reported that the activation of AMPK in adipocytes during hormone-stimulated lipolysis was dependent on a undefined acyl-CoA synthetase (25) that is most likely to be ACSL1 (38). These results in sum suggest a general mechanism through which acyl-CoA synthetases, depending on their physiological location and function, regulate AMPK activation.

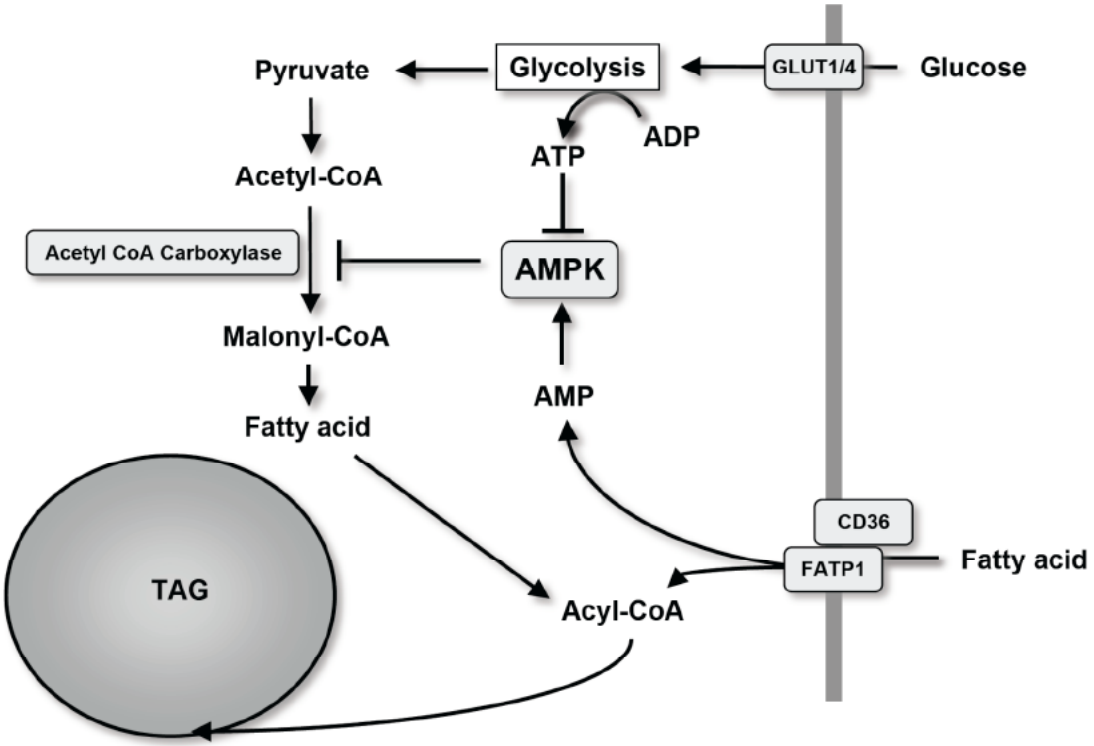

Figure 5. Model of long-chain fatty acid-induced AMPK activation during insulin stimulation. Insulin-stimulated glucose uptake increases the flux of glucose through glycolysis. Glycolysis produces ATP which antagonizes AMP-activated protein kinase (AMPK) and promotes *de novo* fatty acid synthesis. Fatty acids enter the adipocyte and are esterified to their CoA-esters via CD36 and FATP1. The utilization of ATP and production of AMP increases intracellular [AMP]/[ATP] and results in the activation of AMPK. AMPK phosphorylates and inhibits ACC, thereby attenuating *de novo* fatty acid synthesis in the presence of exogenous fatty acids.

ACKNOWLEDGMENTS

We would like to thank members of the Bernlohr laboratory for their comments and discussions concerning this manuscript. Supported by ADA 7-06-RA-12 and the Minnesota Obesity Center.

REFERENCES

1. Kampf, J. P., and Kleinfeld, A. M. (2004) *J Biol Chem* **279**, 35775-35780
2. Coburn, C. T., Knapp, F. F., Jr., Febbraio, M., Beets, A. L., Silverstein, R. L., and Abumrad, N. A. (2000) *J Biol Chem* **275**, 32523-32529
3. Lobo, S., Wiczer, B. M., Smith, A. J., Hall, A. M., and Bernlohr, D. A. (2007) *J Lipid Res* **48**, 609-620
4. Zhou, S. L., Stump, D., Kiang, C. L., Isola, L. M., and Berk, P. D. (1995) *Proc Soc Exp Biol Med* **208**, 263-270
5. Stahl, A., Evans, J. G., Pattel, S., Hirsch, D., and Lodish, H. F. (2002) *Dev Cell* **2**, 477-488
6. Trigatti, B. L., Anderson, R. G., and Gerber, G. E. (1999) *Biochem Biophys Res Commun* **255**, 34-39
7. Kim, J. K., Gimeno, R. E., Higashimori, T., Kim, H. J., Choi, H., Punreddy, S., Mozell, R. L., Tan, G., Stricker-Krongrad, A., Hirsch, D. J., Fillmore, J. J., Liu, Z. X., Dong, J., Cline, G., Stahl, A., Lodish, H. F., and Shulman, G. I. (2004) *J Clin Invest* **113**, 756-763
8. Hall, A. M., Smith, A. J., and Bernlohr, D. A. (2003) *J Biol Chem* **278**, 43008-43013
9. Gimeno, R. E., Ortegon, A. M., Patel, S., Punreddy, S., Ge, P., Sun, Y., Lodish, H. F., and Stahl, A. (2003) *J Biol Chem* **278**, 16039-16044
10. Hall, A. M., Wiczer, B. M., Herrmann, T., Stremmel, W., and Bernlohr, D. A. (2005) *J Biol Chem* **280**, 11948-11954
11. DiRusso, C. C., Li, H., Darwis, D., Watkins, P. A., Berger, J., and Black, P. N. (2005) *J Biol Chem* **280**, 16829-16837
12. DiRusso, C. C., Darwis, D., Obermeyer, T., and Black, P. N. (2008) *Biochim Biophys Acta* **1781**, 135-143
13. Zou, Z., Tong, F., Faergeman, N. J., Borsting, C., Black, P. N., and DiRusso, C. C. (2003) *J Biol Chem* **278**, 16414-16422
14. Tong, F., Black, P. N., Coleman, R. A., and DiRusso, C. C. (2006) *Arch Biochem Biophys* **447**, 46-52
15. Richards, M. R., Harp, J. D., Ory, D. S., and Schaffer, J. E. (2006) *J Lipid Res* **47**, 665-672

16. Ortegren, U., Yin, L., Ost, A., Karlsson, H., Nystrom, F. H., and Stralfors, P. (2006) *Febs J* **273**, 3381-3392
17. Stahl, A., Hirsch, D. J., Gimeno, R. E., Punreddy, S., Ge, P., Watson, N., Patel, S., Kotler, M., Raimondi, A., Tartaglia, L. A., and Lodish, H. F. (1999) *Mol Cell* **4**, 299-308
18. Chiu, H. C., Kovacs, A., Blanton, R. M., Han, X., Courtois, M., Weinheimer, C. J., Yamada, K. A., Brunet, S., Xu, H., Nerbonne, J. M., Welch, M. J., Fettig, N. M., Sharp, T. L., Sambandam, N., Olson, K. M., Ory, D. S., and Schaffer, J. E. (2005) *Circ Res* **96**, 225-233
19. Schaffer, J. E., and Lodish, H. F. (1994) *Cell* **79**, 427-436
20. Hatch, G. M., Smith, A. J., Xu, F. Y., Hall, A. M., and Bernlohr, D. A. (2002) *J Lipid Res* **43**, 1380-1389
21. Wu, Q., Ortegon, A. M., Tsang, B., Doege, H., Feingold, K. R., and Stahl, A. (2006) *Mol Cell Biol* **26**, 3455-3467
22. Fryer, L. G., Hajduch, E., Rencurel, F., Salt, I. P., Hundal, H. S., Hardie, D. G., and Carling, D. (2000) *Diabetes* **49**, 1978-1985
23. Viollet, B., Andreelli, F., Jorgensen, S. B., Perrin, C., Flamez, D., Mu, J., Wojtaszewski, J. F., Schuit, F. C., Birnbaum, M., Richter, E., Burcelin, R., and Vaulont, S. (2003) *Biochem Soc Trans* **31**, 216-219
24. Towler, M. C., and Hardie, D. G. (2007) *Circ Res* **100**, 328-341
25. Gauthier, M. S., Miyoshi, H., Souza, S. C., Cacicedo, J. M., Saha, A. K., Greenberg, A. S., and Ruderman, N. B. (2008) *J Biol Chem*
26. Clark, H., Carling, D., and Saggerson, D. (2004) *Eur J Biochem* **271**, 2215-2224
27. Fediuc, S., Gaidhu, M. P., and Ceddia, R. B. (2006) *J Lipid Res* **47**, 412-420
28. Watt, M. J., Steinberg, G. R., Chen, Z. P., Kemp, B. E., and Febbraio, M. A. (2006) *J Physiol* **574**, 139-147
29. Kawaguchi, T., Osatomi, K., Yamashita, H., Kabashima, T., and Uyeda, K. (2002) *J Biol Chem* **277**, 3829-3835
30. Bernlohr, D. A., and Switzer, R. L. (1981) *Biochemistry* **20**, 5675-5681
31. Huang, M., Kozlowski, P., Collins, M., Wang, Y., Haystead, T. A., and Graves, L. M. (2002) *Mol Pharmacol* **61**, 569-577
32. Richieri, G. V., Anel, A., and Kleinfeld, A. M. (1993) *Biochemistry* **32**, 7574-7580
33. Taylor, E. B., Ellingson, W. J., Lamb, J. D., Chesser, D. G., and Winder, W. W. (2005) *Am J Physiol Endocrinol Metab* **288**, E1055-1061
34. Abumrad, N. A., el-Maghrabi, M. R., Amri, E. Z., Lopez, E., and Grimaldi, P. A. (1993) *J Biol Chem* **268**, 17665-17668
35. Febbraio, M., Abumrad, N. A., Hajjar, D. P., Sharma, K., Cheng, W., Pearce, S. F., and Silverstein, R. L. (1999) *J Biol Chem* **274**, 19055-19062
36. Pohl, J., Ring, A., Korkmaz, U., Ehehalt, R., and Stremmel, W. (2005) *Mol Biol Cell* **16**, 24-31
37. Hajri, T., Hall, A. M., Jensen, D. R., Pietka, T. A., Drover, V. A., Tao, H., Eckel, R., and Abumrad, N. A. (2007) *Diabetes* **56**, 1872-1880
38. Lobo, S., Wiczer, B. M., and Bernlohr, D. A. (2009) *J Biol Chem*

CHAPTER 6:

PERSPECTIVES

Brian Wiczer's contribution to this chapter was writing the entire text.

In 1994, Jean Schaffer and Harvey Lodish used a mouse cDNA library to overexpress proteins in mammalian cells in order to identify candidate proteins involved in long-chain fatty acid (LCFA) influx (1). The result of this screen was the identification of a novel protein they called fatty acid transport protein (FATP). Since then, five additional family members have been identified, many resulting in increased LCFA influx when overexpressed in mammalian cell lines (2,3) and yeast (4). However, when FATP1 was identified in 1994, it was not yet appreciated that this family of proteins all were in fact acyl-CoA synthetases and were predicted to have no structural resemblance to traditional transports such as the glucose transporter family. This inspired a model for LCFA influx, termed vectoral acylation, where fatty acids entered a cell driven by a concentration gradient and were immediately esterified with coenzyme A, both maintaining the influx of LCFAs and channeling the fatty acyl-CoAs to various metabolic fates. It has since been shown that members of long-chain acyl-CoA synthetase family can also increase LCFA influx, both using large lipid vesicles (5) and overexpression in cells. While it is still debated whether or not FATPs in fact require their acyl-CoA synthetase activity to elicit LCFA influx, it has become clear that FATPs have varying subcellular localizations and that this often correlates with whether or not they participate in LCFA influx (6-8).

Work contained in Chapter 2 of this thesis characterized the acyl-CoA synthetase activity of FATP4 and has contributed to the biochemical characterization of all FATPs. Despite the fact that both the long-chain and very long-chain acyl-CoA synthetase activities of FATP4 are ~30-fold and 10-fold higher *in vitro*, respectively, than FATP1,

FATP4 has no role in LCFA influx in adipocytes and is completely localized to internal structures (Chapter 3). On the other hand, FATP1 translocates to the plasma membrane upon insulin treatment of adipocytes (Chapter 3, (9)) and this translocation correlates with the necessity of FATP1 in insulin-stimulated LCFA influx but not basal influx (Chapter 3, (10)).

Having a long-chain acyl-CoA synthetase linked to LCFA influx revealed the possibility that FATP1 could regulate fatty acid synthesis, communicating the rates of LCFA influx to the *de novo* lipogenesis pathway via FATP1's production of AMP. The AMP produced would subsequently activate AMPK and attenuate *de novo* lipogenesis. When this hypothesis was investigated (Chapter 5), the data confirmed that insulin-stimulated LCFA influx in adipocytes could in fact activate AMPK and that this activation was attenuated when FATP1 was depleted. However, under the conditions tested, the response of AMPK activation to LCFA influx was transient, reaching maximum activation in ten minutes and dissipating back to baseline ten minutes later. This brings into question the physiological importance of the LCFA-induced AMPK activation. Future experiments will need to be done to determine how this phenomenon occurs *in vivo* while taking into account the coordinate actions of insulin secretion, lipid entrance into plasma, and subsequent lipid clearance.

Despite the established role of FATP1 in insulin-stimulated LCFA influx, the observation that the majority of FATP1 still resides on internal structures begs the existence of functional roles aside from cellular LCFA influx. This is exemplified in

the observation that FATP1 plays an important role in brown adipocytes and nonshivering thermogenesis (11). Uncoupling of the mitochondrial electron transport chain primarily through uncoupling protein 1 results in heat generation, and oxidation of LCFA provides an abundance of electrons for this purpose. While brown adipocyte FATP1-dependent LCFA influx is important during the late-phase of thermogenesis supplying brown adipocytes with additional LCFA, FATP1 is also important during the early-phase of thermogenesis and suggests a mitochondrial function. Additionally, silencing FATP1 in 3T3-L1 adipocytes results in a trended increase in AMPK phosphorylation with elevated ACC phosphorylation (Wiczer, B. M., unpublished) suggesting increased AMPK activity. This is the opposite observation of what would be expected from a purely LCFA influx standpoint but would be consistent with an alteration in mitochondrial metabolism (12,13). Indeed, FATP1 was found localized to mitochondria, and silencing FATP1 decreased TCA cycle function and altered mitochondrial metabolism (Chapter 4). These phenotypes are consistent with the role of FATP1 as a 2-oxoglutarate dehydrogenase complex (OGDH) enhancer via their direct protein-protein interaction (Chapter 4). The proteomic study described in chapter 4 of this thesis also lists several other candidate FATP1-interacting mitochondrial proteins that most likely represent components of a supramolecular complex or complexes.

It is surprising that the acyl-CoA synthetase activity of FATP1 was not required for the OGDH enhancing activity, determined through the absence of ATP and fatty acids. It should be noted that the FATP1 used in these studies was still catalytically active and

remains to be seen if the OGDH enhancing activity of FATP1 relies on functional FATP1. The question still remains as to why an acyl-CoA synthetase would have this additional, non-enzymatic function. While it is conceivable that the catalytic activity of FATP1 is dispensable in the regulation of OGDH, another possibility is that FATP1 utilizes substrates other than LCFAs. This is certainly the case for FATP5, whose primary function is as a bile acid-CoA ligase (8,14). The branched-chain fatty acyl-CoA, phytanoyl-CoA, is a potent inhibitor of OGDH, unlike the mild inhibitory property of palmitoyl-CoA (15). Therefore FATP1 may utilize phytanic acid and other branched-chain fatty acids and would allow FATP1 to act as a regulatory protein by virtue of both its interaction with OGDH and its acyl-CoA synthetase activity. On the other hand, the traditional view is that fatty acids already exist as their CoA derivatives within the mitochondria. This raises the intriguing possibility that FATP1 has an enzymatic activity in addition to its acyl-CoA synthetase activity. Recently, Abe et al. observed that acetyl-CoA synthetase and luciferase, both adenylate-forming enzymes, possess amide bond synthetic activity dependent on the formation of AMP (16). While the physiological significance of this reaction is unclear, it reiterates the idea that FATP1 could catalyze a novel reaction through similar chemistries. Interestingly, a parallel can be drawn with FABPpm, another protein involved in LCFA influx that also has both dual localizations and functions. As discussed in Chapter 1, FABPpm is also known as mitochondrial aspartate aminotransferase 2/glutamate oxaloacetate transaminase 2, and it is unclear if FABPpm must be catalytically active for facilitating LCFA influx while at the plasma membrane. It is interesting to note that FABPpm was also identified in the FATP1 co-immunoprecipitation study in Table 3, Chapter 4 (i.e.,

glutamate oxaloacetate transaminase 2, mitochondrial), as well as other related enzymes involved in amino acid metabolism. It is therefore tempting to speculate that FATP1 also has a role in amino acid metabolism, but further research will be needed to address this hypothesis.

A couple of additional questions arise with the discovery of this mitochondrial role for FATP1. How do the mitochondrial levels of FATP1 correlate with metabolic disorders? Oxidative stress is a major contributor to the onset and persistence of metabolic disorders and much of the cellular oxidative stress derives from the mitochondrion (17-20). Because FATP1 positively regulates TCA cycle activity, it is possible that increasing mitochondrial FATP1 results in increased reactive oxygen species through a parallel change in oxidative equivalents of NADH without proper compensation of detoxifying enzymes. This would contribute to increased cellular oxidative stress and insulin resistance.

On a related note, how is FATP1 mitochondrial localization regulated? A number of mechanisms are known to regulate mitochondrial protein import. Protein structural stability and the rate of unfolding impact the rate of polypeptide chain entrance into the mitochondrion through the import machinery (21,22). Sometimes this allows the protein to remain active during the import process and permits the protein to transiently perform a cellular function while at the outer mitochondrial membrane, such as in the case of the steroidogenic acute regulatory protein (23,24). Sebastian et al. recently found that FATP1 increases both fatty acid oxidation into acid soluble metabolites and

CO_2 when overexpressed in cultured myotubes, and this may function in a larger complex with CPT1 (25), suggesting that FATP1 can exist at the mitochondrial outer membrane. The fatty acid oxidation results partially conflict with those presented in Chapter 4 of this thesis and may have to due with the particular cell line used in combination with effects due to overexpression. Nonetheless, both FATP1's intrinsic structural stability (Chapter 4) and the degree of protein-protein interactions at the outer mitochondrial membrane might impact the rate of FATP1 mitochondrial import. Another more intriguing mechanism of import regulation would be through the status of cellular metabolic processes. Fumarase from *Saccharomyces cerevisiae* is a dually localized protein equally partitioned in the cytosol and mitochondria (26), participating in the glyoxylate shunt and the TCA cycle, respectively. Regev-Rudzki et al. recently showed that if the glyoxylate shunt was inhibited, fumarase became virtually 100% localized to mitochondria (27). This has shown for the first time that the localization of a protein with dual subcellular localization could shift depending upon the status of metabolic processes. Other studies have also reported that fumarase in mammalian liver has a similar dual localization and derives from a single gene product (28), however the localization differences may have more to due with the alternative translational initiation at two in-phase AUG codons. Because such a regulatory mechanisms could apply to FATP1, it will be important to determine the extent that alterations in particular metabolic processes, such as lipid storage, impact FATP1 mitochondrial localization, how this impacts mitochondrial and cellular metabolism, and if this is at all linked to insulin resistance.

The physiological function of FATP4 is still unknown. While studies have shown that FATP4 is essential for maintaining the lipid barrier in the skin (29-31), recent studies have concluded FATP4 has no role in LCFA influx into the intestine despite its high levels of expression (32). Even the work described in Chapter 3 of this thesis has failed to give any better understanding as to the function of FATP4 in adipocytes, other than decreasing the levels of FATP4 improves insulin sensitivity. One possibility is that FATP4 may be important for the formation of sphingomyelin through its very long-chain acyl-CoA synthetase activity. The pro-inflammatory lipid, ceramide, is derived from sphingomyelin. Therefore decreased sphingomyelin would result in decreased ceramide production and increased insulin sensitivity. Another possibility is that FATP4 has a mitochondrial role that is distinct from FATP1. Certainly, the bioinformatics analysis in Chapter 4 indicates that FATP4 is likely to be mitochondrial and has been confirmed in preliminary cellular fractionation studies (Wiczer, B. M., unpublished). Taking a proteomic approach to understanding FATP4 function should yield promising results as it did for FATP1. Future studies will be needed to determine if FATP4 indeed has a mitochondrial role and, through this role, influence cellular energy homeostasis.

In conclusion, the work contained within this thesis has made a large contribution to the understanding the adipocyte FATPs, FATP1 and 4. FATP1 is no longer viewed as simply a protein involved in cellular LCFA influx. It now has a newly appreciated role in the regulation of mitochondrial function through its involvement in TCA cycle function. While on the other hand FATP4 is still a black box, its probable role in the

mitochondrion should make for an exciting story and shed light on how FATP4 promotes lipid accumulation. This is likely a common theme for the FATP family, in which their major function is not directly in LCFA influx but rather in other aspects of metabolism, dependent on their activity, subcellular localization and protein-protein interactions.

REFERENCES

1. Schaffer, J. E., and Lodish, H. F. (1994) *Cell* **79**, 427-436
2. Hatch, G. M., Smith, A. J., Xu, F. Y., Hall, A. M., and Bernlohr, D. A. (2002) *J Lipid Res* **43**, 1380-1389
3. Gimeno, R. E., Ortegon, A. M., Patel, S., Punreddy, S., Ge, P., Sun, Y., Lodish, H. F., and Stahl, A. (2003) *J Biol Chem* **278**, 16039-16044
4. DiRusso, C. C., Li, H., Darwis, D., Watkins, P. A., Berger, J., and Black, P. N. (2005) *J Biol Chem* **280**, 16829-16837
5. Schmelter, T., Trigatti, B. L., Gerber, G. E., and Mangroo, D. (2004) *J Biol Chem* **279**, 24163-24170
6. Hall, A. M., Smith, A. J., and Bernlohr, D. A. (2003) *J Biol Chem* **278**, 43008-43013
7. Hall, A. M., Wiczer, B. M., Herrmann, T., Stremmel, W., and Bernlohr, D. A. (2005) *J Biol Chem* **280**, 11948-11954
8. Watkins, P. A. (2008) *J Biol Chem* **283**, 1773-1777
9. Stahl, A., Evans, J. G., Pattel, S., Hirsch, D., and Lodish, H. F. (2002) *Dev Cell* **2**, 477-488
10. Wu, Q., Ortegon, A. M., Tsang, B., Doege, H., Feingold, K. R., and Stahl, A. (2006) *Mol Cell Biol* **26**, 3455-3467
11. Wu, Q., Kazantzis, M., Doege, H., Ortegon, A. M., Tsang, B., Falcon, A., and Stahl, A. (2006) *Diabetes* **55**, 3229-3237
12. Leverve, X., Guigas, B., Detaille, D., Batandier, C., Koceir, E., Chauvin, C., Fontaine, E., and Wiernsperger, N. (2003) *Diabetes Metab* **29**, 88-94
13. Canto, C., Gerhart-Hines, Z., Feige, J. N., Lagouge, M., Noriega, L., Milne, J. C., Elliott, P. J., Puigserver, P., and Auwerx, J. (2009) *Nature* **458**, 1056-1060
14. Hubbard, B., Doege, H., Punreddy, S., Wu, H., Huang, X., Kaushik, V. K., Mozell, R. L., Byrnes, J. J., Stricker-Krongrad, A., Chou, C. J., Tartaglia, L. A., Lodish, H. F., Stahl, A., and Gimeno, R. E. (2006) *Gastroenterology* **130**, 1259-1269

15. Bunik, V. I., Raddatz, G., Wanders, R. J., and Reiser, G. (2006) *FEBS Lett* **580**, 3551-3557
16. Abe, T., Hashimoto, Y., Hosaka, H., Tomita-Yokotani, K., and Kobayashi, M. (2008) *J Biol Chem* **283**, 11312-11321
17. Mancuso, C., Scapagini, G., Curro, D., Giuffrida Stella, A. M., De Marco, C., Butterfield, D. A., and Calabrese, V. (2007) *Front Biosci* **12**, 1107-1123
18. Gredilla, R., Grief, J., and Osiewacz, H. D. (2006) *Exp Gerontol* **41**, 439-447
19. Gredilla, R., Sanz, A., Lopez-Torres, M., and Barja, G. (2001) *FASEB J* **15**, 1589-1591
20. Cadenas, E., and Davies, K. J. (2000) *Free Radic Biol Med* **29**, 222-230
21. Yamano, K., Kuroyanagi-Hasegawa, M., Esaki, M., Yokota, M., and Endo, T. (2008) *J Biol Chem* **283**, 27325-27332
22. Sato, T., Esaki, M., Fernandez, J. M., and Endo, T. (2005) *Proc Natl Acad Sci U S A* **102**, 17999-18004
23. Bose, M., Debnath, D., Chen, Y., and Bose, H. S. (2007) *J Mol Endocrinol* **39**, 67-79
24. Bose, H., Lingappa, V. R., and Miller, W. L. (2002) *Nature* **417**, 87-91
25. Sebastian, D., Guitart, M., Garcia-Martinez, C., Mauvezin, C., Orellana-Gavalda, J. M., Serra, D., Gomez-Foix, A. M., Hegardt, F. G., and Asins, G. (2009) *J Lipid Res*
26. Sass, E., Blachinsky, E., Karniely, S., and Pines, O. (2001) *J Biol Chem* **276**, 46111-46117
27. Regev-Rudzki, N., Battat, E., Goldberg, I., and Pines, O. (2009) *Mol Microbiol* **72**, 297-306
28. Suzuki, T., Yoshida, T., and Tuboi, S. (1992) *Eur J Biochem* **207**, 767-772
29. Moulson, C. L., Lin, M. H., White, J. M., Newberry, E. P., Davidson, N. O., and Miner, J. H. (2007) *J Biol Chem* **282**, 15912-15920
30. Herrmann, T., Grone, H. J., Langbein, L., Kaiser, I., Gosch, I., Bennemann, U., Metzger, D., Chambon, P., Stewart, A. F., and Stremmel, W. (2005) *J Invest Dermatol* **125**, 1228-1235
31. Herrmann, T., van der Hoeven, F., Grone, H. J., Stewart, A. F., Langbein, L., Kaiser, I., Liebisch, G., Gosch, I., Buchkremer, F., Drobnik, W., Schmitz, G., and Stremmel, W. (2003) *J Cell Biol* **161**, 1105-1115
32. Shim, J., Moulson, C. L., Newberry, E. P., Lin, M. H., Xie, Y., Kennedy, S. M., Miner, J. H., and Davidson, N. O. (2009) *J Lipid Res* **50**, 491-500

BIBLIOGRAPHY

Abe, T., Y. Hashimoto, et al. (2008). "Discovery of amide (peptide) bond synthetic activity in Acyl-CoA synthetase." J Biol Chem **283**(17): 11312-21.

Abumrad, N. A., M. R. el-Maghrabi, et al. (1993). "Cloning of a rat adipocyte membrane protein implicated in binding or transport of long-chain fatty acids that is induced during preadipocyte differentiation. Homology with human CD36." J Biol Chem **268**(24): 17665-8.

Berk, P. D. and D. D. Stump (1999). "Mechanisms of cellular uptake of long chain free fatty acids." Mol Cell Biochem **192**(1-2): 17-31.

Berk, P. D., S. L. Zhou, et al. (1997). "Uptake of long chain free fatty acids is selectively up-regulated in adipocytes of Zucker rats with genetic obesity and non-insulin-dependent diabetes mellitus." J Biol Chem **272**(13): 8830-5.

Bernlohr, D. A. and R. L. Switzer (1981). "Reaction of Bacillus subtilis glutamine phosphoribosylpyrophosphate amidotransferase with oxygen: chemistry and regulation by ligands." Biochemistry **20**(20): 5675-81.

Bose, H., V. R. Lingappa, et al. (2002). "Rapid regulation of steroidogenesis by mitochondrial protein import." Nature **417**(6884): 87-91.

Bose, M., D. Debnath, et al. (2007). "Folding, activity and import of steroidogenic acute regulatory protein into mitochondria changed by nicotine exposure." J Mol Endocrinol **39**(1): 67-79.

Brasaemle, D. L., G. Dolios, et al. (2004). "Proteomic analysis of proteins associated with lipid droplets of basal and lipolytically stimulated 3T3-L1 adipocytes." J Biol Chem **279**(45): 46835-42.

Brunaldi, K., M. A. Miranda, et al. (2005). "Fatty acid flip-flop and proton transport determined by short-circuit current in planar bilayers." J Lipid Res **46**(2): 245-51.

Bunik, V. I. and D. Degtyarev (2008). "Structure-function relationships in the 2-oxo acid dehydrogenase family: substrate-specific signatures and functional predictions for the 2-oxoglutarate dehydrogenase-like proteins." Proteins **71**(2): 874-90.

Bunik, V. I., G. Raddatz, et al. (2006). "Brain pyruvate and 2-oxoglutarate dehydrogenase complexes are mitochondrial targets of the CoA ester of the Refsum disease marker phytanic acid." FEBS Lett **580**(14): 3551-7.

Cadenas, E. and K. J. Davies (2000). "Mitochondrial free radical generation, oxidative stress, and aging." Free Radic Biol Med **29**(3-4): 222-30.

Canto, C., Z. Gerhart-Hines, et al. (2009). "AMPK regulates energy expenditure by modulating NAD+ metabolism and SIRT1 activity." Nature **458**(7241): 1056-60.

Carmen, G. Y. and S. M. Victor (2006). "Signalling mechanisms regulating lipolysis." Cell Signal **18**(4): 401-8.

Cases, S., S. J. Stone, et al. (2001). "Cloning of DGAT2, a second mammalian diacylglycerol acyltransferase, and related family members." J Biol Chem **276**(42): 38870-6.

Cechetto, J. D., S. K. Sadacharan, et al. (2002). "Immunogold localization of mitochondrial aspartate aminotransferase in mitochondria and on the cell surface in normal rat tissues." Histol Histopathol **17**(2): 353-64.
Chabowski, A., S. L. Coort, et al. (2005). "The subcellular compartmentation of fatty acid transporters is regulated differently by insulin and by AICAR." FEBS Lett **579**(11): 2428-32.
Chavez, J. A., T. A. Knotts, et al. (2003). "A role for ceramide, but not diacylglycerol, in the antagonism of insulin signal transduction by saturated fatty acids." J Biol Chem **278**(12): 10297-303.
Chiu, H. C., A. Kovacs, et al. (2005). "Transgenic expression of fatty acid transport protein 1 in the heart causes lipotoxic cardiomyopathy." Circ Res **96**(2): 225-33.
Clark, H., D. Carling, et al. (2004). "Covalent activation of heart AMP-activated protein kinase in response to physiological concentrations of long-chain fatty acids." Eur J Biochem **271**(11): 2215-24.
Claros, M. G. and P. Vincens (1996). "Computational method to predict mitochondrially imported proteins and their targeting sequences." Eur J Biochem **241**(3): 779-86.
Coburn, C. T., F. F. Knapp, Jr., et al. (2000). "Defective uptake and utilization of long chain fatty acids in muscle and adipose tissues of CD36 knockout mice." J Biol Chem **275**(42): 32523-9.
Coe, N. R., A. J. Smith, et al. (1999). "The fatty acid transport protein (FATP1) is a very long chain acyl-CoA synthetase." J Biol Chem **274**(51): 36300-4.
Cohen, P. (2006). "The twentieth century struggle to decipher insulin signalling." Nat Rev Mol Cell Biol **7**(11): 867-73.
Coort, S. L., W. A. Coumans, et al. (2005). "Divergent effects of rosiglitazone on protein-mediated fatty acid uptake in adipose and in muscle tissues of Zucker rats." J Lipid Res **46**(6): 1295-302.
Cupp, D., J. P. Kampf, et al. (2004). "Fatty acid-albumin complexes and the determination of the transport of long chain free fatty acids across membranes." Biochemistry **43**(15): 4473-81.
de Souza, C. J., M. Eckhardt, et al. (2001). "Effects of pioglitazone on adipose tissue remodeling within the setting of obesity and insulin resistance." Diabetes **50**(8): 1863-71.
Dienel, G. A. and L. Hertz (2001). "Glucose and lactate metabolism during brain activation." J Neurosci Res **66**(5): 824-38.
Dirusso, C. C., E. J. Connell, et al. (2000). "Murine FATP alleviates growth and biochemical deficiencies of yeast fat1Delta strains." Eur J Biochem **267**(14): 4422-33.
DiRusso, C. C., D. Darwis, et al. (2008). "Functional domains of the fatty acid transport proteins: studies using protein chimeras." Biochim Biophys Acta **1781**(3): 135-43.
DiRusso, C. C., H. Li, et al. (2005). "Comparative biochemical studies of the murine fatty acid transport proteins (FATP) expressed in yeast." J Biol Chem **280**(17): 16829-37.

Durkot, M. J., L. De Garavilla, et al. (1995). "The effects of dichloroacetate on lactate accumulation and endurance in an exercising rat model." Int J Sports Med **16**(3): 167-71.
Faergeman, N. J., C. C. DiRusso, et al. (1997). "Disruption of the Saccharomyces cerevisiae homologue to the murine fatty acid transport protein impairs uptake and growth on long-chain fatty acids." J Biol Chem **272**(13): 8531-8.
Febbraio, M., N. A. Abumrad, et al. (1999). "A null mutation in murine CD36 reveals an important role in fatty acid and lipoprotein metabolism." J Biol Chem **274**(27): 19055-62.
Febbraio, M., E. Guy, et al. (2002). "The impact of overexpression and deficiency of fatty acid translocase (FAT)/CD36." Mol Cell Biochem **239**(1-2): 193-7.
Fediuc, S., M. P. Gaidhu, et al. (2006). "Regulation of AMP-activated protein kinase and acetyl-CoA carboxylase phosphorylation by palmitate in skeletal muscle cells." J Lipid Res **47**(2): 412-20.
Fernie, A. R., F. Carrari, et al. (2004). "Respiratory metabolism: glycolysis, the TCA cycle and mitochondrial electron transport." Curr Opin Plant Biol **7**(3): 254-61.
Frayn, K. N., B. A. Fielding, et al. (2005). "Adipose tissue fatty acid metabolism and cardiovascular disease." Curr Opin Lipidol **16**(4): 409-15.
Frohnert, B. I. and D. A. Bernlohr (2000). "Regulation of fatty acid transporters in mammalian cells." Prog Lipid Res **39**(1): 83-107.
Frohnert, B. I., T. Y. Hui, et al. (1999). "Identification of a functional peroxisome proliferator-responsive element in the murine fatty acid transport protein gene." J Biol Chem **274**(7): 3970-7.
Fryer, L. G., E. Hajduch, et al. (2000). "Activation of glucose transport by AMP-activated protein kinase via stimulation of nitric oxide synthase." Diabetes **49**(12): 1978-85.
Gaidhu, M. P., S. Fediuc, et al. (2006). "5-Aminoimidazole-4-carboxamide-1-beta-D-ribofuranoside-induced AMP-activated protein kinase phosphorylation inhibits basal and insulin-stimulated glucose uptake, lipid synthesis, and fatty acid oxidation in isolated rat adipocytes." J Biol Chem **281**(36): 25956-64.
Garcia-Martinez, C., M. Marotta, et al. (2005). "Impact on fatty acid metabolism and differential localization of FATP1 and FAT/CD36 proteins delivered in cultured human muscle cells." Am J Physiol Cell Physiol **288**(6): C1264-72.
Gargiulo, C. E., S. M. Stuhlsatz-Krouper, et al. (1999). "Localization of adipocyte long-chain fatty acyl-CoA synthetase at the plasma membrane." J Lipid Res **40**(5): 881-92.
Garland, P. B. (1964). "Some kinetic properties of pig-heart oxoglutarate dehydrogenase that provide a basis for metabolic control of the enzyme activity and also a stoicheiometric assay for coenzyme A in tissue extracts." Biochem J **92**(2): 10C-12C.
Gauthier, M. S., H. Miyoshi, et al. (2008). "AMP-activated protein kinase (AMPK) is activated as a consequence of lipolysis in the adipocyte: potential mechanism and physiological relevance." J Biol Chem.

Gertow, K., M. Bellanda, et al. (2004). "Genetic and structural evaluation of fatty acid transport protein-4 in relation to markers of the insulin resistance syndrome." J Clin Endocrinol Metab **89**(1): 392-9.
Gertow, K., K. H. Pietilainen, et al. (2004). "Expression of fatty-acid-handling proteins in human adipose tissue in relation to obesity and insulin resistance." Diabetologia **47**(6): 1118-25.
Gimeno, R. E., D. J. Hirsch, et al. (2003). "Targeted deletion of fatty acid transport protein-4 results in early embryonic lethality." J Biol Chem **278**(49): 49512-6.
Gimeno, R. E., A. M. Ortegon, et al. (2003). "Characterization of a heart-specific fatty acid transport protein." J Biol Chem **278**(18): 16039-44.
Glatz, J. F., J. J. Luiken, et al. (2001). "Involvement of membrane-associated proteins in the acute regulation of cellular fatty acid uptake." J Mol Neurosci **16**(2-3): 123-32; discussion 151-7.
Gomazkova, V. S. and O. E. Krasovskaia (1979). "[Regulation of alpha-ketoglutarate dehydrogenase complex from pigeon breast muscle]." Biokhimiia **44**(6): 1126-36.
Gredilla, R., J. Grief, et al. (2006). "Mitochondrial free radical generation and lifespan control in the fungal aging model Podospora anserina." Exp Gerontol **41**(4): 439-47.
Gredilla, R., A. Sanz, et al. (2001). "Caloric restriction decreases mitochondrial free radical generation at complex I and lowers oxidative damage to mitochondrial DNA in the rat heart." FASEB J **15**(9): 1589-91.
Guitart, M., A. L. Andreu, et al. (2009). "FATP1 localizes to mitochondria and enhances pyruvate dehydrogenase activity in skeletal myotubes." Mitochondrion.
Hajri, T., A. M. Hall, et al. (2007). "CD36-facilitated fatty acid uptake inhibits leptin production and signaling in adipose tissue." Diabetes **56**(7): 1872-80.
Hall, A. M., A. J. Smith, et al. (2003). "Characterization of the Acyl-CoA synthetase activity of purified murine fatty acid transport protein 1." J Biol Chem **278**(44): 43008-13.
Hall, A. M., B. M. Wiczer, et al. (2005). "Enzymatic properties of purified murine fatty acid transport protein 4 and analysis of acyl-CoA synthetase activities in tissues from FATP4 null mice." J Biol Chem **280**(12): 11948-54.
Hamada, M., K. Koike, et al. (1975). "A kinetic study of the alpha-keto acid dehydrogenase complexes from pig heart mitochondria." J Biochem **77**(5): 1047-56.
Hamilton, J. A. (2003). "Fast flip-flop of cholesterol and fatty acids in membranes: implications for membrane transport proteins." Curr Opin Lipidol **14**(3): 263-71.
Hardie, D. G., S. A. Hawley, et al. (2006). "AMP-activated protein kinase--development of the energy sensor concept." J Physiol **574**(Pt 1): 7-15.
Hatch, G. M., A. J. Smith, et al. (2002). "FATP1 channels exogenous FA into 1,2,3-triacyl-sn-glycerol and down-regulates sphingomyelin and cholesterol metabolism in growing 293 cells." J Lipid Res **43**(9): 1380-9.

Hauser, S., G. Adelmant, et al. (2000). "Degradation of the peroxisome proliferator-activated receptor gamma is linked to ligand-dependent activation." J Biol Chem **275**(24): 18527-33.
Hausler, N., J. Browning, et al. (2006). "Effects of insulin and cytosolic redox state on glucose production pathways in the isolated perfused mouse liver measured by integrated 2H and 13C NMR." Biochem J **394**(Pt 2): 465-73.
He, T. C., S. Zhou, et al. (1998). "A simplified system for generating recombinant adenoviruses." Proc Natl Acad Sci U S A **95**(5): 2509-14.
Hellstrom, L., D. Langin, et al. (1996). "Adipocyte lipolysis in normal weight subjects with obesity among first-degree relatives." Diabetologia **39**(8): 921-8.
Heron-Milhavet, L., M. Haluzik, et al. (2004). "Muscle-specific overexpression of CD36 reverses the insulin resistance and diabetes of MKR mice." Endocrinology **145**(10): 4667-76.
Herrmann, T., F. Buchkremer, et al. (2001). "Mouse fatty acid transport protein 4 (FATP4): characterization of the gene and functional assessment as a very long chain acyl-CoA synthetase." Gene **270**(1-2): 31-40.
Herrmann, T., H. J. Grone, et al. (2005). "Disturbed epidermal structure in mice with temporally controlled fatp4 deficiency." J Invest Dermatol **125**(6): 1228-35.
Herrmann, T., F. van der Hoeven, et al. (2003). "Mice with targeted disruption of the fatty acid transport protein 4 (Fatp 4, Slc27a4) gene show features of lethal restrictive dermopathy." J Cell Biol **161**(6): 1105-15.
Hirsch, D., A. Stahl, et al. (1998). "A family of fatty acid transporters conserved from mycobacterium to man." Proc Natl Acad Sci U S A **95**(15): 8625-9.
Huang, H. M., H. Zhang, et al. (2003). "Inhibition of the alpha-ketoglutarate dehydrogenase complex alters mitochondrial function and cellular calcium regulation." Biochim Biophys Acta **1637**(1): 119-26.
Huang, M., P. Kozlowski, et al. (2002). "Caspase-dependent cleavage of carbamoyl phosphate synthetase II during apoptosis." Mol Pharmacol **61**(3): 569-77.
Hubbard, B., H. Doege, et al. (2006). "Mice deleted for fatty acid transport protein 5 have defective bile acid conjugation and are protected from obesity." Gastroenterology **130**(4): 1259-69.
Hui, T. Y., B. I. Frohnert, et al. (1998). "Characterization of the murine fatty acid transport protein gene and its insulin response sequence." J Biol Chem **273**(42): 27420-9.
Hwang, D. Y. and F. Ismail-Beigi (2002). "Glucose uptake and lactate production in cells exposed to CoCl(2) and in cells overexpressing the Glut-1 glucose transporter." Arch Biochem Biophys **399**(2): 206-11.
Jiang, Z. Y., Q. L. Zhou, et al. (2003). "Insulin signaling through Akt/protein kinase B analyzed by small interfering RNA-mediated gene silencing." Proc Natl Acad Sci U S A **100**(13): 7569-74.
Kaluzny, M. A., L. A. Duncan, et al. (1985). "Rapid separation of lipid classes in high yield and purity using bonded phase columns." J Lipid Res **26**(1): 135-40.
Kampf, J. P. and A. M. Kleinfeld (2004). "Fatty acid transport in adipocytes monitored by imaging intracellular free fatty acid levels." J Biol Chem **279**(34): 35775-80.

Kawaguchi, T., K. Osatomi, et al. (2002). "Mechanism for fatty acid "sparing" effect on glucose-induced transcription: regulation of carbohydrate-responsive element-binding protein by AMP-activated protein kinase." J Biol Chem **277**(6): 3829-35.

Keller, A., A. I. Nesvizhskii, et al. (2002). "Empirical statistical model to estimate the accuracy of peptide identifications made by MS/MS and database search." Anal Chem **74**(20): 5383-92.

Kim, J. H., T. M. Lewin, et al. (2001). "Expression and characterization of recombinant rat Acyl-CoA synthetases 1, 4, and 5. Selective inhibition by triacsin C and thiazolidinediones." J Biol Chem **276**(27): 24667-73.

Kim, J. K., R. E. Gimeno, et al. (2004). "Inactivation of fatty acid transport protein 1 prevents fat-induced insulin resistance in skeletal muscle." J Clin Invest **113**(5): 756-63.

Knol, J., L. Veenhoff, et al. (1996). "Unidirectional reconstitution into detergent-destabilized liposomes of the purified lactose transport system of Streptococcus thermophilus." J Biol Chem **271**(26): 15358-66.

Kornfeld, S., M. Benziman, et al. (1977). "Alpha-ketoglutarate dehydrogenase complex of Acetobacter xylinum. Purification and regulatory properties." J Biol Chem **252**(9): 2940-7.

Koves, T. R., R. C. Noland, et al. (2005). "Subsarcolemmal and intermyofibrillar mitochondria play distinct roles in regulating skeletal muscle fatty acid metabolism." Am J Physiol Cell Physiol **288**(5): C1074-82.

Koves, T. R., J. R. Ussher, et al. (2008). "Mitochondrial overload and incomplete fatty acid oxidation contribute to skeletal muscle insulin resistance." Cell Metab **7**(1): 45-56.

Kunkel, S. L., M. Spengler, et al. (1988). "Prostaglandin E2 regulates macrophage-derived tumor necrosis factor gene expression." J Biol Chem **263**(11): 5380-4.

Lazar, M. A. (2005). "How obesity causes diabetes: not a tall tale." Science **307**(5708): 373-5.

Leverve, X., B. Guigas, et al. (2003). "Mitochondrial metabolism and type-2 diabetes: a specific target of metformin." Diabetes Metab **29**(4 Pt 2): 88-94.

Lewis, S. E., L. L. Listenberger, et al. (2001). "Membrane topology of the murine fatty acid transport protein 1." J Biol Chem **276**(40): 37042-50.

Liang, X., Q. Wang, et al. (2008). "The prostaglandin E2 EP2 receptor accelerates disease progression and inflammation in a model of amyotrophic lateral sclerosis." Ann Neurol **64**(3): 304-14.

Linton, M. F. and S. Fazio (2003). "Macrophages, inflammation, and atherosclerosis." Int J Obes Relat Metab Disord **27 Suppl 3**: S35-40.

Lobo, S., B. M. Wiczer, et al. (2009). "Functional analysis of long-chain acyl-coa synthetase 1 in 3T3-L1 adipocytes." J Biol Chem.

Lobo, S., B. M. Wiczer, et al. (2007). "Fatty acid metabolism in adipocytes: functional analysis of fatty acid transport proteins 1 and 4." J Lipid Res **48**(3): 609-20.

Luiken, J. J., F. G. Schaap, et al. (1999). "Cellular fatty acid transport in heart and skeletal muscle as facilitated by proteins." Lipids **34 Suppl**: S169-75.

Luiken, J. J., L. P. Turcotte, et al. (1999). "Protein-mediated palmitate uptake and expression of fatty acid transport proteins in heart giant vesicles." J Lipid Res **40**(6): 1007-16.

Mailloux, R. J., R. Beriault, et al. (2007). "The tricarboxylic acid cycle, an ancient metabolic network with a novel twist." PLoS ONE **2**(1): e690.

Mancuso, C., G. Scapagini, et al. (2007). "Mitochondrial dysfunction, free radical generation and cellular stress response in neurodegenerative disorders." Front Biosci **12**: 1107-23.

Maroon, J. C. and J. W. Bost (2006). "Omega-3 fatty acids (fish oil) as an anti-inflammatory: an alternative to nonsteroidal anti-inflammatory drugs for discogenic pain." Surg Neurol **65**(4): 326-31.

Marshall, S. (2006). "Role of insulin, adipocyte hormones, and nutrient-sensing pathways in regulating fuel metabolism and energy homeostasis: a nutritional perspective of diabetes, obesity, and cancer." Sci STKE **2006**(346): re7.

Martin, G., H. Poirier, et al. (2000). "Induction of the fatty acid transport protein 1 and acyl-CoA synthase genes by dimer-selective rexinoids suggests that the peroxisome proliferator-activated receptor-retinoid X receptor heterodimer is their molecular target." J Biol Chem **275**(17): 12612-8.

Mashek, D. G., M. A. McKenzie, et al. (2005). "Rat long chain acyl-coa synthetase 5 increases fatty acid uptake and partitioning to cellular triacylglcyerol in mcardle-RH7777 cells." J Biol Chem.

Memon, R. A., K. R. Feingold, et al. (1998). "Regulation of fatty acid transport protein and fatty acid translocase mRNA levels by endotoxin and cytokines." Am J Physiol **274**(2 Pt 1): E210-7.

Memon, R. A., J. Fuller, et al. (1999). "Regulation of putative fatty acid transporters and Acyl-CoA synthetase in liver and adipose tissue in ob/ob mice." Diabetes **48**(1): 121-7.

Milger, K., T. Herrmann, et al. (2006). "Cellular uptake of fatty acids driven by the ER-localized acyl-CoA synthetase FATP4." J Cell Sci **119**(Pt 22): 4678-88.

Morrow, J. D. and L. J. Roberts (1997). "The isoprostanes: unique bioactive products of lipid peroxidation." Prog Lipid Res **36**(1): 1-21.

Moulson, C. L., M. H. Lin, et al. (2007). "Keratinocyte-specific expression of fatty acid transport protein 4 rescues the wrinkle-free phenotype in Slc27a4/Fatp4 mutant mice." J Biol Chem **282**(21): 15912-20.

Moulson, C. L., D. R. Martin, et al. (2003). "Cloning of wrinkle-free, a previously uncharacterized mouse mutation, reveals crucial roles for fatty acid transport protein 4 in skin and hair development." Proc Natl Acad Sci U S A **100**(9): 5274-9.

Nagamatsu, K., S. Soeda, et al. (1985). "Lignoceroyl-coenzyme A synthetase from developing rat brain: partial purification, characterization and comparison with palmitoyl-coenzyme A synthetase activity and liver enzyme." Biochim Biophys Acta **836**(1): 80-8.

Naveri, H. K., H. Leinonen, et al. (1997). "Skeletal muscle lactate accumulation and creatine phosphate depletion during heavy exercise in congestive heart failure. Cause of limited exercise capacity?" Eur Heart J **18**(12): 1937-45.

Ortegren, U., L. Yin, et al. (2006). "Separation and characterization of caveolae subclasses in the plasma membrane of primary adipocytes; segregation of specific proteins and functions." Febs J **273**(14): 3381-92.
Ost, A., U. Ortegren, et al. (2005). "Triacylglycerol is synthesized in a specific subclass of caveolae in primary adipocytes." J Biol Chem **280**(1): 5-8.
Pan, Y., K. D. Mansfield, et al. (2007). "Multiple factors affecting cellular redox status and energy metabolism modulate hypoxia-inducible factor prolyl hydroxylase activity in vivo and in vitro." Mol Cell Biol **27**(3): 912-25.
Park, L. C., N. Y. Calingasan, et al. (2000). "Quantitative alpha-ketoglutarate dehydrogenase activity staining in brain sections and in cultured cells." Anal Biochem **277**(1): 86-93.
Pei, Z., P. Fraisl, et al. (2004). "Mouse very long-chain Acyl-CoA synthetase 3/fatty acid transport protein 3 catalyzes fatty acid activation but not fatty acid transport in MA-10 cells." J Biol Chem **279**(52): 54454-62.
Pohl, J., A. Ring, et al. (2004). "New concepts of cellular fatty acid uptake: role of fatty acid transport proteins and of caveolae." Proc Nutr Soc **63**(2): 259-62.
Pohl, J., A. Ring, et al. (2005). "FAT/CD36-mediated long-chain fatty acid uptake in adipocytes requires plasma membrane rafts." Mol Biol Cell **16**(1): 24-31.
Pol, A., S. Martin, et al. (2004). "Dynamic and regulated association of caveolin with lipid bodies: modulation of lipid body motility and function by a dominant negative mutant." Mol Biol Cell **15**(1): 99-110.
Rajala, M. W. and P. E. Scherer (2003). "Minireview: The adipocyte--at the crossroads of energy homeostasis, inflammation, and atherosclerosis." Endocrinology **144**(9): 3765-73.
Randle, P. J., P. B. Garland, et al. (1963). "The glucose fatty-acid cycle. Its role in insulin sensitivity and the metabolic disturbances of diabetes mellitus." Lancet **1**: 785-9.
Razani, B., T. P. Combs, et al. (2002). "Caveolin-1-deficient mice are lean, resistant to diet-induced obesity, and show hypertriglyceridemia with adipocyte abnormalities." J Biol Chem **277**(10): 8635-47.
Regev-Rudzki, N., E. Battat, et al. (2009). "Dual localization of fumarase is dependent on the integrity of the glyoxylate shunt." Mol Microbiol **72**(2): 297-306.
Reshef, L., Y. Olswang, et al. (2003). "Glyceroneogenesis and the triglyceride/fatty acid cycle." J Biol Chem **278**(33): 30413-6.
Richards, M. R., J. D. Harp, et al. (2006). "Fatty acid transport protein 1 and long-chain acyl coenzyme A synthetase 1 interact in adipocytes." J Lipid Res **47**(3): 665-72.
Richards, M. R., L. L. Listenberger, et al. (2003). "Oligomerization of the murine fatty acid transport protein 1." J Biol Chem **278**(12): 10477-83.
Richieri, G. V., A. Anel, et al. (1993). "Interactions of long-chain fatty acids and albumin: determination of free fatty acid levels using the fluorescent probe ADIFAB." Biochemistry **32**(29): 7574-80.
Sass, E., E. Blachinsky, et al. (2001). "Mitochondrial and cytosolic isoforms of yeast fumarase are derivatives of a single translation product and have identical amino termini." J Biol Chem **276**(49): 46111-7.

Sato, T., M. Esaki, et al. (2005). "Comparison of the protein-unfolding pathways between mitochondrial protein import and atomic-force microscopy measurements." Proc Natl Acad Sci U S A **102**(50): 17999-8004.
Sauer, S. W., J. G. Okun, et al. (2008). "Impact of short- and medium-chain organic acids, acylcarnitines, and acyl-CoAs on mitochondrial energy metabolism." Biochim Biophys Acta **1777**(10): 1276-82.
Schaffer, J. E. and H. F. Lodish (1994). "Expression cloning and characterization of a novel adipocyte long chain fatty acid transport protein." Cell **79**(3): 427-36.
Schaiff, W. T., I. Bildirici, et al. (2005). "Peroxisome proliferator-activated receptor-gamma and retinoid X receptor signaling regulate fatty acid uptake by primary human placental trophoblasts." J Clin Endocrinol Metab **90**(7): 4267-75.
Schmelter, T., B. L. Trigatti, et al. (2004). "Biochemical demonstration of the involvement of fatty acyl-CoA synthetase in fatty acid translocation across the plasma membrane." J Biol Chem **279**(23): 24163-70.
Schmidt, M. I., R. L. Watson, et al. (1996). "Clustering of dyslipidemia, hyperuricemia, diabetes, and hypertension and its association with fasting insulin and central and overall obesity in a general population. Atherosclerosis Risk in Communities Study Investigators." Metabolism **45**(6): 699-706.
Sebastian, D., M. Guitart, et al. (2009). "Novel role of FATP1 in mitochondrial fatty acid oxidation in skeletal muscle cells." J Lipid Res.
Shim, J., C. L. Moulson, et al. (2009). "Fatty acid transport protein 4 is dispensable for intestinal lipid absorption in mice." J Lipid Res **50**(3): 491-500.
Smith, C. M., J. Bryla, et al. (1974). "Regulation of mitochondrial alpha-ketoglutarate metabolism by product inhibition at alpha-ketoglutarate dehydrogenase." J Biol Chem **249**(5): 1497-505.
Southam, A. D., J. M. Easton, et al. (2008). "Metabolic changes in flatfish hepatic tumours revealed by NMR-based metabolomics and metabolic correlation networks." J Proteome Res **7**(12): 5277-85.
Stahl, A. (2004). "A current review of fatty acid transport proteins (SLC27)." Pflugers Arch **447**(5): 722-7.
Stahl, A., J. G. Evans, et al. (2002). "Insulin causes fatty acid transport protein translocation and enhanced fatty acid uptake in adipocytes." Dev Cell **2**(4): 477-88.
Stahl, A., D. J. Hirsch, et al. (1999). "Identification of the major intestinal fatty acid transport protein." Mol Cell **4**(3): 299-308.
Stewart, S. A., D. M. Dykxhoorn, et al. (2003). "Lentivirus-delivered stable gene silencing by RNAi in primary cells." Rna **9**(4): 493-501.
Stone, S. J., H. M. Myers, et al. (2004). "Lipopenia and skin barrier abnormalities in DGAT2-deficient mice." J Biol Chem **279**(12): 11767-76.
Student, A. K., R. Y. Hsu, et al. (1980). "Induction of fatty acid synthetase synthesis in differentiating 3T3-L1 preadipocytes." J Biol Chem **255**(10): 4745-50.
Stuhlsatz-Krouper, S. M., N. E. Bennett, et al. (1998). "Substitution of alanine for serine 250 in the murine fatty acid transport protein inhibits long chain fatty acid transport." J Biol Chem **273**(44): 28642-50.

Stuhlsatz-Krouper, S. M., N. E. Bennett, et al. (1999). "Molecular aspects of fatty acid transport: mutations in the IYTSGTTGXPK motif impair fatty acid transport protein function." Prostaglandins Leukot Essent Fatty Acids **60**(5-6): 285-9.

Sutherland, B. W., J. Toews, et al. (2008). "Utility of formaldehyde cross-linking and mass spectrometry in the study of protein-protein interactions." J Mass Spectrom **43**(6): 699-715.

Suzuki, T., T. Yoshida, et al. (1992). "Evidence that rat liver mitochondrial and cytosolic fumarases are synthesized from one species of mRNA by alternative translational initiation at two in-phase AUG codons." Eur J Biochem **207**(2): 767-72.

Talbot, J., J. N. Barrett, et al. (2007). "Stimulation-induced changes in NADH fluorescence and mitochondrial membrane potential in lizard motor nerve terminals." J Physiol **579**(Pt 3): 783-98.

Taylor, E. B., W. J. Ellingson, et al. (2005). "Long-chain acyl-CoA esters inhibit phosphorylation of AMP-activated protein kinase at threonine-172 by LKB1/STRAD/MO25." Am J Physiol Endocrinol Metab **288**(6): E1055-61.

Thompson, B. R., A. M. Muzurkiewicz-Munoz, et al. (2009). "Interaction of Adipocyte Fatty Acid Binding Protein and JAK2: AFABP/aP2 as a Regulator of JAK2 Signaling." J Biol Chem.

Tobias, L. D. and J. G. Hamilton (1979). "The effect of 5,8,11,14-eicosatetraynoic acid on lipid metabolism." Lipids **14**(2): 181-93.

Tong, F., P. N. Black, et al. (2006). "Fatty acid transport by vectorial acylation in mammals: roles played by different isoforms of rat long-chain acyl-CoA synthetases." Arch Biochem Biophys **447**(1): 46-52.

Towler, M. C. and D. G. Hardie (2007). "AMP-activated protein kinase in metabolic control and insulin signaling." Circ Res **100**(3): 328-41.

Trigatti, B. L., R. G. Anderson, et al. (1999). "Identification of caveolin-1 as a fatty acid binding protein." Biochem Biophys Res Commun **255**(1): 34-9.

Turcotte, L. P., J. R. Swenberger, et al. (2000). "Muscle palmitate uptake and binding are saturable and inhibited by antibodies to FABP(PM)." Mol Cell Biochem **210**(1-2): 53-63.

Viollet, B., F. Andreelli, et al. (2003). "Physiological role of AMP-activated protein kinase (AMPK): insights from knockout mouse models." Biochem Soc Trans **31**(Pt 1): 216-9.

Watkins, P. A. (2008). "Very long-chain acyl-CoA synthetases." J Biol Chem **283**(4): 1773-7.

Watt, M. J., G. R. Steinberg, et al. (2006). "Fatty acids stimulate AMP-activated protein kinase and enhance fatty acid oxidation in L6 myotubes." J Physiol **574**(Pt 1): 139-47.

Weimar, J. D., C. C. DiRusso, et al. (2002). "Functional role of fatty acyl-coenzyme A synthetase in the transmembrane movement and activation of exogenous long-chain fatty acids. Amino acid residues within the ATP/AMP signature motif of Escherichia coli FadD are required for enzyme activity and fatty acid transport." J Biol Chem **277**(33): 29369-76.

Weiss, R. G., V. P. Chacko, et al. (1989). "Comparative 13C and 31P NMR assessment of altered metabolism during graded reductions in coronary flow in intact rat hearts." Proc Natl Acad Sci U S A **86**(16): 6426-30.
Wessel, D. and U. I. Flugge (1984). "A method for the quantitative recovery of protein in dilute solution in the presence of detergents and lipids." Anal Biochem **138**(1): 141-3.
Willems, H. L., T. F. de Kort, et al. (1978). "Determination of pyruvate oxidation rate and citric acid cycle activity in intact human leukocytes and fibroblasts." Clin Chem **24**(2): 200-3.
Wlodek, D. and M. Gonzales (2003). "Decreased energy levels can cause and sustain obesity." J Theor Biol **225**(1): 33-44.
Wu, Q., M. Kazantzis, et al. (2006). "Fatty acid transport protein 1 is required for nonshivering thermogenesis in brown adipose tissue." Diabetes **55**(12): 3229-37.
Wu, Q., A. M. Ortegon, et al. (2006). "FATP1 is an insulin-sensitive fatty acid transporter involved in diet-induced obesity." Mol Cell Biol **26**(9): 3455-67.
Xu, Y., T. J. Cook, et al. (2005). "Effects of di-(2-ethylhexyl)-phthalate (DEHP) and its metabolites on fatty acid homeostasis regulating proteins in rat placental HRP-1 trophoblast cells." Toxicol Sci **84**(2): 287-300.
Yamano, K., M. Kuroyanagi-Hasegawa, et al. (2008). "Step-size analyses of the mitochondrial Hsp70 import motor reveal the Brownian ratchet in operation." J Biol Chem **283**(40): 27325-32.
Yamauchi, T., J. Kamon, et al. (2001). "The mechanisms by which both heterozygous peroxisome proliferator-activated receptor gamma (PPARgamma) deficiency and PPARgamma agonist improve insulin resistance." J Biol Chem **276**(44): 41245-54.
Zhang, J., D. I. Phillips, et al. (2004). "Human skeletal muscle PPARalpha expression correlates with fat metabolism gene expression but not BMI or insulin sensitivity." Am J Physiol Endocrinol Metab **286**(2): E168-75.
Zhou, S. L., D. Stump, et al. (1995). "Mitochondrial aspartate aminotransferase expressed on the surface of 3T3-L1 adipocytes mediates saturable fatty acid uptake." Proc Soc Exp Biol Med **208**(3): 263-70.
Zimmermann, R., J. G. Strauss, et al. (2004). "Fat mobilization in adipose tissue is promoted by adipose triglyceride lipase." Science **306**(5700): 1383-6.
Zou, Z., C. C. DiRusso, et al. (2002). "Fatty acid transport in Saccharomyces cerevisiae. Directed mutagenesis of FAT1 distinguishes the biochemical activities associated with Fat1p." J Biol Chem **277**(34): 31062-71.
Zou, Z., F. Tong, et al. (2003). "Vectorial acylation in Saccharomyces cerevisiae. Fat1p and fatty acyl-CoA synthetase are interacting components of a fatty acid import complex." J Biol Chem **278**(18): 16414-22.